DEPARTAMENTO DE CIÊNCIAS DA VIDA

FACULDADE DE CIÊNCIAS E TECNOLOGIA
UNIVERSIDADE DE COIMBRA

The Role of PDGF in the Regulation of the Intracellular Pool of MMP-2: MMP-2 Contribution to SNALP Internalization in Glioma Cells

Dissertação apresentada à Universidadede Coimbra para cumprimento dos requisitos necessários à obtenção do graude Mestre em Biologia Molecular e Celular, realizada sob a orientação científica da Professora Doutora Concieição Pedroso da Lima (Universidade de Coimbra) e a Doutora Ana Luisa Cardoso (Centro de Neurociências e Biologia Celular da Universidade de Coimbra).

Angelo Serani

2013

Acknowledgments

I would like to express my gratitude to my supervisor, Dr. Ana Luisa Cardoso, whose expertise, understanding, and patience, added considerably to my experience. I appreciate her vast knowledge and skill in many areas, and her assistance in writing reports. Most important, a special thanks to let free and supported my imagination. She provided me with direction, technical support and became more of a mentor and friend, than a supervisor.

I would like to express my deep gratitude and respect to Prof. Maria Concienção Pedroso da Lima, for the help, the availability and access to all the best for the realization of this project.

A very special thanks goes out to Prof. Carlos B. Duarte and Prof. Lorella Canzoniero to granted me the opportunity to take part in this project.

My sincere thanks go to the various members of "Vector and Gene therapy" group, they provided a friendly and cooperative atmosphere at work and also useful feedback and insightful comments on my work. In particular to Pedro, Carlos, Ricardo and Joana, for their friendship and because they was always a great support in all my troubles in my new life and studies in this country.

I am deeply and forever indebted to my mother, my family, my friends and my beloved for their love, support and encouragement throughout my entire life.

Table of Content:

Abbreviations

AKT/PKB	Ak-Thymoma/Protein Kinase B
AP	Activating Protein
BBB	Blod Brain Barrier
C/EBP	Ccaat-enhancer-binding proteins
CDK	Cyclin-dependent kinase
CDKN	Cyclin-dependent kinase inhibitor
CEF	Chichen Embryo Fibroblast
CHD5	Chromodomain-helicase-DNA-binding protein 5
Cltx	Chlorotoxin
CNS	Central Nervous System
CREB	cAMP response element-binding
Crk	Proto-oncogene c-Crk
CSF	Colony stimulating factor
DMEM	Dulbecco's Modified Eagle Medium
E2F	Eukaryotes transcription factors
ECM	Extracellular matrix
EGFR	Epidermal Growth Factor Receptor
ERK	Extracellular signal-regulated kinases
Ets	E-twenty six Transcription factor
FAK	Focal Adhesion Kinase
FOXO	Forkhead box, sub-group O
GBM	Glioblastoma multiforme
Gbr2	Growth factor receptor-bound protein 2
GFAP	Glial fibrillary acidic protein

GPI	Glicosyl Phosphatidyl inositol
HBV	Hepatitis B virus
HGG	High Grade Gliomas
LGG	Low Grade Gliomas
LOH	Loss of Heretozygosity
MAPK	Mitogen-activated protein kinases
MDM2	Mouse double minute 2 homolog
MMP	Matrix Metalloproteinases
MT-MMP	Membrane Type - Matrix Metalloproteinases
mTOR	Mammalian target of rapamycin
NGF	Nerve growth factor
p14-ARF	Protein 14 - alternate reading frame
p16-Ink4a	Protein 16 - Cyclin-dependent kinase inhibitor 2A
p21	Protein 21
p27Kip1	Cyclin-dependent kinase inhibitor 1B
p53	Protein 53
PDCD4	Programmed Cell Death Protein 4
PDGF	Platelet-derived growth factor
PDK	Phosphoinositide-dependent kinase
PEG	Polyethylene glycol
PI3K	Phosphoinositide 3-kinase
PI3KC	Phosphatidylinositol 3-Kinase Catalytic
PI3KR	Phosphoinositide-3-Kinase, Regulatory Subunit
PIP2	Phosphatidylinositol (4,5)-bisphosphate
PIP3	Phosphatidylinositol (3,4,5)-trisphosphate
PLC	Phospholipase C
PTB	Phosphoprotein binding domain

Ras	Rat sarcoma protein
RB	Retinoblastoma
RES	Reticuloerndothelial system
RTK	Receptor tyrosine kinase
SGK1	Glucocorticoid regulated kinase 1
SH2	Src Homology 2
Shc	SHC-adaptor protein
SNALP	Stable Nucleic Acid Lipid Pasricles
SOS	Son of sevenless homolog
Sp1	SpecificityÿProteinÿ1
Src	Sarcoma (Schmidt-Ruppin A-2) viral oncogene homolog
STI571	Imatinib Mesylate
TfR	Transferrin Receptor
TGF	Transforming growth factor
TIMP	Tissue Inhibitor of Metalloproteinases
TORC-2	Transducer of regulated CREB protein 2
TP53	Tumor protein p53
VEGF	Vascular Endothelial growth factor
WHO	World Health Organization

Abstract

Glioblastoma multiforme is one of the most aggressive forms of astrocytic tumors, characterized by a low survival rate and a high invasive capacity. These properties are, in part, related with the expression of Matrix Metalloproteinases-2 (MMP-2), a proteinase involved in extracellular matrix remodeling, which in normal conditions is involved in new vessel formation, wound healing and, more generally, in tissue remodeling.

In glioblastoma, MMP-2 has been shown to be deregulated, contributing to tumor cell migration and metastization. Several studies have tried to elucidate the structure and activation mechanism of this protein and it has been possible to identify a number of proteins crucial to the control of the physiologic activity of MMP-2. Due to their important role in cellular remodeling and tissue growing, PDGF, and other similar growing factors, belong to the family of MMP-2 regulators and have been strictly connected with the expression and activation of this specific metalloproteinase. It has also been shown that Chlorotoxin, a toxin extracted from the deathstalker scorpion (*Leiurus quinquestriatus*) venom, is able to specifically blind cells that exhibit MMP-2 at their surface and may itself interfere with the tumor invasive capacity.

In the last few years, a wide series of lipid-based drug-delivering particles has been developed with the purpose of increasing the specificity and internalization of anti-tumor drugs. Stable nucleic acid lipid particles (SNALPs), a particular variety of lipid-based particles, have been used in combination with Chlorotoxin to target glioma cells. This technology, which can be used to deliver nucleic acid-based drugs, such as siRNAs or miRNAs, aims to be a valid therapeutic alternative to the conventional and mostly ineffective treatments of glioblastoma.

With this work, we aimed to clarify the MMP-2 regulatory mechanism and delineate a quantitative relation between the expression of this protein at the cell surface and the ability of Chlorotoxin-associated SNALPs to target glioblastoma cells.

We observed that the PDGF pathway presents a regulatory mechanism that, on one hand, leads to a latency between MMP-2 gene stimulation and the increase in the levels of this protein and, on the other hand, stimulates a limiting negative feedback loop that reduces MMP-2 expression after a massive PDGF stimulus. A similar discrepancy between mRNA and protein levels was also observed after siRNA-mediated silencing of MMP-2. However, we were able to detect the presence of extracellular vesicles

containing MMP-2 in the culture medium of glioma cell lines. The accumulation of MMP-2 in these structures revealed the presence of a second pool of intracellular MMP-2 protein, separated from the cytoplasmic MMP-2, which can help to explain the delayed changes observed in MMP-2 protein levels.

Considering the time-frame necessary to modulate MMP-2 protein levels, and in order to study MMP-2 contribution to Cltx-targeted SNALP internalization, we formulated a transfection protocol able to efficiently reduce MMP-2 protein and mRNA levels before SNALP transfection.

Comparison between MMP-2 fluctuations and Cltx-mediated SNALP uptake led us to confirm the existence of a direct relation between MMP-2 and the Cltx-targeting process. However, we observed that MMP-2, by itself, only accounted for a slight influence in SNALP internalization and we found that siRNA-mediated downregulation of TIMP-2, an inhibitor of MMP-2 activation, was able to induce a remarkable increase in SNALP uptake, which led us to conclude that MMP-2 is not the only intervenient in the internalization process.

Taken together, the results presented in this work contribute to clarify the role of PDGF in MMP-2 regulation and suggest the possibility that TIMP-2 may be involved in a regulatory feedback mechanism of the MMP-2 pathway, while simultaneously playing a role in Cltx-mediated particle uptake.

Introduction

1. INTRODUCTION

1.1 Glioblastoma

The primary tumors of Central Nervous System (CNS) include a wide range of pathological entities, each with specific and different neurological characteristics and development.

Glial tumors comprise about 40% of all CNS tumors [1] and according to the World health organization (WHO) can be divided into two macro-groups of gliomas: Low-Grade Gliomas (LGG) define as first and second grade tumors, which comprise non-anaplastic tumors and well circumscribed astrocytomas, usually benign line, most of the times removable by surgery, and High Grade Gliomas (HGG) represent grade III-IV in the WHO classification and they present as undifferentiated and anaplastic gliomas.

Glioblastoma multiforme (GBM), the most aggressive form of astrocytic tumors, displaying a rapid progression that is accompanied by particular poor prognosis of patients. Indeed, despite modern diagnostics and treatments, the median survival time, after diagnosis of this tumor, does not exceed 15 months [1].

Histo-pathological attributes of GBM include cellular polymorphism, high mitotic activity, vascular thrombosis and, as a basic diagnostic characteristic, this kind of tumor presents a predominant microvascular proliferation and necrosis. However the heterogeneity of the brain region where it first appears and the rapid invasive growth of GBM can provoke discrepancies in histological diagnosis [2].

Apart from these primary attribute, the low survival rate of GBM come from many other factors as brain regeneration incapability, resistance of tumor cells to conventional treatments and difficulty to find efficient therapies able to act across the blood brain barrier.

Common strategies, such as chemotherapy or radiotherapy, help to improve prognosis, increasing patient's survival. In fact, removal of 98% or more of the tumor has been associated with a significantly longer survival time, especially if the surgery is guided by a fluorescent dye [3,4]. However, it has been observed that, after surgical removal, tumors recur predominantly within 1 cm of the resection cavity. This is mainly due to the fact that at the time of surgery, cells from the bulk tumor have already invaded

normal brain tissue. Therefore one of the most important hallmarks of malignant gliomas is their invasive behavior.

1.1.1 Epidemiologic Features

Glioblastoma multiforme may present itself at any age, but typically affects adults, with increasing incidence until age 85. The median age at diagnosis is 64 years, with more than 80 % of diagnosed glioblastoma patients being older than 55 years and only 1 % younger than 20 years. Males are more commonly affected by glioblastoma multiforme, with an incidence rate almost 1.6 times higher than females. The glioma incidence is generally higher in the Western world compared to less developed countries [1]. The major reason is probably under-ascertainment of the glioma incidence in developing countries due to limited access to health care, variations in diagnostic practices, and incomplete reporting of glioma cases [3, 4]. However, some reports also indicate that ethnic differences in glioma susceptibility may exist. For example, in the United States glioblastoma multiforme is more frequent in Caucasians than in people of African and Asian descent. A 1-2 % annual increase in the total brain tumor incidence occurred through the 1980s and 1990s, which primarily is thought to reflect the improved clinical diagnosis of neurological diseases after introduction of high resolution neuroimaging in the early 1980es. However, a true rise in incidence for at least some types of brain tumors cannot be excluded, but such evidence is yet to be demonstrated for glioblastoma multiforme [3].

For the majority of gliomas no underlying carcinogenetic causes can be identified. So far, the only established environmental risk factor reported is exposure to high-dose, ionizing radiation [3, 5]. Several epidemiological studies have also demonstrated an association between increased glioma risk and other environmental factors, including severe head injury, dietary risk factors, occupational risk factors, and exposure to electromagnetic fields. However, the data regarding the suggested risk factors remain inconclusive, since other studies failed to identify any link between these risk factors and glioma development [3, 4, 6]. More consistent reports suggest a protective effect of allergic diseases and infections in GBM, indicating that immune surveillance mechanisms stimulated by these conditions can inhibit glioma development [3, 5].

Genetic predisposition has been observed in 5-10 % of glioma cases [4]. Rare genetic syndromes associated with an increased risk of glioma, such as neurofibromatosis 1 and

2, tuberous sclerosis, retinoblastoma (RB) 1, Li-Fraumeni syndrome, Turcot's syndrome, and multiple hamartoma only account for few cases. Gliomas have also been observed to run in families, not affected by the listed syndromes, but implicated susceptibility genes remain have not been identified yet. In addition, the causal relationship between glioma and common polymorphisms in genes involved in detoxification of carcinogens, cell cycle regulation, and DNA repair mechanisms have been investigated only to reveal vague or no association [4, 5].

1.1.2 Histological Features

Glioblastoma multiforme lesions are typical large at the time of diagnosis and may occupy much of a brain lobe. The lesions are often located in the sub cortical white matter of the cerebral hemispheres and frequently extend across the border of the frontal lobe into the temporal lobe. Tumor infiltration often progresses into the adjacent cortex and through the corpus callosum into the contra-lateral hemisphere [7].
The tumor mass of glioblastoma multiforme is characterized by being poorly delineated and having a high degree of regional heterogeneity. Highly proliferating cancer cells are usually found in the peripheral, hypercellular zone of the tumor, whereas the central tumor area consists mainly of necrotic tissue, comprising up to 80 % of the total tumor mass. Histopathologically, the lesions typically exhibit cellular hyperplasia in peripheral zones harboring cancer cells with atypical nuclei, increased mitotic activity, cellular pleomorphism and poor differentiation. A diagnostic feature of glioblastoma multiforme is the presence of areas with vascular hyperplasia, necrosis or both in the tumor tissue. Another hallmark of glioblastoma multiforme is rapid invasion of the surrounding brain tissue, especially along myelinated brain structures such as the corpus callosum or within perivascular spaces. Infiltrating tumor cells are dispersed within the normal brain tissue surrounding the contrast-enhancing tumor border at high-resolution scans. These satellite cancer cells are thought to be the origin of local tumor recurrence after therapy, since the infiltrating cells escape surgical resection and high-dose radiotherapy of the primary tumor mass. Despite the highly infiltrative nature of glioblastoma multiforme, it tends to invade neither the subarachnoidal space nor the vessel lumen and, therefore distant metastasis are rarely found, both within and outside the CNS [7].
Glioblastoma multiforme lesions most commonly occur as primary glioblastoma without clinical evidence of a preceding lesion within the CNS [8]. Only about 5 % of glioblastoma

multiforme cases progress from lower grade astrocytomas into secondary glioblastoma [8].The time to progression is highly variable, with time intervals ranging from less than 1 to more than 5 years before occurrence of glioblastoma multiforme. Primary lesions typically affect older patients with a mean age of 62 years at diagnosis, whereas secondary glioblastoma in contrast develop in younger patients with a mean age of 45 [9].

1.2 Genetic Characterization of Glioblastoma

Phenotypically, primary and secondary glioblastoma are indistinguishable. However, the two glioblastoma multiforme subtypes display distinct genetic abnormalities, suggesting that their malignant transformation occurs through different genetic pathways. Primary glioblastoma in adults is associated with epidermal growth factor receptor (EGFR) overexpression and mutation, loss of heterozygosity (LOH) of chromosome 10q, mutation of the phosphatase and tensin homology (PTEN) gene, and deletion of the p16 gene.

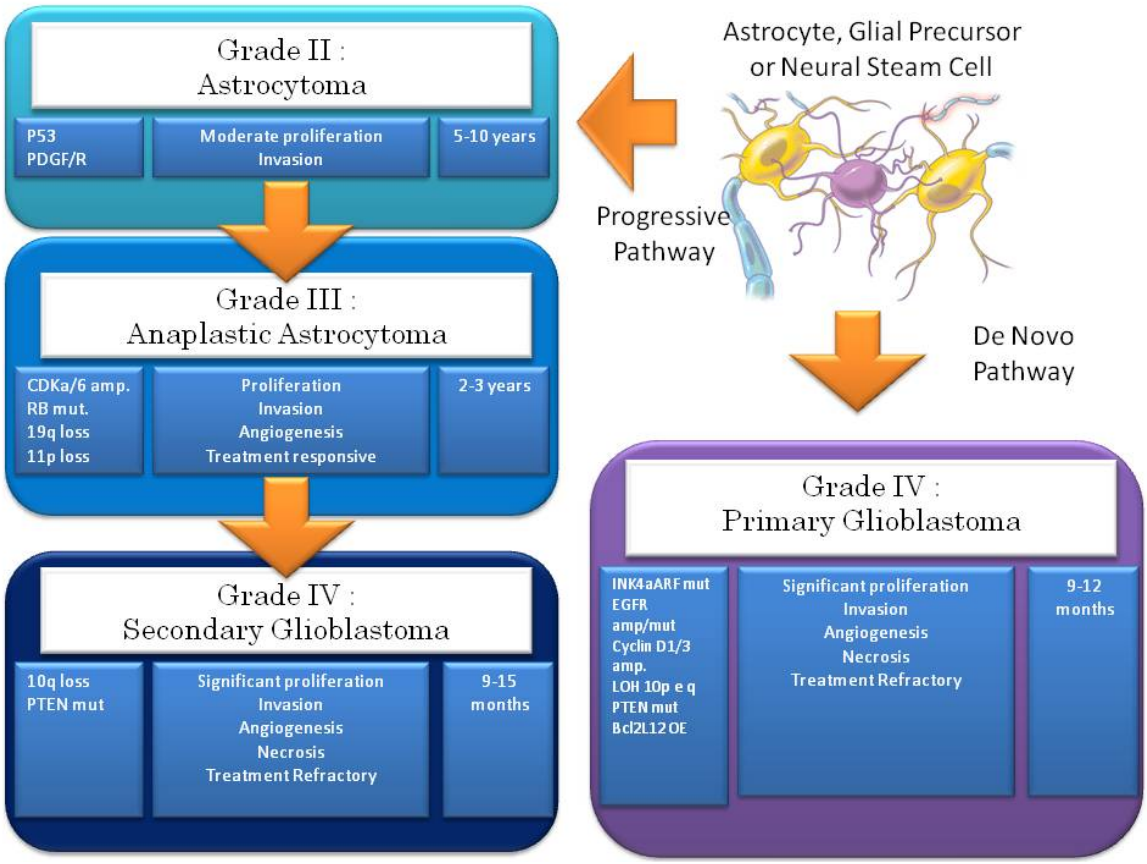

Figure 1. Astrocytic tumor progression, genetic and histological attributes

In contrast, mutations in the p53 gene, LOH of chromosome 10q, and abnormalities in the pathway regulating the tumor suppressor RB are frequently found in secondary glioblastoma multiforme. Overall, these genetic alterations in both primary and secondary glioblastoma multiforme result in overactivation of several mitogenic signaling pathways that ultimately leads to uncontrollable growth of the affected cells [8, 10].

Frequent mutations of cell cycle regulatory genes in glioma have underscored the importance of these genes in cellular proliferation and senescence. The RB and p53 pathways, which regulate cell cycle progression primarily by governing the G1-to-S-phase transition, are major targets of inactivating mutations in GBM. The absence of these cell cycle guardians renders tumors particularly susceptible to inappropriate cell division driven by constitutively active mitogenic signaling effectors, such as phosphoinositide 3-kinase (PI3K) and mitogen-activated protein kinase (MAPK). Relevant genetic targets and inherent pathways involved in primary and secondary GBM evolution will be further explored below.

The Rb pathway. In quiescent cells, hypophosphorylated RB blocks proliferation by binding and sequestering the E2F family of transcription factors, which prevents the transactivation of genes essential for progression through the cell cycle [11].

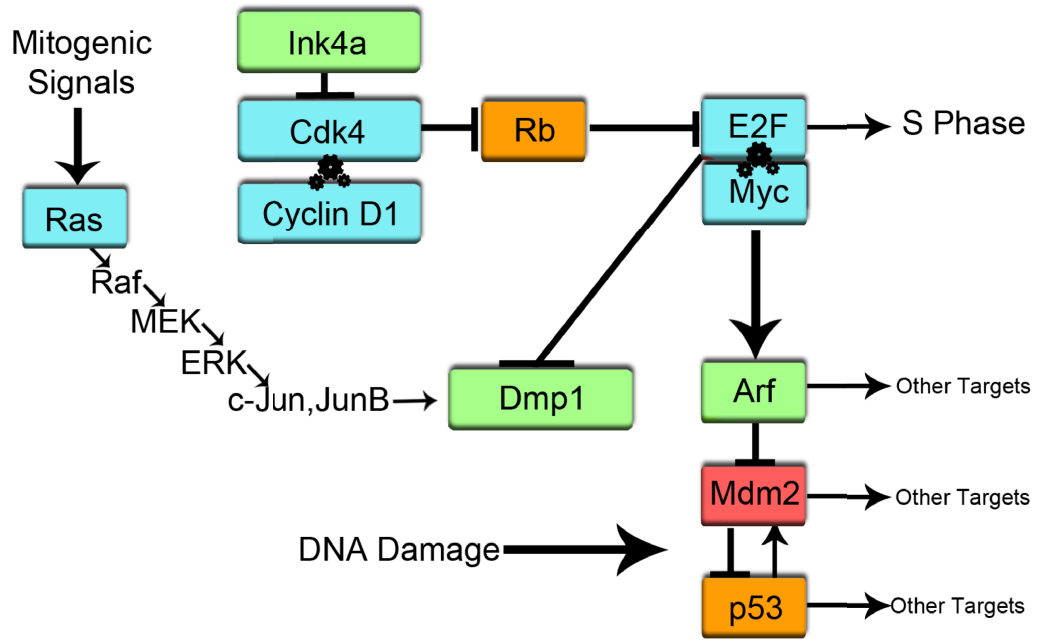

Figure 2. Schematic reproduction of Rb and p53 pathways

Upon mitogenic stimulation, the activation of the MAPK cascade leads to the induction of cyclin D1 and its association with the cyclin-dependent kinases CDK4 and CDK6, as well as the degradation of the CDK2/cyclin E inhibitor, p27Kip1 [12]. These activated CDK complexes in turn phosphorylate RB, enabling E2F transactivation of its direct transcriptional targets which govern S-phase entry and progression [13].

Gliomas circumvent RB-mediated cell cycle inhibition through several possible genetic alterations. The *Rb1* gene, which maps to chromosome 13q14, is mutated in 25% of high-grade astrocytomas and the loss of 13q typifies the transition from low- to intermediate-grade gliomas [14]. Moreover, amplification of the *CDK4* gene on chromosome 12q13-14 accounts for the functional inactivation of RB in 15% high-grade gliomas. *CDK6* can also be found to be amplified but at a lower frequency [15]. RB activity is also frequently lost through the inactivation of a critical negative regulator of both *CDK4* and *CDK6*, $p16^{Ink4a}$ [16]. This gene is one of two transcripts generated at the *CDKN2A* locus on chromosome 9p21 (in addition to $p14^{ARF}$) and is predominantly inactivated by allelic loss or hypermethylation in 50%–70% of high-grade gliomas and 90% of cultured glioma cell lines [17]. Consistent with its role as an important glioma tumor suppressor, $p16^{Ink4a}$ is also a critical inhibitor of progenitor cell renewal in the subventricular zone of aging mice [18]. The importance of the inactivation of the RB pathway in glioma progression is evidenced by the near-universal and mutually exclusive alteration of RB pathway effectors and inhibitors in both primary and secondary GBM [19]. However, numerous in vitro and in vivo assays have demonstrated that the neutralization of this pathway alone is insufficient to abrogate cell cycle control to the extent needed for cellular transformation, suggesting that other important cell cycle regulation pathways complement the activity of RB pathways preventing gliomagenesis [20].

The p53 pathway. The p53 tumor suppressor prevents the propagation of cells with unstable genomes, predominantly by halting the cell cycle at the G1 phase or instigating a program of apoptosis or proliferative arrest [21]. Upon being post-translationally modified by various genotoxic and cytotoxic stress-sensing agents, p53 is stabilized, binding and transcriptionally regulating the promoters of more than 2500 potential effector genes [22]. The best characterized of these effectors is the transcriptional target *CDNK1A,* which encodes the CDK2 inhibitor p21 [23]. Although this gene has not been found to be genomically altered in gliomas, its expression is frequently abrogated by p53

functional inactivity, as well as by mitogenic signaling through the PI3K and MAPK pathways.

The p53 pathway is nearly invariably altered in sporadic gliomas: loss of p53, through either point mutations that prevent DNA binding or loss of chromosome 17p, is a frequent and early event in the pathological progression of secondary GBM [24].

The second protein encoded by *CDKN2A,* $p14^{ARF}$, was also been shown to be an important accessory to p53 activation, under conditions of oncogenic stress, due to its neutralization of the p53 ubiquitin ligase, MDM2 [25]. The MDM2 gene was originally discovered to be amplified in a spontaneously transformed murine cell line, and to be a key negative regulator of p53 during normal development and in tumorigenesis. Concordantly, the chromosomal region containing *MDM2,* 12q14-15, is amplified in 10% of primary GBM, the majority of which contain intact p53. The discovery of the *MDM2*-related gene, *MDM4* (chromosome1q32), which inhibits p53 transcription and enhances the ubiquitin ligase activity of MDM2, prompted the finding that the p53 pathway is also inactivated by the amplification of MDM4 in 4% of GBM with neither TP53 mutation nor *MDM2* amplification [26]. Additionally, the recently discovered tumor suppressor gene *CHD5* (chromodomain helicase DNA-binding domain 5), which maps to chromosome1p36 and is frequently hemizygously deleted in human gliomas that have 1p loss, has been shown to maintain p53 levels by facilitating expression ofp19Arf (mouse $p14^{Arf}$ ortholog), and thus represents an additional mechanism for inactivation of this critical pathway [27].

Mitogenic signaling pathways. Many mitogens and their specific membrane receptors are present in over active form in gliomas. Proliferation of normal cells requires activation of mitogenic signaling pathways through diffusible growth factor binding, cell–cell adhesion, and/or contact with extracellular matrix (ECM) components. These signals are transduced intracellularly by transmembrane receptors that typically activate the PI3K and MAPK signaling pathways.

In contrast, tumor cells acquire genomic alterations that greatly reduce their dependence on exogenous growth stimulation, enabling inappropriate cell division, survival, and motility through the constitutive activation of these pathways. While gliomas overcome the normal impositions on the control of mitogenic signaling through multiple mechanisms, activation of receptor tyrosine kinases (RTKs), discussed in detail below, appears to be the predominant mechanism.

MAPK proliferation signals can be transduced through the MAPK pathway by both integrins and RTKs. Integrins are membrane-bound ECM receptors that mediate the interaction between the ECM and the cytoskeleton. Upon adhesion to ECM, integrins bind cytoplasmic anchor proteins that coordinate the binding of integrins to actin filaments, thus creating a focal adhesion complex. Multiple molecules of focal adhesion kinase (FAK) cluster at these complexes and become activated by cross-phosphorilation, activating a signal transduction cascade that leads to extracellular signal regulated kinase (ERK) phosphorilation either through activation of Ras, or through Src-dependent phosphorilation of p130Cas [28]. Ras-GTP in turn phosphorylates Raf kinase, which phosphorylates MEK, which phosphorylates ERK, which enters the nucleus and phosphorilate nuclear transcription factors that induce the expression of genes promoting cell cycle progression, such as cyclin D1. RTKs activate the MAPK pathway when activated by growth factor signaling, mutation, or overexpression. As discussed in

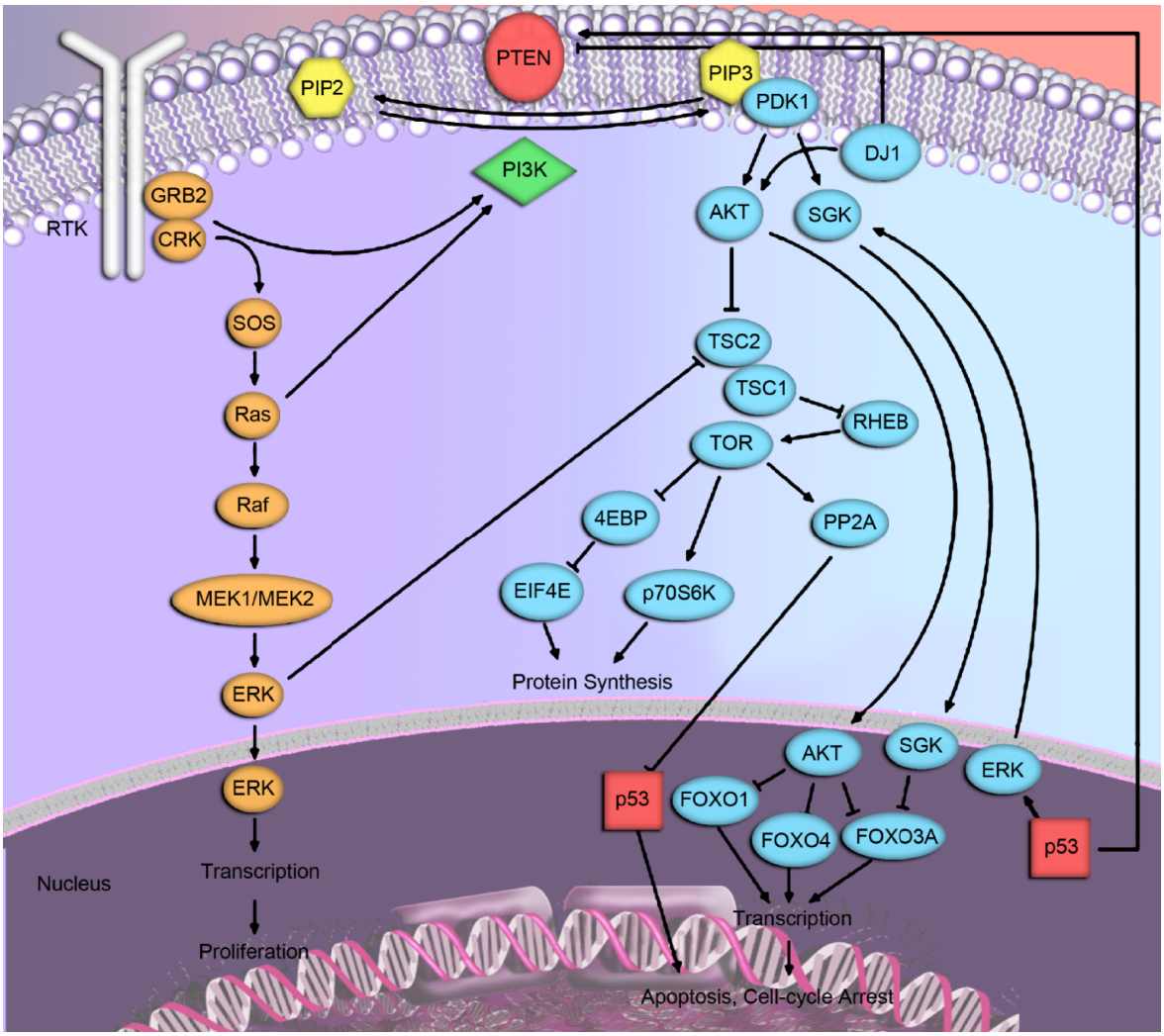

Figure 3. Schematic reproduction of the pathways associated to RTK stimulations.

more detail below, RTK activation results in receptor dimerization and cross-phosphorylation, creating binding sites for adaptor protein complexes such as Grb2/SOS, which in turn activates Ras. While constitutively activated, mutated forms of Ras are found in 50% of all human tumors, few Ras mutations have been found in gliomas. Despite this, high levels of active Ras-GTP are found in advanced astrocytomas [29], suggesting that a more relevant mechanism for MAPK-dependent mitogenic signaling in GBM may be related to inappropriate activation of RTKs and/or integrins.

PI3K/PTEN/AKT. The class I PI3Ks catalyze the mitogen-stimulated phosphorylation of phosphatidylinositol 4,5-bisphosphate (PIP2) to produce phosphatidylinositol 3,4,5-triphosphate (PIP3). This creates docking sites for a multitude of signaling proteins containing domains capable of binding either to PIP3 itself or to the 5-dephosphorylated product, PIP2. The class I-A PI3Ks are heterodimers that are recruited to activated RTKs and adaptor proteins via their regulatory subunit (of which there are five know isoforms, encoded by three genes: p85α, p55 α, and p50α (PIK3R1); p85β (PIKR2); and p55γ (PIKR3)).

Since the regulatory subunits appear, thus far, to be functionally equivalent, the class I-A PI3Ks are currently defined by the catalytic isoform present: p110α, p110β, and p110δ, encoded by the PIK3CA, PIK3CB, and PIK3CD genes, respectively [30]. Evidence for the importance of p110α in cell transformation derives from the discovery of a vir-PIK3CA oncogene in avian sarcoma virus with potent transforming activity in chicken embryo fibroblasts (CEFs) [31]. PIK3CA gain-of-function point mutants have been detected in a variety of cancers, including malignant gliomas such as GBM, in which the frequency of mutation has been cited in some studies to be as high as 15% [32].

The action of class I PI3K enzymes is directly antagonized by the PIP3-phosphatase encoded by the PTEN gene located at 10q23.3 [33]. PTEN is a major tumor suppressor that is inactivated in 50% of high grade gliomas by mutations or epigenetic mechanisms, each resulting in uncontrolled PI3K signaling in these tumors [34]. In mouse models, brain-specific inactivation of PTEN caused overgrowth of the mouse brain and aberrant proliferation of astrocytes both *in vivo* and *in vitro*. An elegant mouse model of astrocytoma has been developed in which the Rb family proteins are inactivated by GFAP-directed expression of SV40 T antigen [35, 36]. In this model system, PTEN inactivation was associated with increased angiogenesis, in a close parallel with the observed progression of high-grade disease in humans when loss of PTEN [37].

While regulation of PI3K signaling is critical to controlling cell growth and survival, a number of recent studies have pointed additional mechanism by which PTEN may act to suppress transformation and tumor progression.

Of the many signaling proteins that are recruited to the membrane and activated by binding to PIP3, the phosphoinositide-dependent kinase (PDK1) and Akt/PKB (also the cellular homolog of a viral oncoprotein), have to been shown to be required for tumorigenesis in $PTEN^{+/-}$mice and for growth of $PTEN^{-/-}$embryonic stem (ES) cells as tumors in nude mice [21]. In response to PI3K activation, PDK1 and the mammalian target of rapamycin (mTOR, acting in the rapamycin-insensitive TORC2 complex) activate Akt via phosphorylation of two key residues, T308 and S473, respectively. Assessment of the phosphorylation status of these residues is often the method of choice for monitoring PI3K pathway activity in cell lines and primary tumors, including GBM samples, 85% of which have been reported to display activated Akt [38, 39].

PI3K–MAPK–p53–RB pathway interactions. While the PI3K, MAPK, p53, and RB pathways are often considered as distinct entities, there is significant cross-talk among the pathways that serve to reinforce the inappropriate regulation of any single pathway perturbation. For example, because p53 enhances *PTEN* transcription and represses the expression of p110α [40], the loss of p53 in cells with constitutively active RTK signaling can further potentiate PI3K pathway activation. Therapies aimed at reactivating p53 in GBM may be compromised by MAPK and PI3K intervention in the activity of p53 and its effectors. MAPK signaling activates c-myc, which binds the miz-1 transcriptional repressor to block *p21* gene induction [41], while Akt impacts on p53 function by phosphorylation of Mdm2 [42] in addition to the direct inhibition of p21 discussed earlier. Moreover, these pathways can negate each other: p53 can inhibit activated FOXOs by inducing the expression of the kinase SGK1, which phosphorylates and exports FOXOs from the nucleus. Conversely, FOXOs can inhibit p53 transcriptional activity by increasing its association with nuclear export receptors that translocate P53 back to the cytoplasm [43]. The recent finding that Sprouty2, a gene involved in suppression of Ras signaling during oncogene-induced senescence, is also a direct transcriptional target of FOXO emphasizes the complexity of cross-talk that exists between the Ras/MAPK and PI3K pathways [44]. The complicated interplay among these critical molecules highlights the need for detailed dissection of the pathways that

are aberrant in each tumor to accurately guide the choice of combination therapies that can simultaneously target multiple pathways.

RTKs. Gliomas may activate receptor-driven pathways by different mechanisms: overexpression of both ligands and receptors leading to an autocrine loop, genomic amplification, and/or mutation of the receptor leading to constitutive activation in the absence of ligand. The EGF and platelet-derived growth factor (PDGF) pathways play important roles in both CNS development and gliomagenesis, as described in the following section, and targeted therapy against these potentially critical signaling pathways is currently under vigorous basic and clinical investigation.

1.3 Platelet-derived growth factor (PDGF)

1.3.1 The PDGF family

Platelet-derived growth factor is a family of dimeric disulfide-bonded polypeptide chains, with growth stimulatory action primarily on connective tissue cells [45]. The family consists of homo- and heterodimers of the two classical PDGF A- and B-chains (PDGF-AA, -BB, and -AB), as well as homodimers of the recently identified family members PDGF-C and -D (PDGF-CC and -DD) [46]. The A- and B-chains of PDGF contain, in addition to the mature ≈100-amino acid sequence, an N-terminal propeptide and a signal peptide that is removed in the Golgi apparatus following formation of the disulfide-bonded dimer in the endoplasmic reticulum. The B-chain is also processed in the carboxy-terminus. Furthermore, PDGF-B and the long splice variant of PDGF-A contain a C-terminal retention sequence, which can mediate interaction with components of the extracellular matrix [47-50]. The mature forms of PDGF-A and PDGF-B contain eight conserved cysteine residues, with the second and fourth being involved in interchain disulfide bonds and the other six in disulfide bonds within the chain [49]. The solution structure of mature PDGF-BB showed an anti-parallel arrangement of the two subunits, where each subunit contains a tight cystine knot and three protruding loops (84). Two loops extend in one direction (loop 1 and 3) and the other in the opposite direction (loop 2). Thus, the anti-parallel subunit arrangement will bring loop 2 of one subunit in proximity of loop 1 and 3 of the other subunit. The most important amino acids involved

in receptor binding have been mapped to loop 1 and 3, with some contribution of loop 2 through diverted mutagenesis [48]. Hence, both chains in the dimeric ligand will contribute to each of the two receptor binding epitopes. Interestingly, PDGF shows structural similarity to the closely related vascular endothelial growth factor (VEGF) [51] as well as to the more distantly related nerve growth factor (NGF) and transforming growth factor-ß (TGF-ß) molecules [52].

The different PDGF isoforms exert their biological effects by binding to two structurally related tyrosine kinase receptors, the PDGF α- and ß-receptors. The PDGF receptors are composed of five extracellular immunoglobulin-like domains, a transmembrane part, and an intracellular part with a split tyrosine kinase domain. The three N-terminal immunoglobulin domains mediate ligand binding, whereas the fourth immunoglobulin domain is involved in receptor dimerization [53]. Based on kinase domain sequence similarity, the split tyrosine kinase domain, and the presence of 5 extracellular Ig domains, PDGF receptors as classified as belonging to the class III of receptor tyrosine kinases, alongside with the stem cell factor receptor c-Kit, the colony stimulating factor (CSF-1) receptor, and Flt3 [54]. Homodimeric PDGF α-receptor complexes are formed after stimulation with PDGF-AA, -AB, -BB, whereas PDGF ß-receptor homodimers are formed after stimulation with PDGF-BB. Furthermore, PDGF-AB and -BB can induce formation of αß-receptor heterodimers and stimulation of cells expressing α- and ß-receptors with PDGF-CC or -DD results in activation of both receptor types [55].

1.3.2 Signaling of PDGF receptors

Dimerization is a general mechanism for the activation of cell surface receptors, including the PDGF receptors [46]. Ligand binding to PDGF receptors leads to formation of a dimeric receptor complex, where each receptor in the complex is believed to phosphorylate the other [56]. Autophosphorylation of a critical regulatory tyrosine within the kinase domain, Tyr849 and Tyr857 in the α- and ß-receptor, respectively, leads to up-regulation of the intrinsic tyrosine kinase activity [57]. Dimerization of PDGF receptors has also been shown to protect the receptors from dephosphorylation by tyrosine phosphatases [58]. Autophosphorylation of the regulatory tyrosine is followed by phosphorylation of tyrosine residues located outside of the kinase domain, which creates docking sites for signal transduction molecules containing phosphotyrosine recognition

motifs, such as the Src Homology 2 (SH2) and phosphotyrosine binding (PTB) domains. The PDGF α- and ß-receptors contain at least 8 and 11 autophosphorylation sites, respectively, and a large number of SH2 domain containing proteins are known to bind to specific phosphotyrosine residues in the activated PDGF receptors . The SH2 domain is a conserved ≈100 amino acid motif that binds to phosphorylated tyrosine residues located within a defined amino acid sequence. The SH2 domain-containing signal transduction molecules fall into three functional categories; those with intrinsic enzymatic activity, such as SHP-2, Src, PLC-γ, and RasGAP, adaptor proteins such as Grb2, Crk, Shc, Nck, and the p85 regulatory subunit of PI3-K, and transcription factors such as STAT proteins. Each SH2 domain-containing protein that binds to the PDGF receptors may potentially initiate a signal transduction pathway [46].

1.3.3 PDGF in malignant disease

The first indications that PDGF can be involved in tumorigenesis came with the discovery of homology between the simian sarcoma viral oncogene v-*Sis* and PDGF-B [59, 60]. The transforming activity of the Sis gene product occurs by autocrine stimulation of PDGF receptors. Moreover, PDGF-A was shown to be able to transform cells expressing the PDGF α-receptor [59]. Malignant cells in various human tumors have been shown to co-express PDGF ligands and receptors, which is a prerequisite for autocrine growth promotion by PDGF [46]. In human glioma, PDGF α-receptor and PDGF A-chain expressing tumor cells occur with increasing frequency in high grade as compared to low grade tumors. In particular, PDGF α-receptor expression was observed in tumors that did not overexpress the EGF receptor. Furthermore, some cases of glioblastoma multiforme show an amplified PDGF α-receptor gene, with subsequent receptor overexpression [61]. Recently, expression of PDGF-C and PDGF-D was demonstrated in human glioma cells [62]. Expression of dominant-negative PDGF or PDGF ß-receptor mutants could inhibit growth of glioma cell lines with autocrine PDGF A-chain/PDGF α-receptor loop [63]. Moreover, therapy of PDGF-A/PDGF α-receptor expressing human glioblastoma xenografts with the PDGF antagonist STI571 induced proliferative arrest and subsequent reduction of tumor growth [64]. In summary, PDGF ligand and receptor co-expression has been demonstrated in several different malignant diseases. Furthermore, inhibition of PDGF signaling has been shown to block the growth of experimental glioblastomas. Taken together, these findings provide a rationale for

clinical trials with PDGF antagonists in diseases with putative activation of the PDGF system.

1.4 Matrix Metalloproteinases 2 (MMP-2)

1.1.1 The MMP Family

A key requirement for cells to reach distant target sites is the ability to traverse the protein fibers of the extracellular matrix (ECM) which are present in all tissue types [65]. Basement membranes represent a specialized form of the ECM that separate epithelium or endothelium from stroma by a dense layer of ECM. To overcome these matrix barriers, migrating cells require specific proteolytic enzymes. In addition to serine- and cysteine-proteinases, the matrix metalloproteinases (MMPs) in particular are capable of degrading ECM components. Consequently, MMPs have been found to be involved in various physiologic and pathologic processes [66].

In addition to having the ability to degrade the ECM, MMPs have a number of other organo-mercurial compounds and inhibited by tissue inhibitors of metalloproteinases (TIMPs). Finally, these enzymes are calcium-dependent, which is important for their inhibition [67].

Until now, at least 24 zinc-dipendent metalloproteinases were found and classified as a subgroup in the matrixin family.

The MMPs family can be divided, according to the activity of its components in: Collagenases (MMP-1, -8, -13, -18) have the ability to cleave interstitial collagens I,II and III at specific sites close to the N-terminus and can digest other ECM and non-ECM molecular components [68]; Stromelysins 1 and 2, MMP-3 and -10 respectively, which in addiction degrade ECM are able to activate other MMPs, and Matrilysins 1 and 2 (MMP-7 and -26), which process cell surface molecules as pro-α-defenin, Fas-ligand, pro-TNF-α and E-cadherins and also digest a number of ECM components [69]. A fourth group is constituted by Membrane-Type MMPs (MT-MMP) which are six metalloproteinases that present a transmembrane segment and an intracellular codon in the N-Terminal part of the molecule. This group is constituted by MMP-14, -15, -16 and -24, known as Membrane-Type -1 to -4 MMP and, in addition, MMP-17 and -25, that are Glicosyl-phosphatidyl-inositol (GPI) anchored proteins.

With exception of MT4-MMP they are all capable of activating and MT1-MMP also presents a colagenolytic activity on type I, II and III [70].

The fifth and last classed group of MMPs, which has and high relevance for this work, represents Gelatinase A (MMP-2) and B (MMP-9). These proteins readily digest denatured collagens and gelatins and present three repeats of a type II fibronectin domain inserted in the catalytic domain, which bind to gelatin, collagens, and laminin [71]. Moreover MMP-2, but not MMP-9, digests type I, II, and III collagens [72, 73].

1.4.2 General Structural Features of MMP-2

MMP-2 is characterized by the typical structure of the MMP family, presenting a 660 amino acid sequence which is secreted as zymogen.

The pro-peptide sequence of pro-MMP-2 forms a globular domain characterized by the presence of hydrophobic interactions and hydrogen bonds. The "Cysteine Switch" motif (PRCGXPD) is a characteristic structure found in pro-domains of all the MMPs. The SH group of the cysteine present in this motif interacts with the zinc ion present in the catalytic domain conferring to the pro-domain the ability to inactivate the protein [74].

The central core of this protein is composed by three fibronectine type II domain and the catalytic domain. The fibronectine-like repeats are inserted in the fifth ß-strand and in the helix 2. The catalytic domain consist of two antiparallel ß-sheets connected with a short α-helix and stabilized by two disulfide bond [75], forming a hydrophobic pocket accessible from the outside. This pocket is a structural hallmark of this domain and allows substrate binding. The architecture of the catalytic domain is known as matrixin fold [76] and consists of a five-stranded ß-sheet and three α-helices. A peculiar characteristic of this segment is the presence of the zinc binding motif

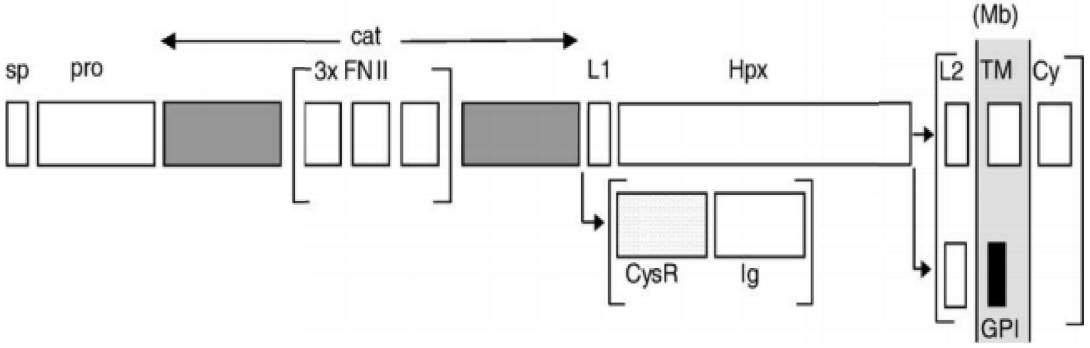

Figure 4. Domain structures of the MMP family. **sp**: signal sequence, **pro:** pro-domain, **cat:** catalytic domain, **FNII:** fibronectin type II motif, **L1:** linker 1, **Hpx:** Hemopexin-like domain, **L2:** linger 2, **Mb:** plasma membrane, **TM:** transmembrane domain, **Cy:** cytoplasmatic domain, **CysR:** cysteine rich domain, **Ig:** Immunoglobulin domain, **GPI:** glycosylphosohatidilinositol anchor.

(HEXXHXXGXXH) which is involved, as previously described, in the inactivation of the protein [74]. This structure is highly conserved in MMPs and is unaffected by the insertion of the fibronectin domains.

The last segment of the protein is the Hemopexine-like domain, lined with the catalytic domain by a hinge peptide. It was shown trough changes in this peptide in other MMPs, that probably helps to determine substrate specificity [76]. The Memopexine-like domain shows a four-propeller fold [77, 78], in which the first and second propeller blades are oriented toward the catalytic domain and are linked to the first fibronectin-like domain by a hydrogen bound, turning blades 3 and 4 away from the catalytic domain. These two last blades constitute the binding site of the tissue inhibitor of matrix metalloproteinases-2 (TIMP-2) and they may contribute to the formation of a groove that may be involved in substrate binding [74].

1.4.3 Structure of TIMP-2 and MT1-MMP

TIMP-2 polypeptide chain can be fully traced in the electron density to an extent of 180 of the total 194 residues. Only the last 14 residues, which represent the acidic tail of the

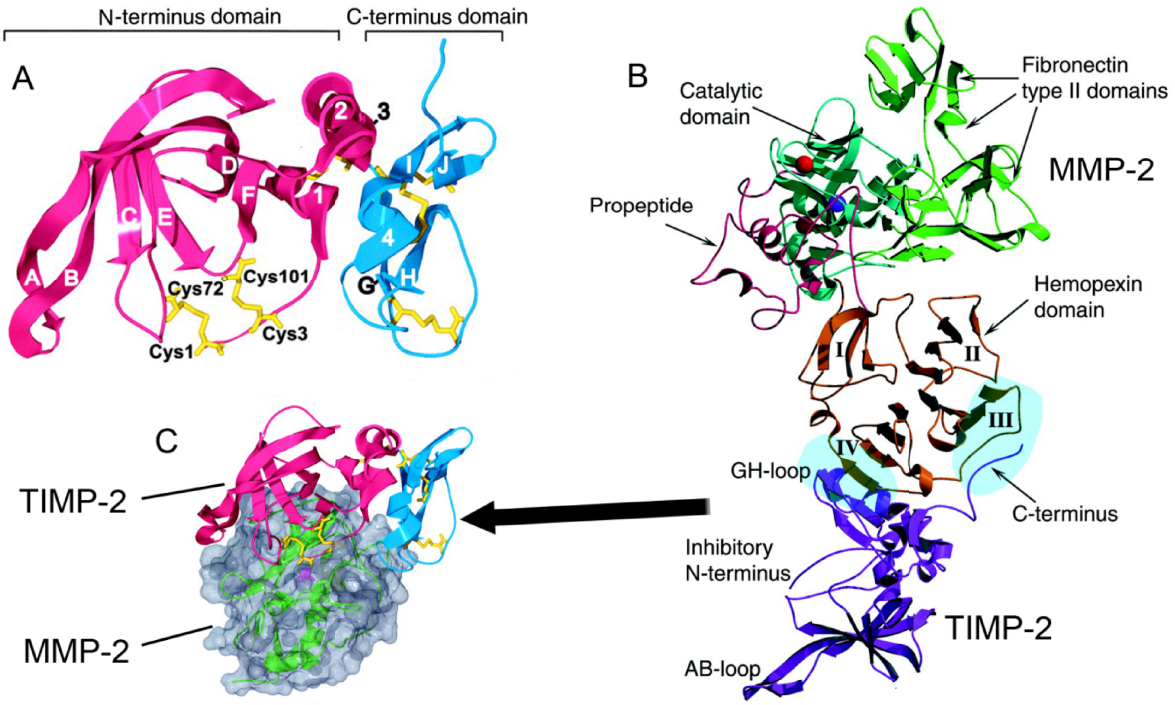

Figure 5. Structural insight into the complex formation of MMP-2 with TIMP-2. A. Tree dimensional structure of TIMP-2. **B.** of the proMMP-2/TIMP-2 complex. Overall conformation: the proteinase and inhibitor interact via their C-terminal domains. The catalytic site of MMP-2 and the inhibitory active site of TIMP-2 are turned away from each other. This topology excludes an inhibitory interaction between the proteinase and inhibitor and implies that both proteins remain fully functional in the complex. Catalytic and structural Zn2+ ions are colored red and Ca2+ ion purple. The ß-propeller blades of the hemopexin domain are numbered from I to IV. Two light blue ellipsoids in blades III and IV indicate two areas of interaction between proMMP-2 and TIMP-2 molecules. **C.** Different perspective of the MMP-2/TIMP-2 complex

protein are not visible and, thus, presumably flexible [77]. The overall shape of this protein can be described as a wedge, composed by a large N-terminal, consisting of a closed five-stranded ß-barrel, which are able to bind to the central core of MMP-2 or MT1-MMP, producing the inactivation effect, and a C-terminal (~60 aa), which forms ß-turn structure [79].

The N-terminal part resembles the so-called OB-fold, already described in a number of oligosaccharide/oligonucleotide-binding proteins and forms the edge that interacts with the catalytic domain of MMP-2 or MT1-MMP. Five residues in this terminal section bind to the active-site cleft of MMP-2 or MT1-MMP in a quasi-substrate-like manner, with Cys1 packed directly above the catalytic zinc ion of the metalloproteinases and the following amino acids inserted in the hydrophobic pocket of the catalytic domain, forming intermolecular hydrogen bonds similar to those formed by the substrate [80].

While the N-terminal part is in intimate contact with the active site of the target MMP,

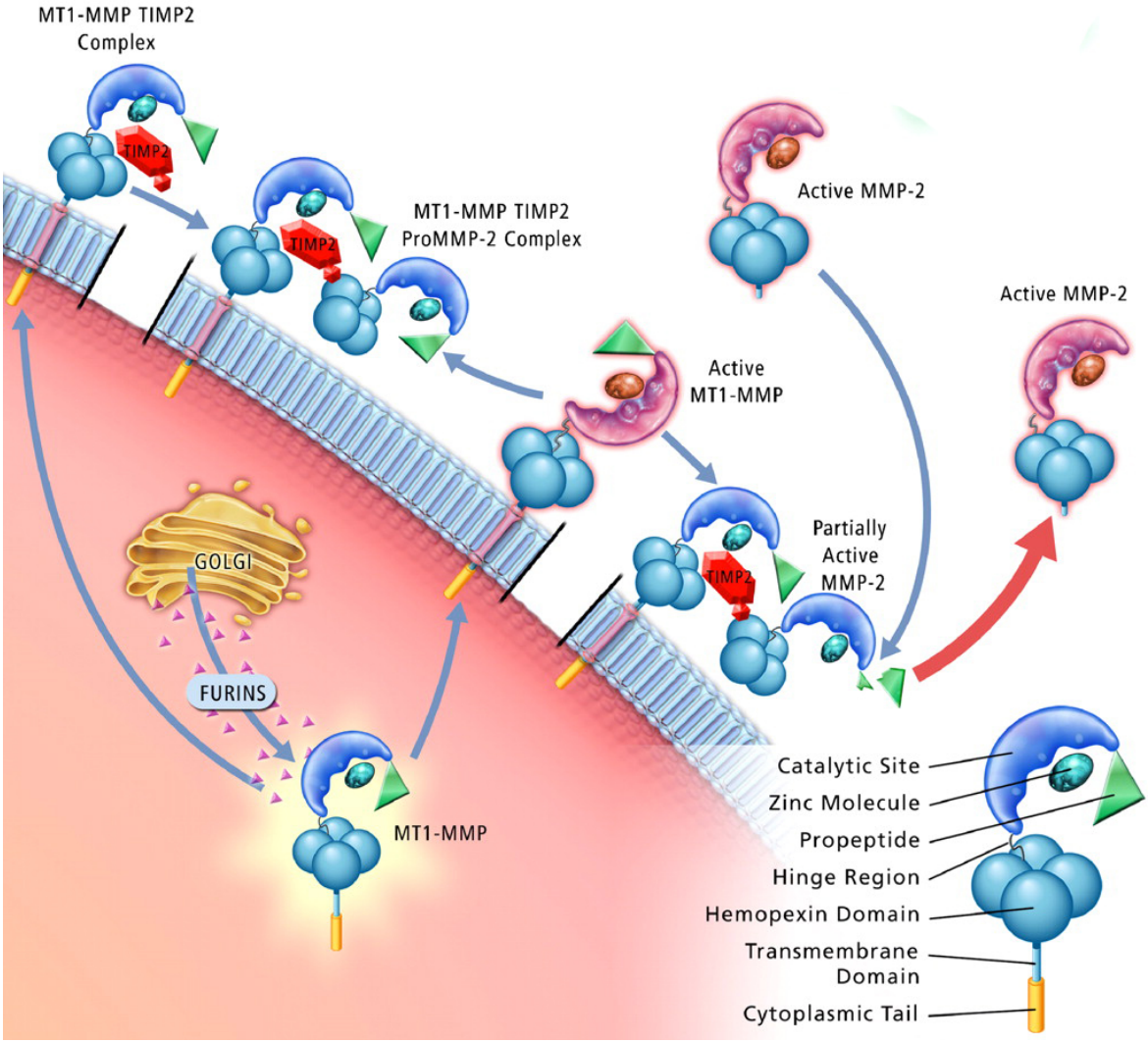

Figure 6. Schematic rapresentation of the MMP-2 activation mechanism.

the C-terminal part seems to have only minor impact on the tightness of the interaction with the MMP. However, it is critical to other functions, such as binding of TIMP-2 to pro-MMP, which is an essential step in the activation process of pro-MMP-2, and inhibition of angiogenesis [79]. In fact it was shown that the negatively charged C-Terminal tail of TIMP-2 has the ability to establish electrostatic interaction with the positively charged residues on blades 3 and 4 of the MMP-2 Hemopexin-like domain, especially with three particular Lys residues (Lys566-568).

Of all the MT-MMPs, MT1-MMP is the one studied in more detail. This protein follows the general structure of the MMP family resembling a notched spherical molecule. Interestingly, MT1-MMP lacks a fibronectin-like domain and presents a transmembrane domain. This protein has 8 additional residues between ß-strands II and III that constitute a central element for MMP-2 activation [81]. The cytoplasmic tail of this protein seems to play an important role during protein trafficking to the membrane surface In fact, fine mapping of this segment has shown a particular interaction between a Leu-Leu-Tyr motif and the μ2 subunit of AP-2, a component of clathrin-coated vesicles involved in the internalization of the complex.

1.4.4 Activation Mechanism of MMP-2

The timely degradation of extracellular matrix is an important feature of development, morphogenesis, tissue repair and remodeling. This event is precisely regulated under normal physiological conditions, and its deregulation is related with several disease, such as arthritis, nephritis chronic ulcers, fibrosis, and cancer where uncontrolled ECM remodeling is one of the main causes of cancer cell mobility.

MMP-2 is produced as a latent pro-form of 72 kDa that is cleaved in a intermediary form of 64 kDa and finally activated as a 62 kDa protease.

The activation of MMP-2, involved in ECM remodeling, is the result of a fine regulated construction of a activation complex. Studies involving the extraction of this complex have shown that it is composed by MT1-MMP, TIMP-2 and Integrin αvß3 which participate in the formation of a MMP-2 receptor [82].

As mentioned previously, the TIMP-2 N-Terminal domain has the ability to insert in the catalytic domain of the MMPs. Therefore an increasing ion the amount of this inhibitor protein on the cell surface leads to the inhibition of the MT1-MMP autoinactivation ability, contributing to increase of the active form of MT1-MMP [83].

Formation of the MT1-MMP•TIMP-2 complex allows on a hand, that the inhibitory ability of TIMP-2 remains focused only on MT1-MMP, and on the other hand that the C-Terminal domain remains free [84]. This domain is characterized by a negatively charged surface, which is able to bind the positively charged hemopexine-like domain of MMP-2, originating MT1-MMP•TIMP-2•MMP-2 complex.

The cleavage the pro-peptide of MMP-2 requires another active MT1-MMP free from the influence of TIMP-2 in the vicinity of the ternary complex, so that the pro-peptide of MMP-2 can be cleaved and the metalloprotease transforms into the 64 kDa latent form.

As latent protein, MMP-2 shows a trans-autoproteolytic ability, whereby the cysteine switch motif can be removed from the catalytic domain. The role of integrin αvβ3 in the MMP-2 activation pathway is to support the maturation of MMP-2 by supplying additional latent metalloproteinase to the ternary complex. It was shown by confocal microscopy analysis that MT1-MMP and integrin αvβ3 are colocalized on the cell surface. Moreover integrin αvβ3 specifically binds the hemopexine-like domain of MMP-2 [85]. These two characteristics allow the accumulation of the MMP-2 and its ternary receptors on the invasive front of the cells where they can be activated and start to digest the ECM.

Some considerations should be made on the characteristics and concentrations of the components of this activation complex. TIMP-2 concentration on the cell surface must be fine regulated, since a low concentration of this inhibitor leads to inactivation of a part of the pool of MT1-MMP. On the other hand, a very high concentration of TIMP-2 allow inhibition of the whole pool of the MT1-MMP, preventing the MT1-MMP mediated cleavage of the MMP-2 pro-peptide and also binding MMP-2 trough the inactivating N-Terminal domain. Therefore, this activation model requires that the concentration of TIMP-2 remains half of the concentration of MT1-MMP and equal to the concentration of MMP-2.

1.4.5 The Role of Chlorotoxin (Cltx) in the MMP-2 mediated ECM digestion

Chlorotoxin is a 36 amino acid peptide isolated from *Leiurus quinquestriatus* venom. The main characteristic of this peptide is the presence of a tyrosine that can be labeled with radioactive iodine and eight cysteine residues that conjugate to form four disolfure bonds

[86] conferring a highly folded shape to the peptide. Cltx is the first ligand discovered to bind whit high affinity to small conductance Cl^- channels. Moreover, it was initially found to specifically bind glioma cells rather than normal astrocytes *in vivo* [87]. This peculiarity led to a more profound investigation on the surface Cltx receptors present on the glioma cell surface. Initially, a membrane component of about 72 kDa, with a molecular mass similar to the CLC ion channel family was identified as being able to bind to this toxin. However, more in depth studies helped to reveal the nature of the cell surface receptor of Cltx. The use of Actigel ALD allowed to form a His-Cltx bond between the toxin and a proteic cluster on the membrane. Isolation and purification of this complex led to the discovery that this putative receptor is composed by MMP-2 and the Activation Complex [82].

The binding of CTX to the protein complex results in the uptake of the complex together with the chloride ion channel ClC-3, by cells into membrane lipid rafts, which decreases the number of active chloride ion channels of the cell surface and, thereby, suppresses the chloride ion current [88].

Modification of the cell shape and the formation of invadopode, events required during cell invasion, are based on the ability of cells to decrease their volumes by decreasing cytoplasm content. This skill depends on the intracellular transportation of Cl^-, K^+ and water, in which chloride ion channels plays a critical role. A higher resting potential is present in glioma cells and the excretion of cytoplasm content is likely to be driven by the outflow of Cl^- [89, 90]. Theoretically, this explains the fact that Cltx suppresses

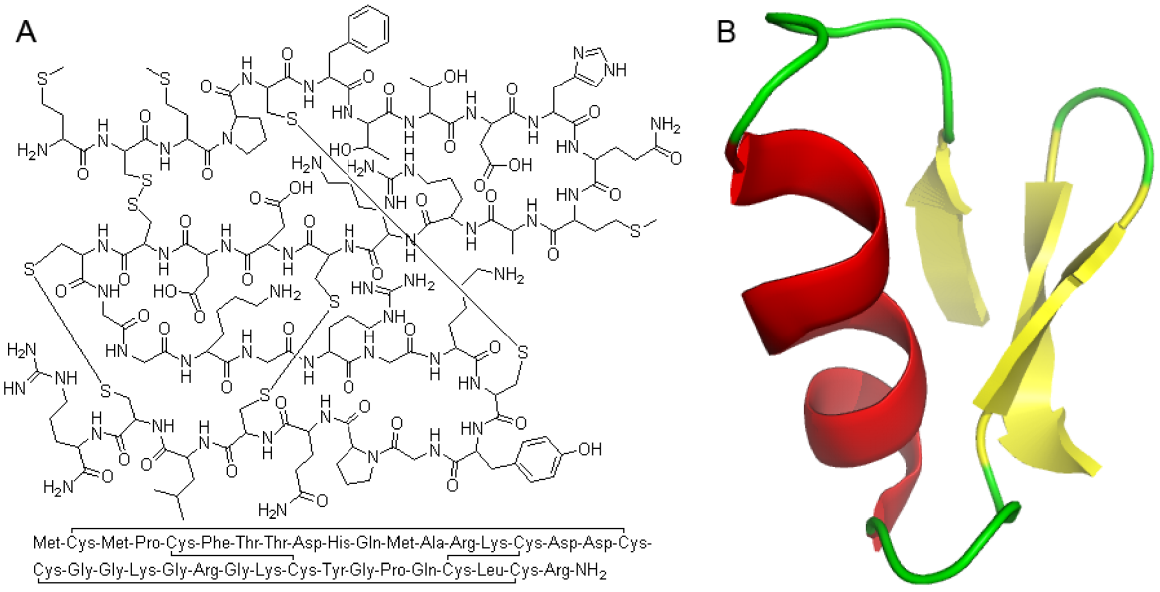

Figure 7. Chemical structure (**A**) and tree dimensional rendering (**B**) of Chlorotoxin

metastasis and tumor growth in gliomas. First, as a chloride ion channel blocker, Cltx inhibits the volume shrinkage of tumor cells by blocking chloride channels, thereby compromising the metastatic capacity of the glioma cells. Second, the interactions between Cltx and MMP-2 also contribute the anti-invasive and anti-metastatic capacity of Cltx, mainly due to Cltx-mediated inhibition of MMP-2 activity and enhanced endocytosis of MMP-2, which decreases the amount of this protein present at the cell membrane [86, 91]. These characteristics make Cltx an efficient drug against tumor invasiveness, a perfect compound for imaging diagnostics and, as will be next described, a good ligand for lipidic drugs delivery systems.

1.5. Strategy of Glioblastoma Treatment

1.5.1 Conventional Treatment

Standard therapy for newly diagnosed glioblastoma multiforme consists of surgery followed by radiotherapy with concomitant and adjuvant chemotherapy. Complete surgical resection of the tumor is not possible due to its highly infiltrative growth, but surgical removal is performed to maximally reduce tumor size to the maximum. Subsequent postoperative radiotherapy is delivered by partial-field external beam irradiation, targeting brain tissue at a 2-3 cm margin around the operative cavity [10].

The main chemotherapeutic agent used for treatment of glioblastoma multiforme is temozolomide, an oral alkylating agent with reasonable penetration of the normal blood-brain barrier [92]. Despite the best available treatment, tumor recurrence is observed in almost all patients diagnosed with glioblastoma multiforme, and its mean time is only of 6.9 months from the time of diagnosis [2]. Therapy of recurrent glioblastoma consists of tumor reoperation due to symptoms of the mass effect are evident, radiotherapy, various combinations of conventional chemotherapeutics, and experimental therapies [93, 94]. Common side effects accompanying glioblastoma multiforme therapy include toxicity to adjacent brain structures, toxicity to proliferating cells of non-neuronal tissues and unwanted long-term effects like cognitive deficits and epilepsy due to neuronal damage [93].

Despite recent progress in the therapeutic management of glioblastoma multiforme, the five year patient survival is still less than 5 %, and the disease can be considered incurable due to the high rate of recurrence [1]. The reasons for this are both the late stage of the disease at the time of diagnosis, and the inability of available therapies to efficiently eradicate all glioblastoma cells. Advances in glioblastoma multiforme therapy are clearly required to improve patient survival and reduce the side effects of medical treatment. Recent advances in understanding glioma biology hold promises for the development of therapeutics that specifically target the tumor compartment and multiple experimental therapies based on this approach are currently in development [95].

1.5.2 Targeted Cancer Therapy

In general, research has focused on two different drug targeting strategies in a variety of solid tumors: targeting drugs directly to cancer cells [96] or targeting drugs to the tumor vasculogenesis [97-99]. The first strategy promotes specific interaction of the drug with the cancer cells to exert its effects, whereas targeting drugs to tumor endothelial cells aims at decreasing the tumor capability to build up new vases and to promote the subsequent starvation of cancer cells.

Independently of the targeting strategy, the chosen target molecule must obey certain principles. First of all, the target must be highly specific for the tumor cells in order to achieve selective targeting. If the target molecule is expressed by cells of other tissues, this could result in off-target side effects and toxicity. The target molecule must also be abundantly expressed in the tumor area to ensure sufficient interaction between the drug and the target cells. Furthermore, a stable expression of the target molecule is of great importance, in order to prevent down-regulation of the target molecule during malignant progression of the tumor and during treatment with targeted therapeutics.

Unfortunately, it has proven difficult to identify molecular targets that meet all of the this criteria, either in cancer cells or in tumor endothelial cells [100, 101]. Despite difficulties in the identification of optimal targets, extensive research in targeted cancer therapies during the last decades has generated a variety of targeting strategies and agents that have shown potential to be used in the clinical therapy of glioblastoma multiforme.

1.5.3 Targeting of the Cancer Cells

Targeted accumulation of the therapeutic drug in the tumor compartment can also be achieved either by promotion of drug uptake through binding of the drug to the target molecule (e.g. an internalizing cell surface receptor) or by administration of high drug doses, which is possible only if there are few off-target side effects. [95, 96] However, an obstacle for direct targeting of cancer cells is that the drug of choice needs to penetrate into the tumor to exert its therapeutic effects. In glioblastoma multiforme the high intratumoral interstitial pressure and the still partially intact blood-brain barrier in lesions areas act as barriers [102, 103], reducing the tumoral delivery of blood-born tumor-targeted drugs [96, 100].

Drugs that target cancer cells directly can be divided into two main groups, based on the mechanism of interaction with their target. The first group, known as molecular targeted drugs, aims at interfering with intracellular signaling pathways which are overactivated in glioblastoma and drive cellular proliferation, survival and invasion [104]. Molecular targeted drugs exert their anticancer effects by binding directly to a target molecule involved in cellular signaling and thereby inhibiting the normal functions of this molecule [95, 96].

The second group of drugs targeting cancer encompasses various types of drug carriers. Here, the carrier transporting the cytotoxic drug prevents interaction of the drug with healthy cells, and modification of the drug carrier with a ligand or antibody directs the drug carrier towards a specific surface molecule of cancer cell. The main objective of the target molecule is to establish contact between the carrier and the cancer cell, facilitating the uptake of the drug into the intracellular compartment, where it can exert its effects [105].

Various strategies to improve the efficacy of molecular targeted drugs are currently being investigated in clinical trials. They include the combination of molecular targeted drugs with conventional therapy or with other targeted drugs, selection of patients on the basis of biomarkers and development of new and more powerful drugs against the same or newly discovered targets.

Numerous targeted drug carriers have been studied preclinically in animal models of glioblastoma multiforme. However, few have progressed to clinical trials. The investigated drug carriers include protein toxins and doxorubicin-liposomes, targeted

primarily to the transferrin receptor or to interleukin receptors, which are overexpressed on the surface of glioblastoma cells [106, 107]. Targeted protein toxins are the only tumor-directed drug carriers that are currently in clinical trials for glioblastoma multiforme. These large drugs must be delivered locally into the tumor through an invasive procedure, known as convection-enhanced delivery, based on infusion of the drug through catheters inserted in the brain. [108, 109].
Targeted liposomes are another important type of drug carriers that have been suggested for the therapy of glioblastoma multiforme and which will be more extensively discussed in the following section.

1.5.4 Different type of Liposomes

Liposomes are lipid bilayer vesicles within the 50-1000 nm range, which contain an aqueous core. Unilammellar liposomes consist of a single lipid vesicle with an aqueous core, whereas multilammeller liposomes contain several lipid vesicles inside each other. Liposomes can be prepared from various mixtures of natural and synthetic lipids, and the chosen lipid composition is an important determinant of the *in vitro* and *in vivo* liposomal characteristics [110]. Liposomes are well suited to act as drug carriers, since they have the ability to transport many different types of drugs at high concentrations. Hydrophilic and amphiphilic drugs can be encapsulated into the aqueous core, whereas hydrophopic drugs can be incorporated into the lipid bilayer [111].
To control the cellular fate of liposomes, they can be modified with various surface molecules, such as polymer-coatings and targeting agents. Based on such modifications, unilammellar liposomes have been divided into several types. The first liposomes to be investigated were unilammellar liposomes between 100-500 nm without any surface modifications, named conventional liposomes. Investigating various formulations of conventional liposomes revealed that *in vivo* circulation time and other pharmacokinetic parameters were closely related to the size, lipid composition and charge of these liposomes [111]. For example, small liposomes (<100 nm) containing gel-state phospholipids and cholesterol had a significantly longer circulation time than larger liposomes of the same lipid composition [112]. In addition, neutral liposomes were generally found to have a longer circulation time than electrostatically charged liposomes [111]. The fast removal of conventional liposomes from the circulation is

predominantly caused by a rapid liposomal uptake by the macrophages of the reticulo-endothelial system (RES) in the liver and spleen [111]. To overcome this problem liposomes coated with linear polyethylene glycol (PEG) molecules was developed, limiting the rapid uptake by the RES and significantly prolonging the half life of circulating liposomes to about 20 hours in mice and rats [113] and up to 45 hours in humans [114]. PEG are commonly grafted to the liposomes by modification of the PEG molecules with a hydrophobic residue at one end, typically a phospholipid, which then can be incorporated into the bilayer of the liposomal membrane. Still concerning conventional liposomes and PEGylated liposomes, liposome size was also found to be an important factor in liposomal clearance after intravenous injection [111]. Prolonged circulation was especially observed for small liposomes with a size of 70-200 nm and a high degree of homogeneity [115]. In contrast, 300-400 nm PEGylated liposomes avoided significant entrapment in the liver, but not in the red pulp and marginal zone of the spleen [116]. Thus, the biodistribution pattern of liposomes can significantly be altered by changing the basic structure of both conventional and PEGylated liposomes.

The next step in the development of liposomes as drug carriers involved preparation of liposomes that were conjugated with a targeting ligand. This enabled targeting of the liposomes towards specific molecules expressed by the target cell population, promoting close interaction of the liposomes with the target cell and allowing cellular internalization.

Two different approaches investigated for the conjugation of liposomes are coupling the targeting ligand directly to the lipid bilayer, which was explored for both conventional and PEGylated liposomes and coupling of the targeting ligand to the distal end of surface grafted PEG-chains of PEGylated liposomes [117].

When choosing a targeting ligand for liposomal conjugation, it is not only important to ensure that the ligand binds specifically to a target highly expressed by the target cell, but several other considerations must also be taken into account to choose the best type of targeting ligand and chemical method to attach of the ligand to the liposome.

First of all, conjugating a ligand to the surface of a liposome may increase the rate of liposome uptake by the RES, despite the presence of PEGylation. Next, the immune system might attack the ligand or other parts of the ligand-conjugated liposomes and cause an unwanted immune reaction [118]. The extent of antibody development depends on the type of ligand employed, for example, small peptides or Fv fragment are usually less immunogenic than a complete foreign antibody [119, 120]. Based on these principles,

it is understandable that the amount of conjugated ligand must be well balanced to establish successful binding to its target, while maintaining a long circulation time. Using liposomes with a lower ligand-density may extend the liposome circulation time and improve the chance of interaction with targets located in tissues with limited blood flow, although such liposomes might not bind to the same target as efficiently *in vitro* compared to liposomes with high ligand density.

1.5.5 In vivo liposomes behavior

The behavior of the various formulations of liposomes has been extensively studied at the cellular level both *in vitro* and *in vivo*, as well as at the whole organism level *in vivo*. As mentioned above, the fate of liposomes *in vivo* is determined by the structure and components of the liposomes, such as size, lipid composition, PEGylation, and the presence of targeting ligands on the liposome surface.

The predominant administration route for liposomes is by intravenous injection, after which the liposomes circulate in the blood. Due to the large size of liposomes, the lining of the blood vessels act as a barrier and the liposomes can only extravasate at sites with discontinuous or fenestrated endothelium [111]. Both the liver and spleen have fenestrated endothelium and therefore, liposomes that do not exceed the size of the fenestrae are prone to accumulate in these organs. However, liposome accumulation within these organs has been demonstrated not to depend solely on the size of the particles, but also on their lipid composition. For example liposomes that present a significant larger size than the pore size of the liver fenestrae, but that also have high fluidity were found to accumulate in the liver in a high degree. Accumulation of liposomes in the liver and the spleen promotes the interaction with inherent macrophages of the RES, which are the main source of liposome elimination from the body. Depending on the size and lipid composition of the liposomes, liver hepatocytes may also play an important role in removing liposomes from the blood. No convincing study has demonstrated a significant uptake of liposomes by other cell types easily accessible from the blood, such as cell of the endothelium or circulating blood cells [117].

Several theories exist for the mechanisms of liposome removal by the RES, and why PEGylation of the liposomes can slow down this process. In the circulation, liposomes of various compositions unspecifically adsorb serum proteins. One theory depends that the opsonization of liposomes by macrophages occurs through receptor-mediated trigged by

liposome-bound proteins [111]. Some of the identified proteins contribute to this process include fibronectin, complement factors, ß2-glycoprotein, C-reactive protein, and α2-macroglobulin [121-125]. After the receptor-mediated endocytosis of liposomes, lysosomal digestion of the liposome membrane releases the liposomal content into the cytoplasm. Several theories have been proposed to explain why PEGylation increases the circulation times of liposome. One of the most popular views suggests that the PEG-chains act as a steric barrier, preventing macromolecules such as the mentioned opsonins from interacting with the liposomal membrane. Due to the lack of liposome opsonization the rate of macrophage uptake is significantly reduced [111].

Long-circulating liposomes have a higher probability of encountering their target cells, especially if these cells are located in an area with limited blood supply. A longer circulation also increase the probability of extravasation and accumulation at sites with increased vascular permeability, such the tumoral tissue [117]. Increasing the circulation time will increase the number of times a liposome passes through a specific tissue, thereby increasing the probability of interaction with its target cell or increasing the probability of intratumoral extravasation through the EPR effect. Several possible mechanisms explaining the interaction of liposomes with cells, after accumulation in the target tissue, have been described. First of all, unspecific binding or absorption of liposomes to the cell surface can occur through the electrostatic association, and untargeted liposomes can deliver their drug load by this mechanism.

When in close contact with the cell, lipophilic drugs encapsulated in the liposomal membrane can be transferred to the cell membrane, while encapsulated hydrophilic drugs can be released, in some circumstances, from absorbed liposomes and taken up into the cells. Both these processes are not fully understood, but it is clear that the lipid composition and charge of the liposomal membrane and the physiochemical characteristics of the drug in question are of great importance. Another suggested mechanism by which liposomes can deliver their content to the cellular compartment is through fusion of the liposomal lipid membrane with the cellular membrane, thereby inducing cytoplasmic release of the liposome content. However, no experimental evidence clearly indicates that cellular fusion occur when using standard conventional or PEGylated liposome and in general specific fusion-inducing agents are believed to be required for stimulation of this process [117]

Two primary mechanisms have been proposed to explain how targeted liposomes can increase the cellular uptake of liposomes, depending on both the properties of the target

molecule and the targeting ligand. When targeting the liposomes to a cell surface receptor at a site where binding induce internalization of the whole complex, the liposomes can be internalized through receptor-mediated endocytosis into the intracellular compartment of cancer cells. Some liposomes have the ability to destabilize the endosomal membrane, through lipid-lipid or protein-lipid interactions, resulting in the releasing of their cargo into the cytoplasm, before lisosmal digestion can occur. However, even liposomes targeted to a non-internalizing molecule have demonstrated high intracellular accumulation of the transported drug. A likely explanation for this phenomenon is that binding of the liposome to its membrane target keeps the liposomes in close contact with target cells long enough to facilitate diffusion of the encapsulated drug into the cells or internalization of the liposomes by unspecific mechanism [126].

1.5.6 RNA interference thought Liposomes delivery system.

At present, RNAi is defined essentially as a naturally occurring and evolutionary conserved mechanism by which short dsRNAs trigger a sequence-specific inhibition of gene expression that can be implemented for the treatment of a variety of human diseases with a known genetic origin.

Intensive investigation on the RNAi mechanism identified small interfering RNAs (siRNAs) as the genuine effectors of the genetic interference [127]. Synthetic siRNAs can easily be produced through large-scale chemical synthesis and the majority of reports on RNAi therapeutics have focused on siRNA for the activation of gene silencing.

Before siRNA molecules can reach the desired intracellular location, many extra- and intracellular barriers have to be overcome. Obviously, the efficiency with which siRNAs can by-pass these obstacles will have major implications on the extent and duration of gene silencing and, consequently, on the determination of a clinically relevant dosing interval. Several concepts and strategies have been proposed to improve the siRNA pharmacokinetics and eventually their therapeutic performance.

It is well known that siRNAs are rapidly degraded in the extracellular environment. When naked (i.e. uncomplexed, formulated in saline) siRNA is injected intravenously, it is recognized and cleaved by RNase type A endonucleases [128-130] or 3' exonucleases [131-133] limiting the serum half-life of the siRNAs to a time frame lower than 30 minutes.

Besides degradation by RNases, the short *in vivo* half life of siRNAs is also influenced by their rapid renal clearance. Since siRNAs are highly hydrophilic (~40 negatively charged phosphate groups per siRNA molecule) and have a molecular weight (~14 kDa) far below the cut-off for glomerular filtration (~60 kDa), one can expect renal clearance to be prominent.

Moreover, in the case of treatment of brain disease, one more obstacle to be considered is the blood brain barrier (BBB) which limits passage of charged molecules into the brain tissue.

In an attempt to overcome these impediments, breakthroughs in of lipid particle technology led to the design of a novel type of lipid bilayer containing a mixture of cationic and fusogenic lipids coated with diffusible polyethylene glycol. These new particles were called Stable Nucleic Acid Lipid Particles (SNALP) and are in the 120~140 nanometer diameter size range preserving a the lipid combination that protects the siRNAs from serum nucleases and allows cellular endosomal uptake and subsequent cytoplasmic release of the siRNAs.

An important study has shown success in achieving a significant and long-term reduction of HBV activity using three daily injections of siRNA followed by a weekly administered maintenance dose accomplishing persistent *in vivo* anti-HBV activity of siRNAs over time [134, 135]. A more recent report, using SNALP technology to deliver anti-ApoB siRNA in cynomolgus monkeys, describes a marked reduction in plasma ApoB protein levels for more than ten days after a single injection [135].

In addition, the systemic delivery of these targeted siRNA nanoparticles, twice a week for more than four weeks resulted in long-term inhibition of tumor cell engraftment and tumor growth in many murine therapeutic models such as Ewings sarcoma.

Many delivery strategies have been attempted to direct the nanoparticles to a specific target. Receptor mediated-targeting to the brain can be achieved by directly coupling of a targeting ligand to a drug molecule or by encapsulating drugs into nanoparticles that are then actively targeted to receptors on the BBB. Some of the most widely used receptors for this purpose include the transferrin receptor, the insulin receptor, the low-density lipoprotein receptor family, and the diphtheria toxin receptor [136]. When ligands bind to these receptors, they are taken up into the brain endothelial cells by endocytosis. Large molecules or nanoparticles attached to these ligands can be taken up along, enabling intrinsically BBB-impermeable compounds to cross the BBB [137]. Subsequent transcytosis to the abluminal (brain) side is required for entry into the brain and

different nanoparticles have been recovered from the brain parenchyma [138-141], showing the potential of this strategy.

Several ligands have shown good targeting properties in many different studies regarding their ability to facilitate BBB crossing, but it is difficult to compare results from different studies and, therefore, to decide which ligand has the best capacity to target a nanoparticle to the brain.

Regarding this subject, transferrin has been frequently chosen as a target ligand for several particular reasons. First of all, transferrin receptor (TfR) is the most widely studied receptor for BBB targeting. TfR is a transmembrane glycoprotein, consisting of two linked 90-kDa subunits, that can each bind a transferrin molecule. The receptor is highly expressed on immature erythroid cells, placental tissue and rapidly dividing cells [108, 142]. Furthermore it is expressed on hepatocytes and endothelial cells of the blood–brain barrier and, most importantly, in glioma cells, which have shown a high metabolic requirement for iron with consequent increase of the TfR on the cell surface.

The major role of this receptor is the regulation of the cellular uptake of iron from transferrin, a plasma protein which transports iron in circulation. Cellular iron uptake from transferrin is initiated by the binding of holo-transferrin to the transferrin receptor, followed by endocytosis [143]. Since iron-bound transferrin has a high affinity for the TfR, it has been used as a ligand for targeting to brain endothelial cells [144, 145]. However, this application is limited *in vivo*, because endogenous levels of transferrin are high, resulting in nearly saturated transferrin receptors. Nevertheless, successful brain targeting using transferrin as a targeting ligand has been accomplished in vivo [146, 147].

Chlorotoxin, another interesting ligand for brain targeting, has been shown to have ananti-invasive effect and also the ability to be highly selective for glioma cells. Chlorotoxin "receptor", MMP-2, is expressed mainly in glioma tumor cells and its downregulation has also been shown to reduce malignant invasiveness. Therefore these characteristics make Cltx a good ligand for SNALP delivering system in glioblastoma treatment. It was shown, as will be better explained in after section, that Cltx-SNALPs are very effective in mediating nucleic acid delivery to tumor cells both *in vivo* and *in vitro* [148].

Objectives

2. Objectives

Due to its importance in glioma invasiveness and location at the cell surface, matrix metalloproteinase-2 has been used as a target for the development of targeted lipid-based drug delivery strategies. The main goal of the present study was to evaluate the influence of this protein on Chlorotoxin-mediated SNALP binding and internalization in glioma cells. The specific aims of this project were:

- To evaluate the contribution of PDGF, an important growth factor related with glioblastoma, to MMP-2 protein levels.

- To identify the major molecular pathways and their specific intervenients involved in the regulation of MMP-2 protein levels.

- To clarify the dynamics between MMP-2 mRNA and protein levels and investigate the existence of an intracellular vesicular pool of this protein.

- To modulate MMP-2 mRNA and protein levels using RNA interference tools and lipid-based delivering particles.

- To clarify the relation between MMP-2 protein levels and the ability of Chlorotoxin-targeted SNALPs to bind and be internalized by glioma cells.

Materials and methods

3. Materials and methods

3.1 Materials

Sunitinib malate (Sutent®) was kindly offered by Pfizer (Basel, Switzerland). The lipids 1,2-dioleoyl-3-(dimethylammonium) propane (DODAP), 1,2-dioleoyl-3-(trimethyl ammonium) propane (DOTAP), 1,2-distearoyl-sn-glycero-3-phosphocholine (DSPC), N-palmitoyl-sphingosine-1-[succinyl(methoxypolyethylene glycol) 2000] (C16 PEG2000 Ceramide), 1,2-distearoyl-sn-glycero-3-phospatidylethanolamine-N-[maleimide (poly ethyleneglycol)-2000] ammonium salt (DSPE-PEG-MAL), L-α- phosphoethanolamine-N-(lissaminerhodamine B sulfonyl) (Rho-PE), 1,2-dipalmitoyl-sn-glycero-3-phosphoethanol amine-N-(7-nitro-2-1,3-benzoxadiazol-4-yl) ammonium salt (NBD-PE) and Cholesterol were acquired from Avanti Polar Lipids (Alabaster, AL, USA).
The 36 aminoacid long peptide chlorotoxin (MCMPCFTTDHQMARKCDDCCGGKGRGK CYGPQCLCR), the MMP-2 siRNA (target-sequence: GGAGAGCUGCAACCUGUUUTT), the TIMP-2 siRNA (target sequence: GGAUCCAGUAUGAGAUCAATT) and the scramble siRNA (UAAGGCUAUGAAGAGAUATT) were synthesized by Genecust (Dudelange, Luxembourg). All other reagents were obtained from Sigma-Aldrich unless stated otherwise.

3.2 Cell lines and culturing conditions

The GL261 mouse glioma cell line was kindly supplied by Dr. Perez-Castillo (Universidad Autónoma de Madrid, Madrid, Spain); the parental U87 human GBM cell line was a kind gift from Dr. Peter Canoll (Columbia University, New York, USA). HEK293-T human embryonic kidney cells were obtained from the American Type Culture Collection (Manassas, VA, USA). All cell lines were maintained in culture in DMEM containing 4.5 g/L glicose (Invitrogen, Carlsbad, CA, USA) and supplemented with 10% heat-inactivated FBS (Gibco, Paisley, Scotland), 100 U/mL penicillin (Sigma), 100 μg/mL streptomycin (Sigma), 10 mM HEPES. Cells were cultured at 37°C under a humidified atmosphere containing 5% CO2.

A modified U87 cell line overexpressing PDGF-B (U87-PDGF) was derived from parental U87 cells through infection with a PDGF-B retrovirus. Briefly, a 0.8 kb fragment encoding PDGF-B-hemagglutinin (HA) was inserted into the MCS1 region of the retroviral vector PQ-MCS1-IRES-eGFP. U87 cells infected with the same retroviral vector but without the PDGF-B-HA construct were used as a control. The infected cells were plated onto 10 cm culture dishes at a 90% confluence and were incubated for 48 h in serum-free basal media. PDGF-B determination was performed in the conditioned media using an ELISA kit (R&D Systems, Minneapolis, MN, USA). Parental U87 conditioned media had undetectable levels of PDGF-B, while U87-PDGF conditioned media had a mean PDGF-B concentration of 353 ng/ml.
For SNALP-mediated or lipoplex-mediated transfection, all cell lines were plated in 12-well plates (U87: $8x10^4$ cells/well, GL261: $7x10^4$ cells/well and U87-PDFG: $6x10^4$ cells/well) for cell viability studies, protein and mRNA extraction or flow cytometry studies) 24 hours before transfection, except when stated otherwise.

3.3 Isolation of membrane vesicles from conditioned medium

Cells were prepared as already described and collected at 100% flask confluence. Conditioned medium was obtained by centrifugation at 600 x g for 15 minutes and then 1500 x g for 15 minutes to remove cells and large debris. The supernatants were centrifuged at 100,000 x g for 1 hour at 4°C. Pellet vesicles were resuspended in RIPA lysis buffer. Proteins were extracted as described.

3.4 Liposome and lipoplex preparation and transfection

Cationic liposomes composed of DOTAP:cholesterol (1:1 molar ratio) were prepared as previously described by Campbell [149] for *in vitro* application. Briefly, a mixture of 10 µl of DOTAP and 13 µl of cholesterol in chloroform (from stock solutions of 100 mg/ml DOTAP and 40 mg/ml cholesterol), were dried under nitrogen in order to obtain a thin lipid film. The film was dissolved in 70 µl of ultrapure ethanol and the resulting ethanol solution was injected into 930 µl of HBS buffer, employing a 250 µl Hamilton syringe to obtain a final lipid concentration of 1.43 mM DOTAP (1 mg/ml). The liposomes were stored at 4 °C until use.

Tf-lipoplexes or Fa-lipoplexes were prepared by pre-incubating a given volume of the liposome suspension with iron saturated (halo) human transferring (32 μg/μg of siRNA) or folic acid (40 μg/μg of siRNA) for 15 min, followed by the addition of the necessary volume of siRNA stock solution to achieve a final siRNA concentration of 25, 50 or 100 nM in each well and a 2/1 lipid/siRNA charge ratio. The mixture was further incubated for 15 min at room temperature before cellular delivery and remained in contact with the cells for 4h in OptiMEM medium (Gibco). After this period, the OptiMEM medium medium was removed, cells were washed once with PBS and fresh medium was added to each well. The cells were further incubated for different periods of time, according to each specific experiment.

In certain experiments the commercial reagent Lipofectamine RNAi Max (Invitrogen) was also used as a delivery vector for siRNAs according to the manufacturer's instructions.

3.5 Preparation and purification of targeted SNALPs

CTX-coupled (targeted) SNALPs were prepared by the postinsertion method [150,151] Briefly, CTX was modified with the addition of thiol groups upon reaction with freshly prepared 2-iminothiolane hydrochloride (2-IT, in HBS, pH 8), at a molar ratio of 1:10 (CTX:2-IT). The reaction occurred under gentle stirring for 1 h, in the dark, at room temperature (RT). Thiolated CTX was then coupled to DSPE-PEG-MAL micelles, prepared in MES buffer pH 6.5 [153], by a thioesther linkage (1:1, protein:micelles molar ratio). The coupling reaction was performed overnight (at RT), in the dark, with gentle stirring. For the non-targeted SNALPs (NT), postinsertion was performed with plain micelles (without conjugated ligand), which were prepared by adding HBS (pH 8.0) to the DSPE-PEG-MAL micelles. The neutralization of free maleimide groups in the micelles was carried out upon incubation with ß-mercaptoethanol at a maleimide:ß-mercaptoethanol molar ratio of 1:5, under stirring for 30 min (at RT). The insertion of CTX-DSPE-PEG-MAL conjugates or plain DSPE-PEG-MAL micelles into the preformed liposomes, at 1 or 4 mol % (relative to the total lipid concentration), was performed upon incubation in a water bath at 39°C for 16 h (in the dark). Targeted and NT SNALPs were

purified by size exclusion chromatography on a Sepharose CL-4B column, using HBS (pH 7.4) as washing buffer to remove nonconjugated micelles and chemical reagents used during SNALPs preparation.

3.6 Characterization of SNALPs

The final total lipid concentration in SNALPs was assessed by cholesterol quantification (using the Liebermann-Burchard test) [152]. The quantification of encapsulated asOs/siRNAs was performed with the DNA-intercalating probe SYBR® Safe (Life Technologies, USA), in the presence of the detergent octaethylene glycol monododecyl ether (C12E8) (Sigma). The encapsulation efficiency was calculated from the formula [(asO/total lipid) final molar ratio/ (asO/total lipid) initial molar ratio] × 100. The extent of nucleic acid protection resulting from the encapsulation of the asOs/siRNAs into the liposomes was determined by evaluating the ability of the SYBR® Safe probe to intercalate into the asOs/siRNAs in the absence of C12E8.

The amount of Cltx associated with SNALPs was determined using with the BCA Protein Assay Kit at 562 nm (Pierce, Rochford, IL, USA), using a Cltx standard curve, in a microplate reader (SpectraMax Plus 384, Molecular devices). The insertion efficiency was calculated from the formula [(CTX/total lipid) final molar ratio/(CTX/total lipid) initial molar ratio] × 100.

SNALPs size distribution was assessed by photon correlation spectroscopy, using an N5 submicrometer particle size analyzer (Beckman Coulter, Miami, FL, USA). Measurements were made at a 90° angle and at 20°C. Zeta potential measurements of targeted and NT SNALPs were performed at RT, using a Zetasizer Nano ZS™ (Malvern Instruments, UK).

3.7 Assessment of SNALP cellular association and internalization by flow cytometry

To evaluate the extent of cellular association and internalization of SNALPs, cells were plated into 12-well plates. Twenty-four hours after plating, cells were incubated with targeted (Cltx-coupled or bovine serum albumin (BSA)-coupled) or non-targeted

liposomes, encapsulating FAM-labeled oligonucleotides, for 4 h at 4ºC (association only) or 37°C (association and internalization). Subsequently, cells were washed twice with cold phosphate buffer saline (PBS, pH 7.4), detached from the plates by exposure to a trypsin solution (5 min, 37ºC) and washed twice with PBS. Cells were then ressuspended in 350 µL of cold PBS and immediately analyzed in a FACS Calibur flow cytometer (BD, Biosciences). FAM fluorescence was evaluated in the FL-2 channel and a total of 30,000 events were collected for each sample (unless stated otherwise). The data were analyzed using the Cell Quest software (BD).

3.8 Cell viability Assay

Cell viability was determined by the Alamar blue assay. This assay measures the redox capacity of cells and allows the determination of cell viability without detachment and death of adherent cells. Briefly, 1ml of DMEM supplemented with 10% FBS containing 10% of the rezazurin dye was added to each well. After 2 hours of incubation at 37°C, 200µl of cell medium were collected from each well and transferred to 96-well plates. The optical density of each well was measured at 570 and 600 nm in a microplate reader and cell viability was calculated as a percentage with respect to control cells, using the formula: $(A_{570} - A_{600})$ of treated cells x 100/$(A_{570} - A_{600})$ of control cells.

3.9 RNA extraction and cDNA synthesis

For mRNA extraction, cells were washed once with PBS and frozen at -80ºC in their plates until the day of extraction. Total mRNA was extracted using the NZY Total RNA Isolation kit (NzyTech), according to the instructions of the manufacturer, at room temperature. mRNA conversion into cDNA was performed using the ZNT First-Strand cDNA synthesis Kit (NzyTech). For each sample, cDNA was produced from 25 ng of total RNA in an iQ5 thermocycler (Bio-Rad), by applying the protocol advised in the respective kit. The cDNA was further diluted 1:50 with RNase-free water prior to quantification by qPCR.

3.10 qPCR quantification of mRNA expression

Quantification of MMP-2 mRNA levels was performed in an One Step Plus (Applied Biosysyems using 96-well microtitre plates and the iQ™ SYBR® Green Supermix Kit (Bio-Rad). The primers for the target gene (MMP-2) and the reference gene (HPRT1) were pre-designed by Qiagen. A master mix was prepared for each primer set, containing a fixed volume of SYBR Green master mix, water and the appropriate amount of each primer to yield a final concentration of 150 nM. For each reaction, performed in duplicate, 10 µl of master mix were added to 2 µl of template cDNA. The reaction conditions consisted of enzyme activation and well-factor determination at 95°C, for 1 min and 30 s, followed by 40 cycles at 95°C for 10 s (denaturation), 30 s at 55°C (annealing) and 30 s at 72°C (elongation). The melting curve protocol consisted of 1 min heating at 55°C followed by eighty 10 s steps, with 0.5°C increases in temperature at each step. The percentage of mRNA knockdown was determined following the Pfaffl method for relative mRNA quantification, in the presence of target and reference genes with different amplification efficiencies. The amplification efficiency for each target or reference gene was determined according to the formula: $E=10^{(-1/S)}$, where S is the slope of the standard curve obtained for each gene.

3.11 Protein extraction and quantification

Total protein extracts were prepared from cultured U87, U87-PDGF, HEK-293T or GL261 cells. Following cell lysis at 4ºC in RIPA lysis buffer (50 mM Tris, pH 8.0, 150 mM NaCl, 50 mM EDTA, 0.5% sodium deoxycholate, 1% Triton X-100) containing a protease inhibitor cocktail (Sigma), 2 mM DTT and 0.1 mM PMSF, the concentration of protein lysates was determined using the Bio-Rad Dc protein assay (Bio-Rad). Total protein extracts, containing 25 or 50 µg of total protein, were prepared and mixed in a proportion of 5:1 with loading buffer (20% glycerol, 10% SDS, 0.1% bromophenol blue). The extracts were then incubated for 5 min at 95ºC and loaded onto a 10% or 8 % polyacrylamide gel for electrophoretic separation.

3.12 Western blot analysis

After electrophoresis, the proteins were blotted into a PVDF membrane, which was blocked in 5% nonfat milk and further incubated with anti-MMP2, anti-c-Jun, anti-AKT, anti-PTEN or anti-PDCD4 primary antibodies (1:1000) (Cell Signaling, Beverly, MA, USA) overnight at 4ºC, and with the appropriate alkaline phosphatase-labeled secondary antibody (1:20000) (Amersham, Uppsala, Sweden) for 2 h at room temperature. Equal protein loading was shown by reprobing the membranes with anti-α-tubulin or anti- α-actin antibodies (1:10000) (Sigma) and with a secondary anti-mouse antibody. The membranes were washed several times with TBS/T (25 mM Tris-HCl, 150 mM NaCl, 0.1% Tween-20), incubated with ECF (alkaline phosphatase substrate) for 5 min (at RT) and then submitted to fluorescence detection at 570 nm using a VersaDoc Imaging System Model 3000 (Bio-Rad). For each membrane, the band intensity was analyzed using the ImageJ software.

3.13 Statistical Analysis

All data are presented as mean independent experiments. One way analysis of variance (ANOVA) combined with Tukey posthoc test was used for multiple comparison (unless stated otherwise) and considered significant when $p<0.05$. Statistical differences are presented at probability levels of $p<0.05$, $p<0.01$, $p<0.001$. Calculation were performed with Prism 5 (GraphPad, San Diego, CA, USA)

Results

4. Results

4.1 Characterization of the MMP-2 level in glioma cells

It is known that MMP-2 presents a complex activation process, which involves many different proteins and presents several levels of regulation. In order to recognize the different protein intermediates that originate during the activation process, we first analyzed MMP-2 levels by western blot in the different cell lines used in this work.

According to several studies, western blot analysis of MMP-2 usually shows a 72 kDa band which corresponds to the pro-form of the protein. In our results, each cell line presents a different quantity of this precursor (data not shown). In addition to the 72 kDa, we observed several other bands located around 200, 150 and 100 kDa. U87, U87-PDGF and H293-T cells showed a similar band pattern, while the GL261 glioma cell line presented a band at 200 kDa approximately and two other bands at 140 and 120 kDa, respectively.

Mathematical analysis of each band through comparison with the distance between the bands of Bio-Rad precision Plus Protein™ Standard has shown that the detected bands correspond to proteins or protein complexes of 169 kDa, 126 kDa and 100 kDa for the U87, U87-PDGF and H293-T cell lines. The polynomial regression used for this study also confirmed that the MMP-2 pro-form band presented the supposed correct weight of 72 kDa. Since, according to earlier reports, the high molecular weight bands were not expected, we considered that these bands might originate from the cross-reactivity of the polyclonal antibody with similar epitopes present on different proteins. To exclude this,

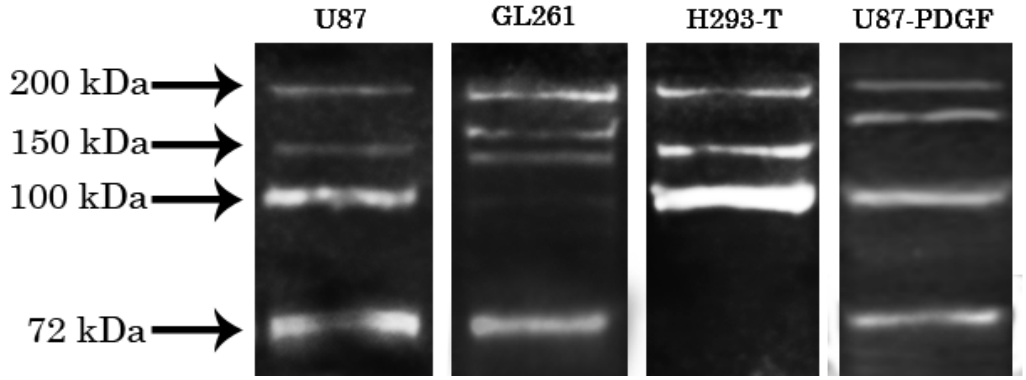

Figure 8. MMP-2 protein bands in parental U87, Gl261, H293-T and U87-PDGF cells. Cell lines were plated in 12-well plates and, after 24 h, protein extraction was performed and MMP-2 protein levels were analyzed by western blot.

we performed a transfection on GL261 and normal U87 cells with 50nM of anti-MMP-2 or scramble siRNAs (negative control), using Lipofectamine™ as the delivery vector (as described in Material and Methods section).

We were able to observe a decrease of the 72 kDa pro-MMP-2 band of 35.25% in U87 cells and 65.33% in GL261 cells. In what concerns the unknown bands, in U87 cells we found a decrease in the intensity of all bands, but in GL261 cells only the 160 kDa band presented a decrease. These results led us to suppose that the 100 kDa band could correspond to the inactive state of the MMP-2 protein since if we consider that TIPM-2, in its active form, is a protein of 27 kDa able to bind the 72-kDa pro-form of MMP-2, the resulting complex would present the correct 100 kDa weight of the observed band. However, intense studies and mathematical analysis did not show any significant correlation between fluctuations of the 100 kDa band and MMP-2 pro-form protein levels.

4.2 Influence of PDGF on MMP-2 protein level.

The activity of MMP-2 is regulated by several mechanism, including pro-enzyme activation, natural inhibition by TIMP-2 and gene expression. To better characterize the interaction between each single component of the activation pathway and to clarify how MMP-2 could be regulated by a proliferation signal like PDGF we decided to retrace the pathway starting by looking at the gene regulation mechanism.

Sequence analysis of the MMP-2 promoter has revealed a number of potential cis-acting regulatory elements that can be activated by p53, AP-1, Ets-1, C/EBP, CREB, Sp1 and AP-2 and therefore be involved in MMP-2 regulation.

The p53 element does not contribute to MMP-2 activation, probably because the majority

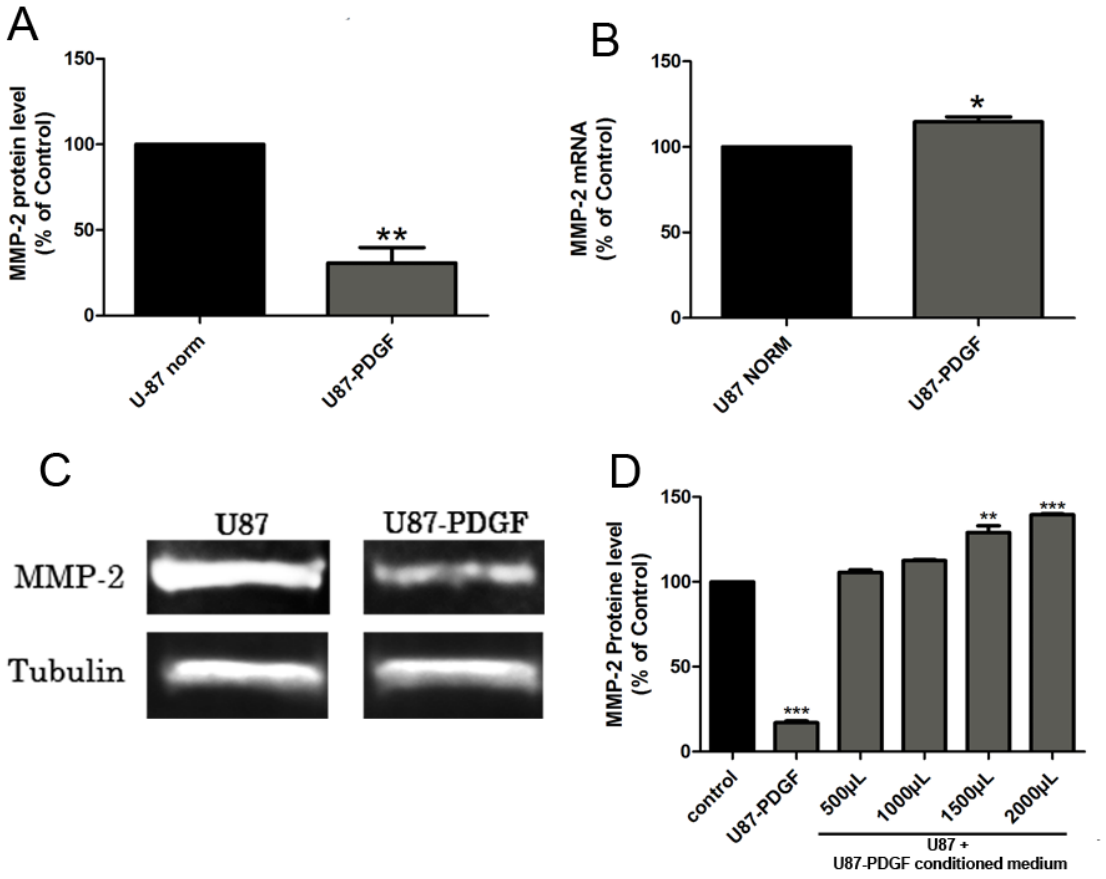

Figure 9. MMP-2 protein and mRNA levels in U87 and U87-PDGF cells. both cell lines were plated in 12-well plates and maintained in culture for 24 hours before protein (**A, C**) and mRNA (**B**) extraction. U87 was also treated with different amounts of U87-PDGF conditioned medium (500µl, 1000µl, 1500µl and 2000µl) for 24 hours before protein extraction. MMP-2 protein levels were quantified by western blot (**A**), (**B**) and (**C**), while MMP-2 mRNA levels were quantified by pPCR (**B**). Results are expressed in % MMP-2 protein or mRNA levels which respect to U87 untreated cells (control) and representative of 3 independent experiments. *p<0.05, **p<0.01, ***p<0.001

of gliomas express a mutant version of this protein. Studies concerning the deletion of several sections of the MMP-2 promoter revealed that the proximal region is essential for MMP-2 regulation. This region is a binding site of Activating Protein 1 and 2 (AP-1 and 2) [153]. The AP-1 enhancer has been shown to be regulated by several proteins including MAPK. In addition other studies have shown how the MMP-2 gene is regulated by MKK-1, through the c-Jun/Sp-1 interaction, by ERK-1 and -2 and by p38 [154]. This framework of genetic domains led us to investigate the possible interaction between PDGF-B, which could act as common chain-ring of all these pathway, and MMP-2 protein levels.

First of all we compared MMP-2 expression between normal U87 and U87-PDGF (U87 cells which have been retrovirally modified to overexpress PDGF-B) (Figure 9A). Unexpectedly, this cell line presented a decrease of 70% in MMP-2 protein levels, with respect to parental U87 cells. Although PDGF is supposed to increase MMP-2 expression in the cell line in which PDGF is overexpressed and in which both autocrine and paracrine effects should be maximized, we found a drastical reduction of protein levels of pro-MMP-2. Thus, to try to understand if the protein decrease resulted from a low genetic activity, we analyzed MMP-2 mRNA levels in samples of U87 or U87-PDGF cells (Figure 1B). Despite the difference observed in protein levels, our results shown a higher MMP-2 mRNA expression in U87-PDGF cells than parental U87. The discrepancy between genetic activity and protein levels led us to suppose that an overstimulation of the PDGF pathway was producing a negative auto-feedback loop. However, the high level of mRNA detected in U87-PDGF implicates that high PDGF expression is also

Figure x. Positive and negative regulation of MMP-2 expression (+) Upregulation of MMP-2 ecpression; (-) Downregulation of MMP-2 expression

influencing MMP-2 at the protein synthesis level or in the way MMP-2 is stored inside the cells.

Considering that one of the genetic characteristic of glioma cells is PTEN mutation, and also considering that this protein is involved in AKT regulation, we decided to investigate PDGF influence in the PDGF-Pi3K-AKT pathway, extending our research to PTEN as a regulator of AKT and Programmed cell death protein 4 (PDCD4) which is regulated by AKT and downregulates AP-1 activity [155,156].

According to previous studies, U87-PDGF conditioned medium had a mean PDGF concentration of 353 ng/ml [157]. In order to mimic the autocrine production of PDGF-B by U87-PDGF, and to quantify the interaction between PDGF-B and MMP-2, parental U87 cells were treated with increasing quantities of conditioned medium, of 500 µL, 1000 µL, 1500 µL and 2000 µL (corresponding approximately to 175, 350, 525 and 700 ng/mL of PDGF-B), over 24 hours. U87-PDGF cells were used as a positive control and untreated parental U87 cells as a negative control. As shown in figure 1C, the progressive increase of conditioned medium led to a progressive increase of MMP-2 protein levels, while, as shown in figure 1A, U87-PDGF presented low MMP-2 levels. In the next set of experiments 1000µl of conditioned medium were considered sufficient and acceptable to mimic the normal quantity of PDGF-B secreted by U87-PDGF and 2000µl were used to double the amount of this factor present in the medium. Since, we also believed that U87-PDGF conditioned medium includes other factors that may influence the pathway under study, such as PDGF-A, to better understand influence of this

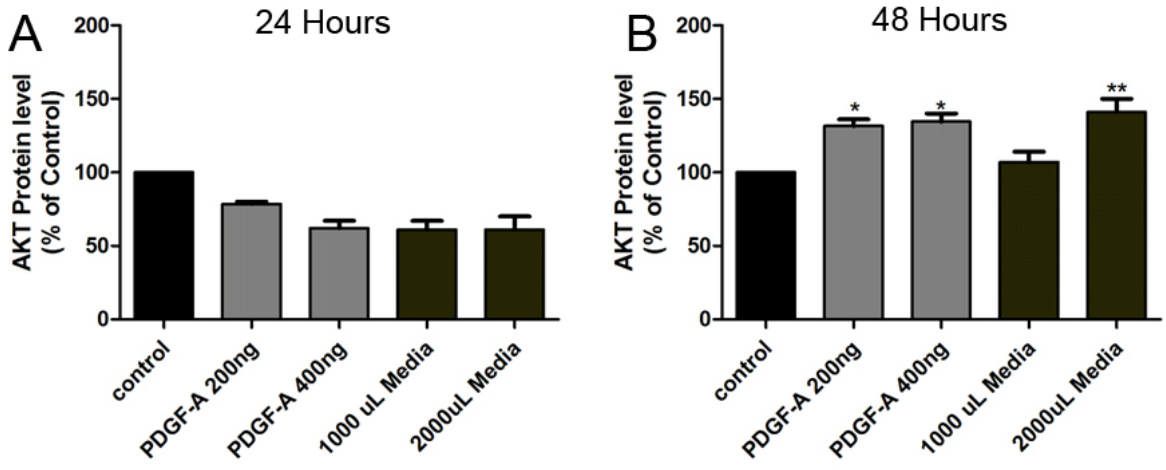

Figure 10. AKT protein concentration at 24 and 48 hours. U87 cells was plated in 12-well plates and treated with 200 ng/µL and 400 ng/µL of PDGF-A dissolved in 2000µl of DMEM and 1000µl, and 2000µl of U87-PDGF conditioned medium with addiction 250µl of DMEM maintained in culture for 24 hours and re-treated with same conditions. Proteins was extracted and quantificated after 24 hours (**A**) and 48 hours (**B**).

growing factor, we incorporated in our tests two new conditions: parental U87 treated with 200 ng/µL and 400 ng/µL of PDGF-A dissolved in DMEM.

Another important factor to consider was the influence of treatment time on the pathway. In fact, we supposed that increasing the exposition of the cells to PDGF contributed to the increase of MMP-2 levels through a linear dynamic range. Therefore, we proceeded to treating parental U87 with two conditioned medium administrations, the first at following cell plating and a second one after 24 hours in culture, extracting protein respectively after 24 and 48 hours. With these new conditions we started to investigate the other intervenients in the PDGF pathway as described below.

As mentioned before, *AKT*, also known as Protein Kinase B (PKB), is one of the most important effectors of PDGF stimulation. In fact this growing factor, though its receptor, is able to phosphorilate Phosphoinositide 3-kinase (Pi3K). This kinase is responsible for the phosphorilation of many substrates included Phosphatidylinositol 4,5-bisphosphate (PIP2), which is converted in Phosphatidylinositol (3,4,5)-trisphosphate (PIP3) on the inside surface of the cellular membrane where AKT is activated. As a consequence of PDGF stimulation, we observed that AKT presented an anomalous behavior. After 24 hours of treatment, the protein levels decreased to 78.50% in the 200nM PDGF-A condition, 62% in the 400nM PDGF-A condition, 61% in the presence of 1000µl U87-PDGF conditioned medium and 61% in the presence of 2000µl U87-PDGF conditioned medium (Figure 10A). This behavior can be explained by the presence of an initial positive feedback on a protein inhibitor which in turn decreased the PDGFR influence on

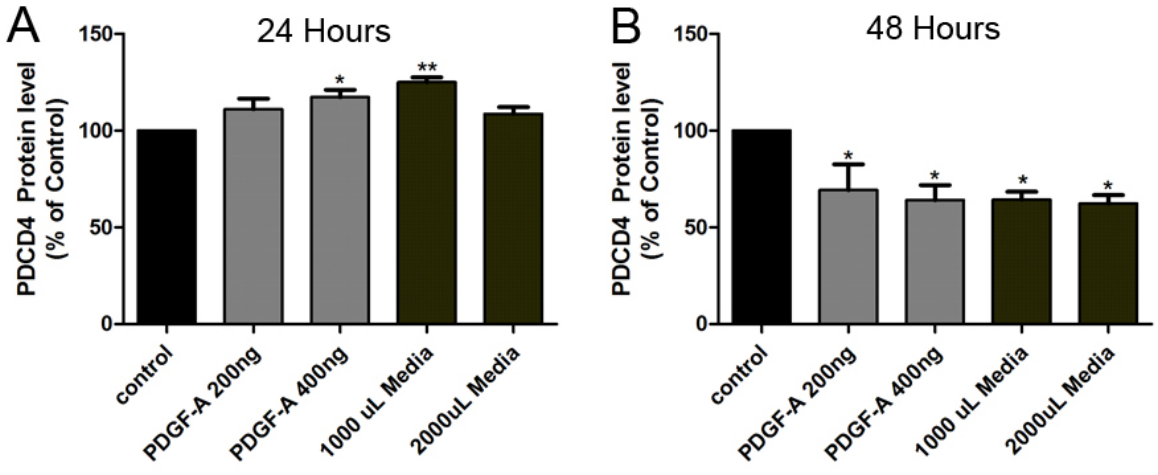

Figure 11. PDCD4 protein concentration at 24 and 48 hours. U87 cells was plated in 12-well plates and treated with 200 ng/µL and 400 ng/µL of PDGF-A dissolved in 2000µl of DMEM and 1000µl, and 2000µl of U87-PDGF conditioned medium with addiction 250µl of DMEM maintained in culture for 24 hours and re-treated with same conditions. Proteins was extracted and quantified after 24 hours (**A**) and 48 hours (**B**).

its intracellular effectors. One of the best candidates for this initial regulation is Transforming Growing Factor - ß (TGF-ß), which was shown to regulate PDGF-B-mediated activation in vascular smooth muscle cell proliferation through its interaction with F-actin stress fibers [158]. However, its role in U87 is still unknown and was not the subject of our study.

After 48 hours of PDGF stimulation, we observed that this supposed inhibition lost its effect and AKT levels, as expected, presented a massive increase with respect to untreated U87, with the 200nM PDGF-A condition showing a protein increase of 131.5%, 400nM PDGF-A showing an increase of 134,5% and 1000µL and 2000µl of conditioned medium showing 107.5% and 136.0% increases respectively (Figure 10B).

Another important component of this pathway, PDCD4, is a target of AKT. Our data suggest how the increasing and decreasing of this protein is a direct consequence of the fluctuations in AKT levels. In the 24 hours experiment PDCD4 was shown to be up-regulated with respect to control, following the down-regulation of AKT during the same time period. In the 200 and 400nM PDGF-A treatment the increase of this protein was of 115% and 120% respectively; in 1000µl of conditioned medium was 123% and in 2000µl of conditioned medium was 110%. In our opinion, this behavior reflects the linear influence which exist between AKT and PDCD4 (Figure 11).

Regarding PTEN, this protein should present an inactivating mutation in GBM cells, as described for many cellular models of this disease.

medium treatment. After 24 hours, PTEN levels were slightly upregulated in all the

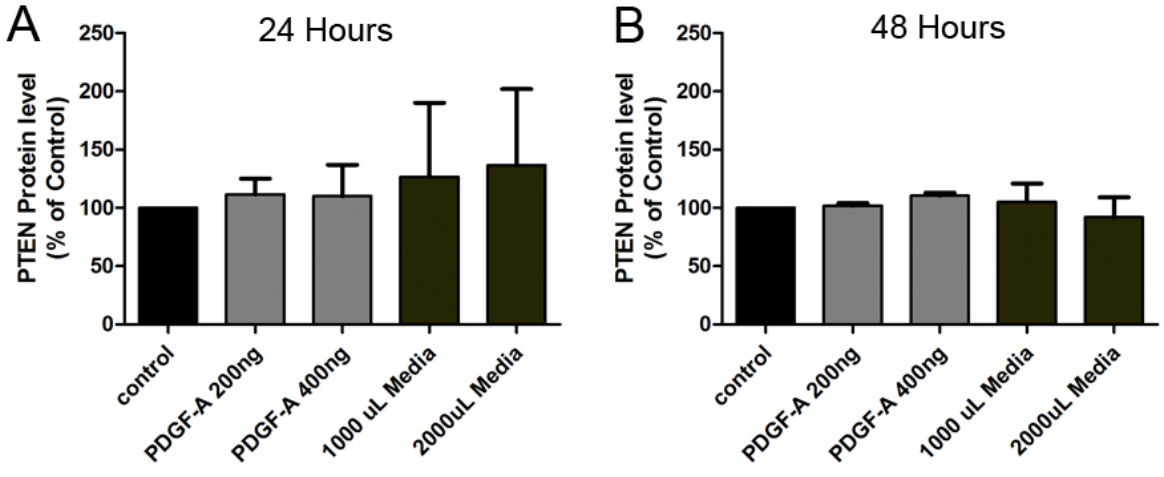

Figure 12. PTEN protein concentration at 24 and 48 hours. U87 cells was plated in 12-well plates and treated with 200 ng/µL and 400 ng/µL of PDGF-A dissolved in 2000µl of DMEM and 1000µl, and 2000µl of U87-PDGF conditioned medium with addiction 250µl of DMEM maintained in culture for 24 hours and re-treated with same conditions. Proteins was extracted and quantified after 24 hours (**A**) and 48 hours (**B**).

conditions, although both PDGF-A treatments were shown to be less efficient in mediating this upregulation, increasing the protein levels only by 10%. On the other hand, 1000µl and 2000 µl of conditioned medium increased PTEN levels to 126% and 136%, respectively but not in a statistically significant way. This behavior reflected the observed downregulation of AKT in the same interval of time. Furthermore, after 48 hours treatment, although PDGF-A treatment did not show a relevant influence in PTEN levels, PDGF conditioned medium exhibited a slight tendency to downregulate PTEN since the treatment with 2000µl led to a 10% decrease in protein levels (Figure 12). This specific response, together with the observed AKT behavior, led us to consider that PTEN was not completely inactivated. Two suppositions can be done regarding this particular behavior. First, there is the possibility that PTEN mutations may influence just the activity of the protein, but still allow the interaction with other regulatory molecules. This theory admits two conditions, 1) PTEN can be downregulated by PDGF by a unspecific mechanism and 2) AKT levels are only linked to the direct stimulation by PDGF, since the PTEN mutation avoids any negative feedback on PIP2. A second supposition regarding this peculiar response considers that the PTEN mutation may have a heterozygous nature. In this situation the non-mutated PTEN can help glioma cells preserve part of the negative feedback on PIP2. This behavior can be explained considering that in the 48 hours condition, in 2000 µl samples, we can observe a PTEN decrease of around 30% with respect to the 24 hours condition and a similar increase in AKT levels.

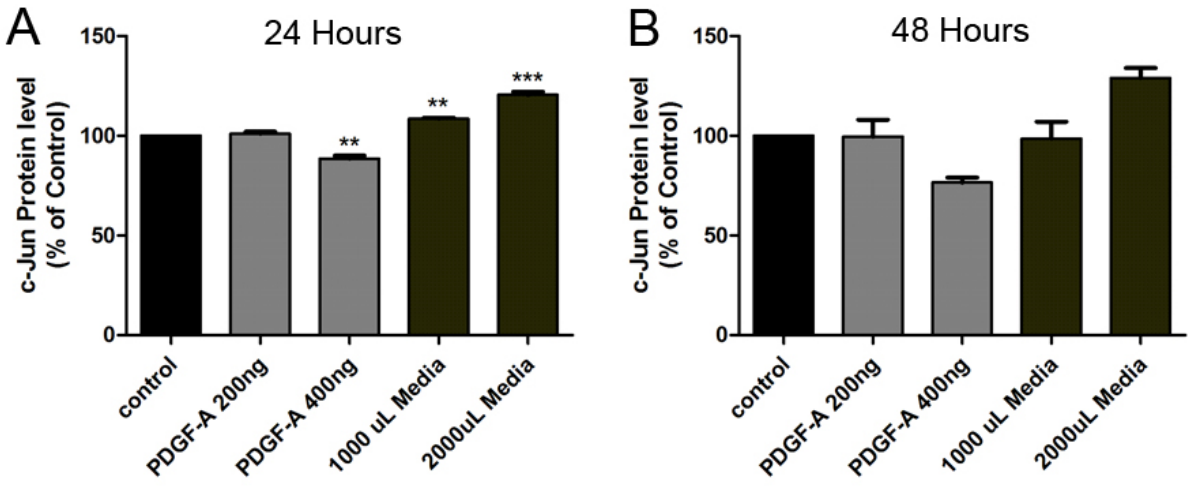

Figure 13. c-Jun protein concentration at 24 and 48 hours. U87 cells was plated in 12-well plates and treated with 200 ng/µL and 400 ng/µL of PDGF-A dissolved in 2000µl of DMEM and 1000µl, and 2000µl of U87-PDGF conditioned medium with addiction 250µl of DMEM maintained in culture for 24 hours and re-treated with same conditions. Proteins was extracted and quantified after 24 hours (**A**) and 48 hours (**B**).

As described previously, c-Jun can positively stimulate MMP-2 gene activity through the interaction with Sp1, as a result of MAPK cascade stimulation. This signaling cascade begins with Ras stimulation through PDGFR. We decided to investigate this pathway to clarify the possibility of a synergistic interaction between the two branches of the PRGFR pathway (AKT and c-Jun pathways). c-Jun has shown a particular behavior in response to our treatment. After 24 hours protein levels were 101% and 88.5%, for 200nM and 400nM PDGF-A samples, respectively and 108.5% for 1000 µl conditioned medium samples, while the 20000 µl samples showed an increase of c-Jun levels to 120%. After 48 hours, unexpectedly, c-Jun levels in the first tree samples were 99%, 76.5% and 98.5% respectively, while in the 2000 µl conditioned medium samples they increased to 129% (Figure 13). This results led us to believe that to increase the concentration of c-Jun and, in consequence, its activity is necessary a high level of PDGF. Moreover, despite the AKT pathway which was shown to present a initial negative regulation, the increase in c-Jun activity is linearly dependent of stimulation with PDGF.

Comparison between U87-PDGF and parental U87, regarding the protein levels analyzed previously can clarify the long term influence of PDGF on these pathways. As shown by the results in figure 3 U87-PDGF presented an upregulation of AKT levels 24 hours after plating to 159%, while PDCD4 showed a downregulation to 77.5% and PTEN presented an increase to 113%. After 48 hours in culture, protein levels in U87-PDGF presented negligible differences compared to parental U87 (AKT: 101%, PDCD4: 102%, PTEN: 100,5%). We propose that this behavior can be explained taking in consideration that during the first 24 hours the cells are not highly confluent and PDGF production is adequate to produce only an autocrine interaction due to an increase in AKT levels and a decrease PDCD4 levels. After the first 24 hours a full growing condition promotes the activation of proliferation pathways, while after 48 hours cell confluence is enough to favor cell to cell interactions that activate a negative feedback on these pathways.

As a final target of this pathway, we proposed that MMP-2 levels are influenced only by the AKT pathway in PDGF-A stimulated cells and 1000µl conditioned medium experimental samples while 2000µl conditioned medium samples the high levels in the medium led to a significant increase in MMP-2, due to the additional stimulation of the c-Jun pathway by PDGF. In addiction our results have shown that MMP-2 does not present a linear interaction with PDGF, as supposed in preliminary experiments.

After a 24 hours stimulus of PDGF-A or U87-PDGF conditioned medium, the pro-form of MMP-2 was upregulated in all samples, to 137% in 200nM and 205% in 400nM PRGF-A, 112% in 1000µl conditioned medium samples and 136% in 2000µl of conditioned medium, results that reflected the experiments described previously (Figure 14A). Surprisingly, after the 48 hours stimuli, pro-MMP-2 levels have shown a decrease to 93% in 200nM PDGF-A samples, 118% in 400nM PDGF-A samples and 100.5% in 1000µl conditioned medium with respect to pro-MMP-2 levels after 24 hours stimulus. However the 2000µl conditioned medium samples showed an increase to 155% (Figure 14B).
To better understand this behavior we also compared the pro-form concentration with the active protein levels. At 24 hours, the levels of the 64 kDa protein were 110% and

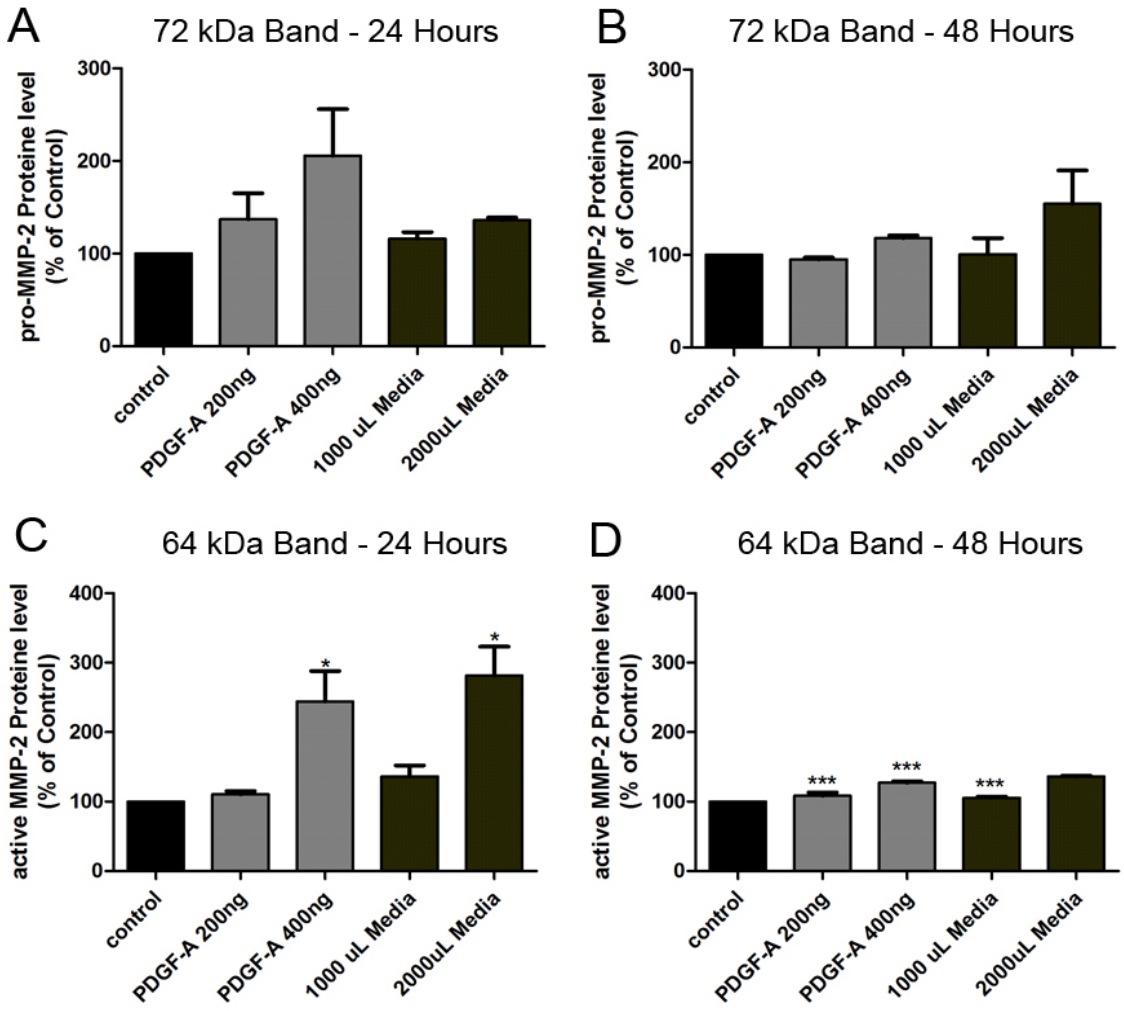

Figure 14. MMP-2 protein concentration at 24 and 48 hours. U87 cells was plated in 12-well plates and treated with 200 ng/µL and 400 ng/µL of PDGF-A dissolved in 2000µl of DMEM and 1000µl, and 2000µl of U87-PDGF conditioned medium with addiction 250µl of DMEM maintained in culture for 24 hours and re-treated with same conditions. Proteins was extracted and quantified after 24 hours (**A** and **B**) and 48 hours (**B** and **D**). **A)** 72 kDa pro-MMP-2 protein concentration after 24 hours **B)** 72 kDa pro-MMP-2 protein concentration after 48 hours **C)** 64 kDa active MMP-2 protein concentration after 24 hours **D)** 64 kDa active MMP-2 protein concentration after 48 hours

244% in 200 and 400nM PDGF-A samples and 136% and 281% in 1000µl and 2000µl conditioned medium samples. In the 48 hours conditions, these values decreased showing a similar tendency to the pro-form MMP-2 protein (200nM PDGF-A samples: 108%; 400nM PDGF-A: 127%; 1000µl conditioned medium: 105%; 2000µl conditioned medium: 136%) (Figure 14C, 14D).

U87 cells response to 2000µl conditioned medium treatment confirmed our supposition that the activation of both AKT and c-Jun pathways is stimulated by high levels of PDGF. These results also illustrate how PDGF has the ability, on one hand, to increase the MMP-2 pro-form levels, as result of the positive a interaction of its pathways with the MMP-2 gene and, on the other hand, to stimulate the activation of MMP-2, leading to an increase of active-form. It is also true that in the first tree conditions, both active- and pro-form of MMP-2 presented a decrease after 48 hours. This behavior may mean that the PDGF stimulus activates MMP-2 more efficiently than it is able to stimulate genetic activity to replace the pro-form converted in active-form. Even in the last condition high gene expression is not sufficient to replace MMP-2 converted to the active-form protein that is rapidly inactivated without the presence of a substrate.

Furthermore, another consideration can be made regarding this behavior: active- and pro- form MMP-2 can be found in two different pools inside the cells, probably with the active form present in vesicles. Whit this perspective, the decrease observed at 48 hours can be described as the ability of the cells to extrude vesicles faster than they can replace them.

To clarify these suppositions we decided to analyze MMP-2 mRNA levels in a shorter

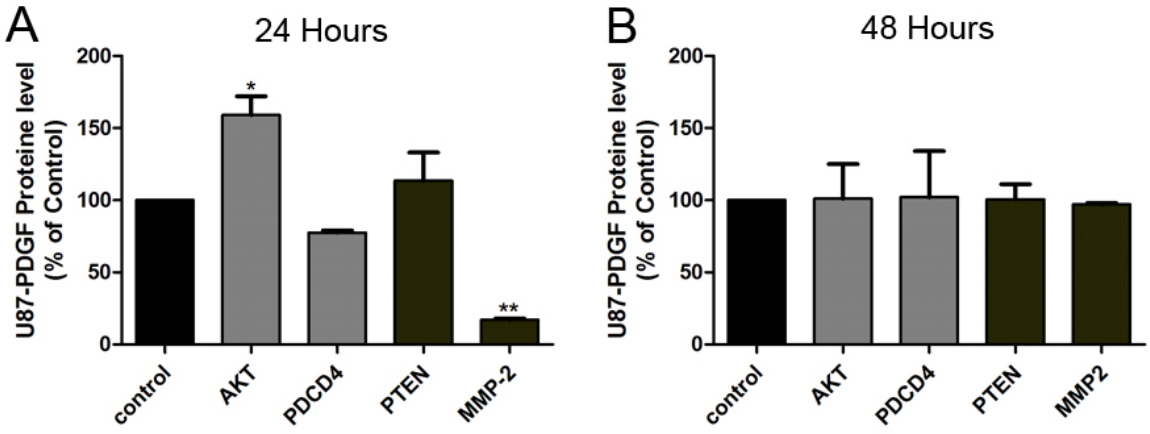

Figure 15. U87-PDGF protein concentration at 24 and 48 hours. U87 cells was plated in 12-well plates and treated with 200 ng/µL and 400 ng/µL of PDGF-A dissolved in 2000µl of DMEM and 1000µl, and 2000µl of U87-PDGF conditioned medium with addiction 250µl of DMEM maintained in culture for 24 hours and re-treated with same conditions. Proteins was extracted and quantified after 24 hours (**A**) and 48 hours (**B**).

time gap.

We performed RNA extraction from the 1000µl and 2000µl conditioned medium samples, after 24, 36, and 48 hour of incubation. Moreover, we decided to consider a new condition in which cells were treated only once after plating, to analyze the possibility that a PDGF massive stimulation could activate an unknown negative feedback loop (in figure 8 we refer to this conditions as 48-t1 for cells treated immediately after plating and after 24 hours and 48-t0 for samples treated only after plating).

The observed results have confirmed our supposition showing a comparable behavior between treatment with 1000µl and 2000µl of conditioned medium. Regarding 1000µl conditioned medium samples, the mRNA levels after 24 hours were 38% of control, after 36 hours these levels decreased even further to 15% and in the 48-t1 condition increase to 114% at 48 hours. Surprisingly, in the 48-t0 condition, the mRNA amount at 48 hours was 170% of control. We found the same fluctuations in the 2000µl conditioned medium samples, where MMP-2 mRNA levels were 38% at 24 hours, 15% at 36 hours, 108% at 48 hours in the 48-t1 condition but were 290% in 48-t0 (Figure 16).

0According to our interpretation of these results, although PDGF is able to activate its receptor, an unspecified negative feedback loop generates a stimulus-response delay on the AKT pathway reducing MMP-2 gene expression. However, this stimulus is also able to promote activation of MMP-2 at 24 hours, producing an increase in the 64 kDa active-form. While the remaining mRNA is being converted into protein, gene activity is not sufficient to replace depleted mRNA pool, which may explain the 24 hour MMP-2 mRNA levels in both conditions and the subsequent decrease after 36 hours. After 48 hours, in

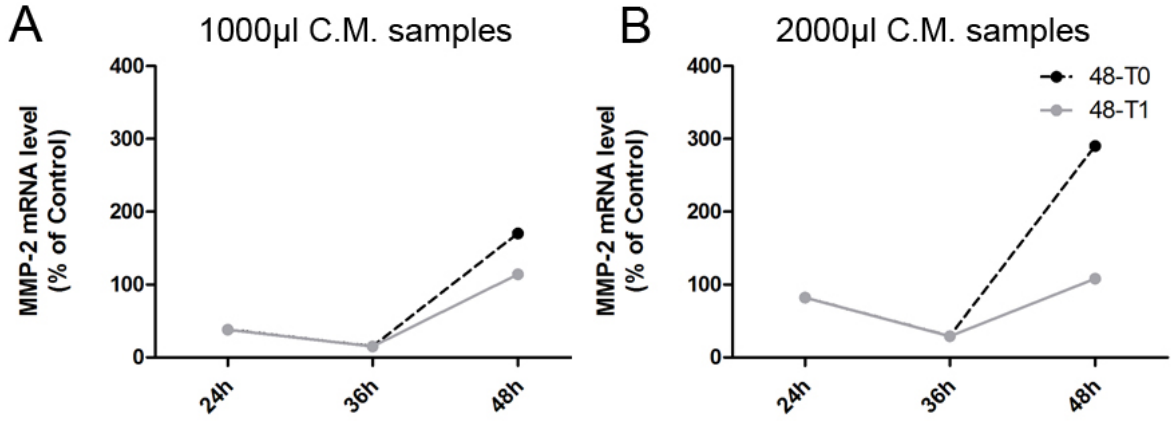

Figure 8. MMP-2 mRNA concentration in progressive time conditions. U87 cells was plated in 12-well plates and treated with 1000µl (**A**), and 2000µl (**B**) of U87-PDGF conditioned medium with addiction 250µl of DMEM. mRNA was extracted after 24, 36 and 48 hours. In black is reported 48 hours conditions treated one at plating time, in gray is reported 48 hours conditions treated at plating time and after 24 hours.

the 48-t1 conditions, PDGF concentration is sufficiently high to overcome the negative feedback loop and increase MMP-2 gene expression. However, as shown in Figure 8, a single stimulus with PDGF (48-t0) was more efficient in increasing MMP-2 mRNA levels. A possible explanation for this phenomenon may be the existence of a limiting feedback mechanism that reduces cell response in the presence of a massive PDGF stimulus. Evidence of a time incongruence between the PDGF stimulus, genetic activity and protein production supports our supposition about the existence of an intracellular pool of pro-MMP-2, ready to be used by the cells in response to PDGF stimulation, to rapidly originate active MMP-2.

4.3 Evaluation of SNALP internalization

The ability of Chlorotoxin (Cltx) to recognize and bind glioma cells, in which the protein MMP-2 is supposed to be involved, was extensively demonstrated by a wide number of research studies.

The choice to use Cltx as a ligand in SNALP formulations aimed to improve several aspects of liposome-based glioblastoma therapies, since the presence of a tumour-specific cell surface epitope in this molecule helps to induce specific internalization in glioma cells and subsequent release of the therapeutic substances from the liposomes.

The results presented in the previous section have shown how a positive stimulus of PDGF can lead to an increase in the active and zymogen form of MMP-2. In order to proceed with our studies, the subsequent logic step was to design an adequate protocol to induce a decrease in the levels of this metalloproteinase in glioma cells, aiming at

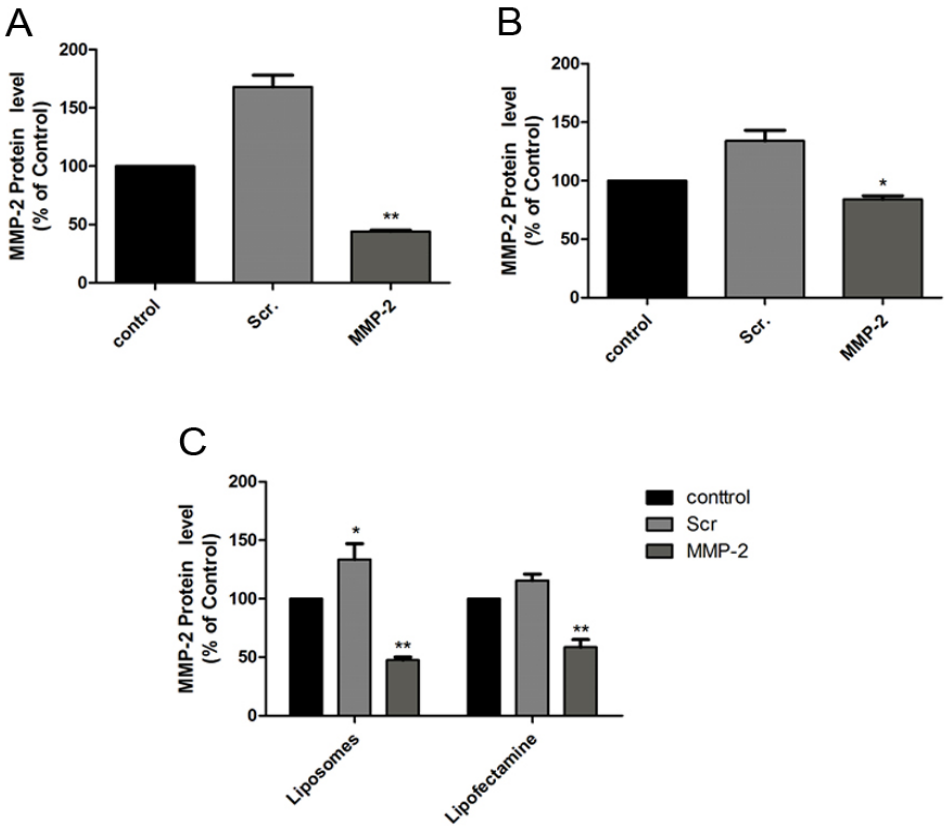

Figure 17. MMP-2 protein levels following U87 and GL261 transfection with anti-MMP2 siRNAs. U87(**A**, **C**) and GL261 (**B**) cells were plated in 12-well plates. After 24 hours, the cells were transfected with **Lipofectamine®** (**A**, **B**, **C**) or transferrin-associated liposomes (**C**) complexed with 50nM of anti-MMP-2 siRNAs (MMP-2) or scramble siRNAs (Scr.). The cells were manteined in culture for 48 hours before protein extraction. MMP-2 protein levels were quantified by western blot. Result are expressed as the percentage of MMP-2 protein levels with respect to untreated U87 or GL261 cells (control) and are representative of three independent experiments. * $p<0.05$, ** $p<0.01$

establishing a qualitative and quantitative relationship between MMP-2 levels on the outside of glioma cells and Cltx-SNAPL internalization.

In order to produce a decrease in MMP-2 levels, we decided to employ the RNAi machinery to silence the mRNA of MMP-2. For this purpose, a pre-validated anti-MMP-2 siRNA sequence was chosen and introduced in glioma cells using non-viral lipid-based delivering particles. In addition, a scramble siRNA sequence (non targeting sequence) was used as a control in all transfection experiments, in order to identify any possible unspecific effects due to the transfection process *per se*.

In our first experiment we compared MMP-2 protein levels in U87 parental cells and GL261 cells treated with Lipofectamine® complexed with the anti-MMP-2 siRNA or the scrambled siRNA at a concentration of 50nM. Our results showed that both cell lines presented a positive response to the transfection process. However, U87 cells were more responsive to the treatment, showing a decrease of 56% in MMP-2 levels, while GL261 presented decrease of only 16% (Figure 17A and 17B).

We also decided to compare, in the U87 cell line, the transfection efficiency of

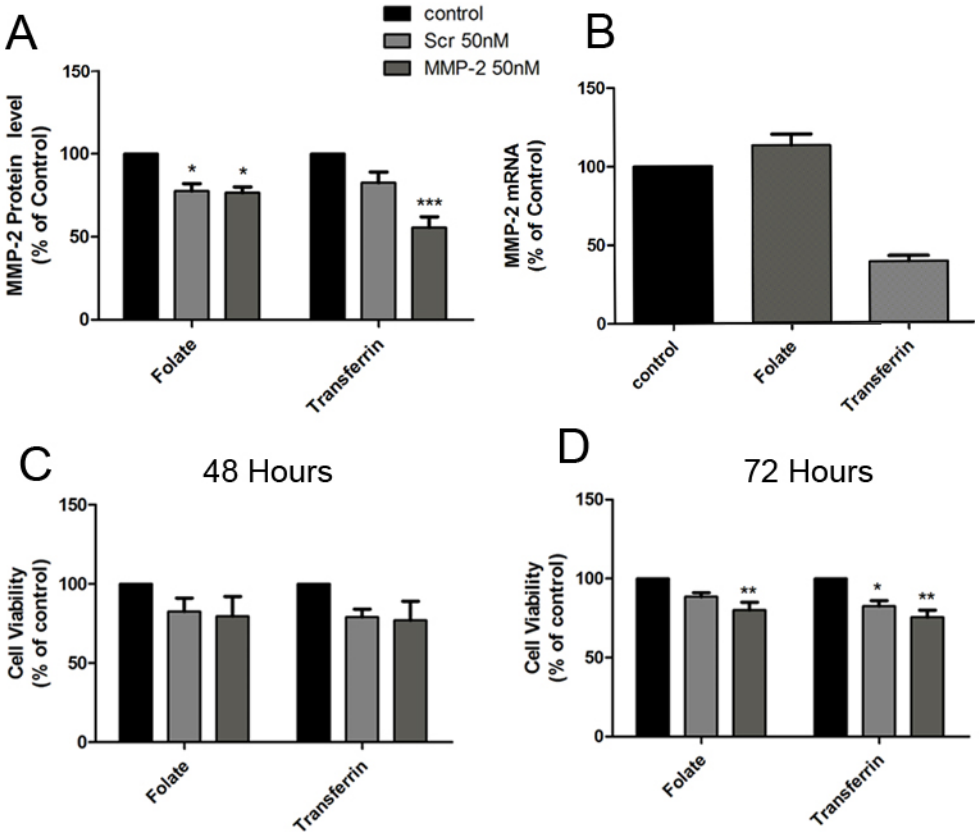

Figure 18. MMP-2 protein and mRNA levels following U87 transfection with anti-MMP2 siRNAs. U87 cells were plated in 12-well plates. After 24 hours the cells were transfected with folate- or transferrin-associated liposomes containing 50nM of anti-MMP-2 (MMP-2) or scramble (Scr.) siRNAs and mantained in culture for 48 hours before RNA extraction **(B)** or 72 hours before protein extraction **(A)**. MMP-2 protein levels were quantified by western blot while MMP-2 mRNA levels were quantified by a qRT-PCR. Cell viability was determined by the Alamar blue assay at 48 and 72 hours **(C, D)**. Result are expressed as the percentage of protein, mRNA or cell viability levels with respect to untreated U87 cells (control) and are representative of three indipendent experiments. * $p<0.05$, ** $p<0.01$

Lipofectamine® with that of DOTAP:Cholesterol liposomes, prepared as described in Material and Methods, and complexed with the targeting ligand tranferrin (Tf-lipoplexes). We used Holo-transferrin (Tf) as a ligand since several studies have confirmed that iron-associated Tf is able to increase the binding and internalization efficiency of lipoplexes *in vitro*, in particular in glioma cell lines.

We observed a decrease in protein levels for both formulations, to 47% in samples treated with Tf-lipoplexes and to 58% in samples treated withLipofectamine® (Figure 17C). Furthermore, cell viability tests presented negligible differences in the toxicity profile of these two conditions (data not shown). These results led us to consider Tf-lipoplexes as a valid alternative to Lipofectamine® to transfect glioma cells in future experiments.

To further confirm our choice of transfection vector we decided to compare MMP-2 downregulation produced by Tf-lipoplexes with that obtained using the same lipid formulation complexed with a different ligand. Folic acid (Fa) was used in these experiments, since its targeting potential has been already demonstrated in many tumor cell lines and many folate-drug conjugates have entered clinical trials for the treatment of several types of cancer [153].

Transfection experiments were performed with 50nM of anti-MMP-2 or scramble siRNAs in U87 cells. MMP-2 mRNA expression was analyzed 48 hours after lipoplex delivery, while protein levels were quantified after 72 hours and cell viability levels were analyzed at both time points (Figure 18).

Our results showed that Tf-lipoplexes were more efficient than Fa-lipoplexes in reducing both MMP-2 mRNA and protein levels, confirming our supposition that transferrin is a good ligand to promote lipoplex delivery in glioma cells. Indeed, MMP-2 protein levels in Tf-lipoplex-treated samples decreased to 55%, while in samples transfected with Fa-lipoplexes only decreased to 76.5%; MMP-2 mRNA levels were 112% for Fa-mediated transfection and 38.5% for Tf-mediated transfection. Finally, cell viability tests showed that both conditions presented negligible differences in terms of cytotoxicity, both at 48 and 72 hours (at 48 hours: Tf-lipoplexes: 79%; Fa-lipoplexes: 77% and at 72 hours Tf-lipoplexes: 80.5% and Fa-lipoplexes: 85.5%).

Once we delineated the transfection conditions regarding the vector and the ligand, the last element which required optimization was the siRNA concentration to be used in future experiments. It was necessary to identify which siRNA concentration presented the best balance between MMP-2 silencing, toxicity and unspecific effects. On the other

hand, it was also important to determine at which time point after transfection MMP-2 protein levels were lower, in order to choose the best moment to perform Cltx-SNALP transfection. With this in mind, experimental conditions were designed to transfect parental U87 cells with increasing concentration of siRNA, 25 nM, 50 nM and 100 nM, respectively, using Tf-lipoplexes. For each siRNA concentration, MMP-2 mRNA levels were measured 48 hours after transfection and MMP-2 protein levels were measured after 48, 72, and 96 hours, while cell viability was measured at each time point.

Cell viability tests (Figure 19) showed, as expected, that particle-mediated toxicity had a tendency to decrease with time. Higher toxicity values could be found for all samples at 48 hours, but were only significant for the 100nM MMP-2 and scramble conditions and for the 50nM scramble condition. After 72 hours, toxicity levels presented a tendency to

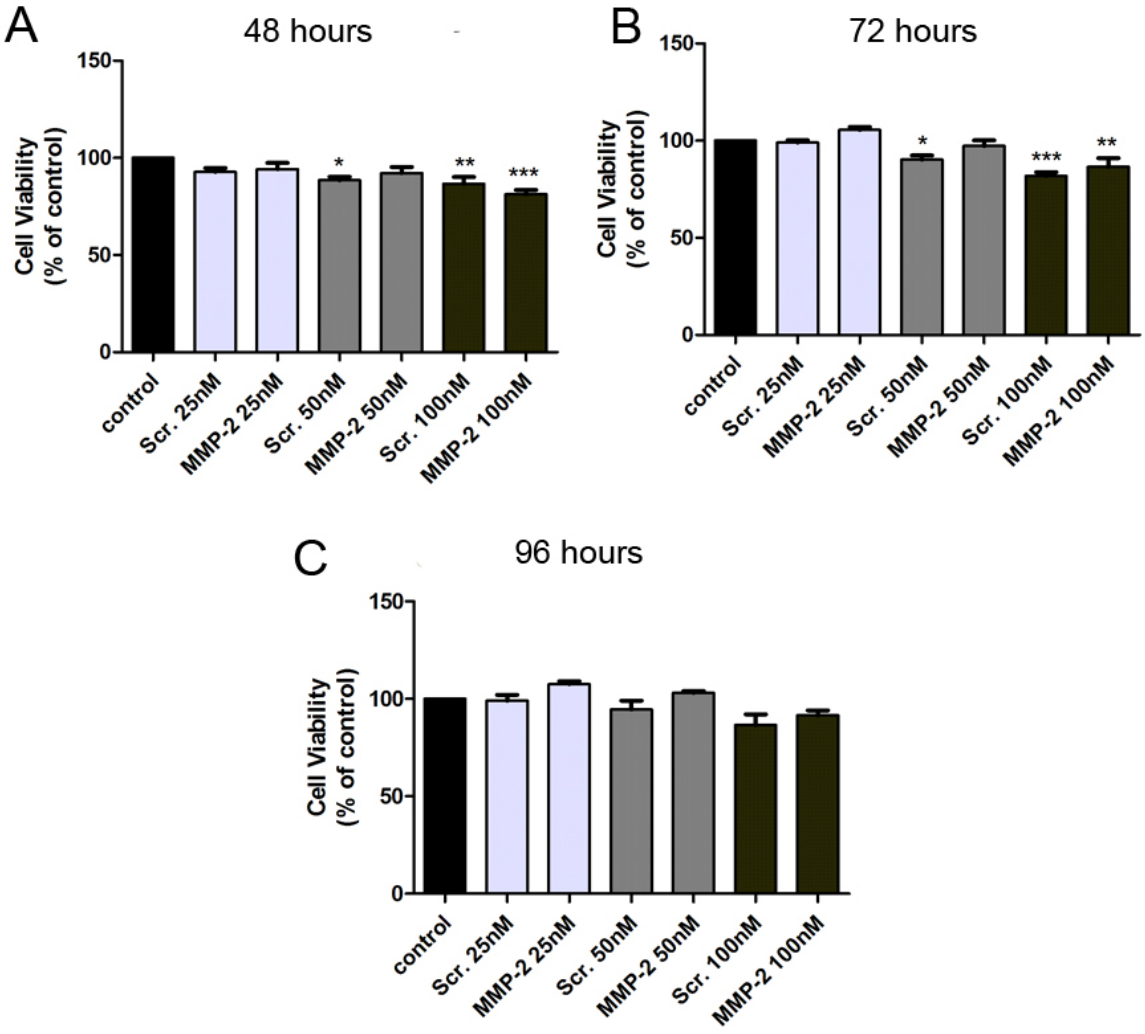

Figure 19. Cell viability following U87 transfection with different siRNA concentrations at different time points. U87 cells were plated in 12-well plates and, after 24 hours, were transfected with transferrin-associated liposomes containing 25nM, 50nM or 100nM of anti-MMP-2 (MMP-2) or scramble (Scr.) siRNAs. Cell viability was determinated by the Alamar blue assay 48 **(A)**, 72 **(B)** and 96 **(C)** hours after transfection. Result are expressed as the percentage of cell viability with respect to untreated U87 cells (control) and are representative of four indipendent experiments. * $p<0.05$, ** $p<0.01$, *** $p<0.001$

decrease, reaching negligible levels in all the conditions at 96 h after transfection.

Regarding MMP-2 protein levels, we found that after transfection the expected decrease in these levels followed a similar but inverse behavior to that found in the previous experiments using PDGF conditioned medium. In particular, we found that the time delay for protein decrease was inversely proportional to the siRNA concentration used in transfection. Forty-eight hours after transfection we found that MMP-2 protein levels were 78% in 25 nM MMP-2 siRNA-treated samples, 77% in 50nM samples and 76% in 100nM samples, which means that all siRNA concentrations showed negligible differences in terms of protein knockdown at this time point. However, after 72 and 96 hours, the knockdown behavior was different for each condition. MMP-2 levels in 25 nM conditions were of 80% and 84% at 72 and 96 hours. The other siRNA concentrations

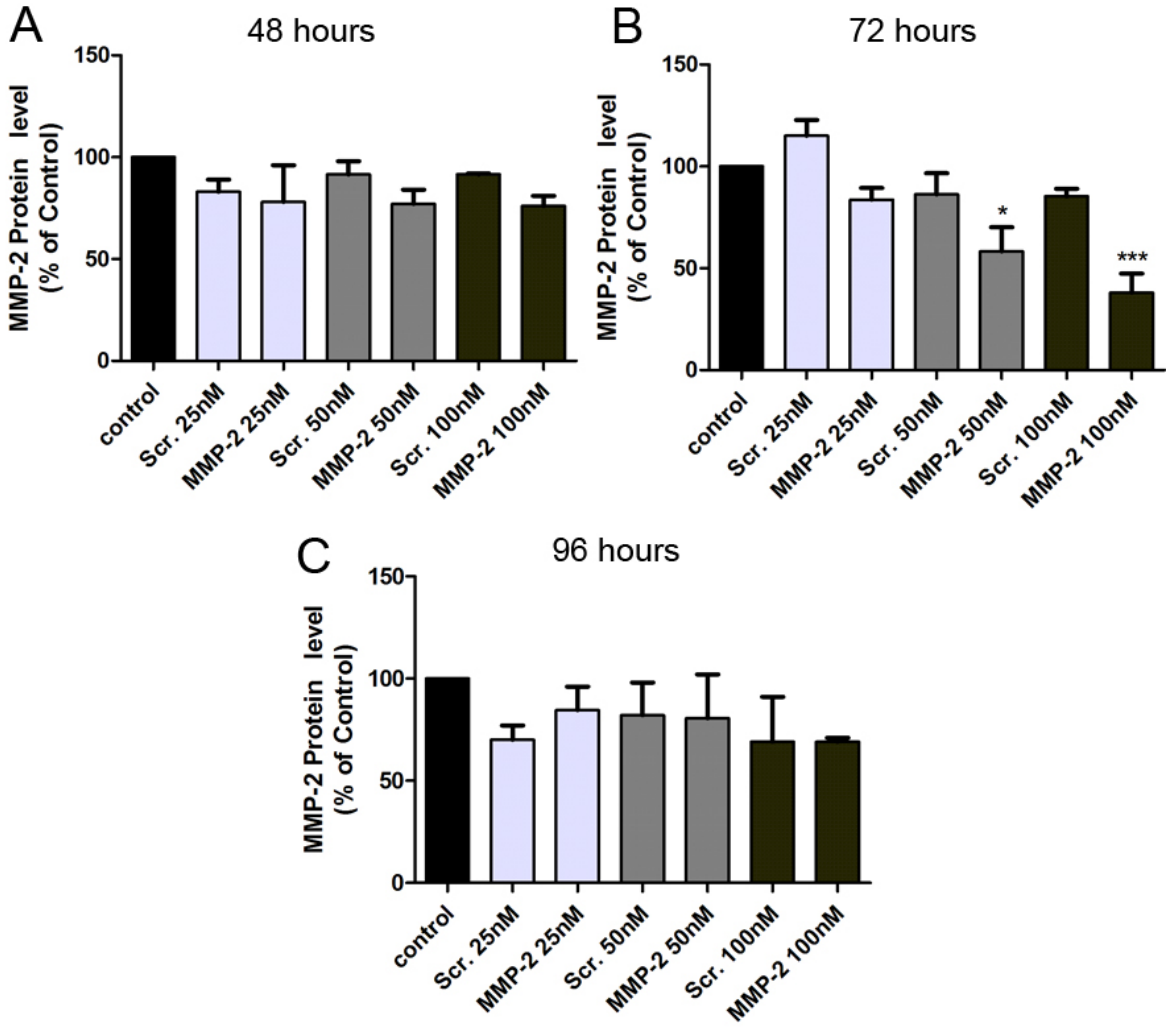

Figure 20. MMP-2 protein levels at different time points following transfection with different anti-MMP2 siRNA concentrations. U87 cells were plated in 12-well plates and, after 24 hours, trasfected with transferrin-associated liposomes containing 25nM, 50nM or 100nM of anti-MMP-2 (MMP-2) or scramble (Scr.) siRNAs. Cells were mantained in culture for 48 **(A)**, 72 **(B)** and 96 **(C)** hours before MMP-2 protein quantification by western blot. Result are expressed as the percentage of MMP-2 protein levels with respect to untreated U87 cells (control) and are representative of three indipendent experiments. * $p<0.05$, ** $p<0.01$, *** $p<0.001$

showed the lowest protein levels 72 hours after transfection and a tendency to restore normal MMP-2 levels after 96 hours (50nM: 53% at 72 hours and 80% at 96 hours; 100nM: 34% at 72 hours and 69% at 96 hours). None of the tested siRNA concentrations revealed concerning unspecific effects, since MMP-2 levels were not reduced significantly at any time point following transfection with the scramble siRNA (Figure 20).

In terms of mRNA levels (Figure 21), the ability of the different siRNA concentrations to decrease MMP-2 levels was not directly comparable with the protein results. In fact, MMP-2 mRNA presented a tendency to be upregulated in samples treated with 25nM of siRNAs 48 h after transfection and mRNA levels were lower in the 50 nM condition with respect to the 100nM condition (respectively 35% and 65%). Taken together, these results led us to choose the 50nM siRNA concentration and the 72 h time point as the optimal conditions to decrease both MMP-2 protein and mRNA levels in U87 cells.

We considered the discrepant results observed between MMP-2 mRNA and protein levels after transfection as an additional evidence in favor of our suppositions concerning the presence of an intracellular pool of MMP-2 in these cells. In addition, we also found evidence in the literature of the existence of membrane adherent vesicles, containing MMP-2 and the other components of the activation mechanism of this metalloproteinase, in the external side of the cellular membrane of human umbilical vein endothelial cells (HUVEC) [154]. Taking in consideration these results, we decided to investigate the existence of similar structures in the cell lines used in this work.

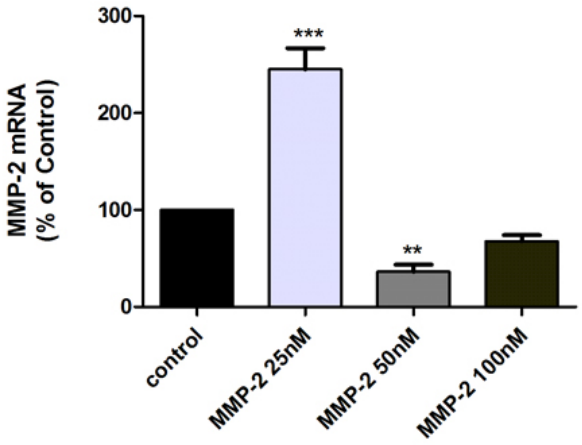

Figure 21. MMP-2 mRNA levels following U87 transfection with different concentrations of anti-MMP-2 siRNAs. U87 cells were plated in 12-well plates and transfected after 24 hours with transferrin-associated liposomes containing 25nM, 50nM or 100nM of anti-MMP-2 siRNAs. Folowing transfection, the cells were maintained in culture for 48 h before RNA extraction and MMP-2 mRNA quantification by qRT-PCR. Result are expressed as the percentage of MMP-2 mRNA levels with respect to untreated U87 cells (control) and are representative of three indipendent experiments. **p<0.01.

For this purpose, we performed a low speed centrifugation to separate culture medium from the cultured cells. We tested medium from three glioma cell lines: U87, U87 PDGF and GL261 and from HEK 293T cells, which served as a control. The cell supernatants were then subjected to ultracentrifugation, in order to separate the vesicles from the liquid components of the cell medium. We extracted and quantified protein in the vesicle fraction immediately after the centrifugation process and proceeded to determine the presence of MMP-2 in this fraction using Western Blot (Figure 22). Our results showed that, in all tested cell lines, the vesicles contained MMP-2, but this was particularly evident in U87 cells. In our opinion, these results help to justify how these cells are able to produce a delay on the MMP-2 pathway, following a positive or negative stimulus, resulting in lagged alterations in the MMP-2 mRNA and protein levels inside the cells.

Based in these preliminary experiments, we formulated a experimental protocol to efficiently modulate MMP-2 protein levels before SNALP transfection. In order to increase MMP-2 levels, we treated U87 cells with one administration of 1000 µl or 2000 µl of U87-PDGF conditioned medium immediately after plaiting and proceeded to incubate cells for 48 hours before performing SNALP internalization studies. In order to achieve the opposite result, the decrease of MMP-2 levels, we transfected U87 cells with Tf-associated liposomes complexed with 50nM of anti-MMP-2 siRNAs and maintained the cells in culture for 72 hours before SNALP delivery.

Aiming at assessing SNALP internalization, U87 cells were transfected with SNALPs containing FAM-labeled oligonucleotides and the intracellular FAM content was measured by flow cytometry 4 hours after particle delivery.

We first compared parental U87 with U87-PDGF cells. We were able to observe a

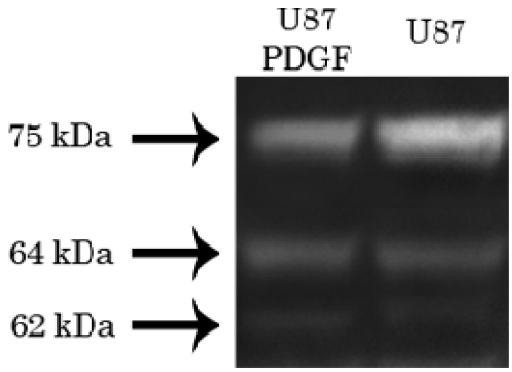

Figure 22. MMP-2 protein content in extracellular vesicles obtained from the culture medium of different cell lines. Medium from all cell lines was collected after 24 h of incubation in the presence of the cells and subjected to ultracentrifugation to separate the vesicle fraction. Following protein quantification, MMP-2 levels in the extracellular vesicle fraction were analyzed by western blot.

significant reduction in SNALP internalization (37,5%) in U87-PDGF cells (Figure 23), although this difference was not as high as expected considering the previous differences observed in MMP-2 levels (U87-PDGF presented a 70% reduction in MMP-2 protein levels with respect to parental U87 cells).

We also tested, in parental U87 cells, SNALP internalization following MMP-2 siRNA-mediated silencing or U87-PDGF conditioned medium treatment (Figure 23). We found that untreated cells, referred as control, presented anomalous lower internalization rates compared to other samples, therefore we compared our results with samples transfected with scramble siRNAs.

Our results show that U87 cells where MMP-2 was silenced before SNALP delivery presented a decrease of 17,5% in SNALP internalization (Figure 24A), while cells treated with U87-PDGF conditioned medium presented a modest increase in intracellular FAM levels of 5.5% for the 1000µl concentration and 9% for the 2000µl concentration (Figure 24B). These results are in agreement with the discrepancy observed between MMP-2 levels and SNALP internalization in parental U87 and U87-PDGF cells.

A similar behavior was found in both U87-PDGF and GL261 cells. In fact, U87-PDGF cells treated with siRNAs anti-MMP2 presented a decrease of 14.8% in intracellular FAM fluorescence levels, while for GL261 a negligible decrease of 3% could be observed. These results led us to conclude that although MMP-2 modulation slightly influenced Chlorotoxin binding to U87 cells, this protein cannot be the only required element involved in SNALP internalization. To test this theory, we decided to intervene in the MMP-2 activation mechanism by modulating the protein levels of the MMP-2 inhibitor TIMP-2 using RNA interference (Figure 24C). We employed a similar transfection

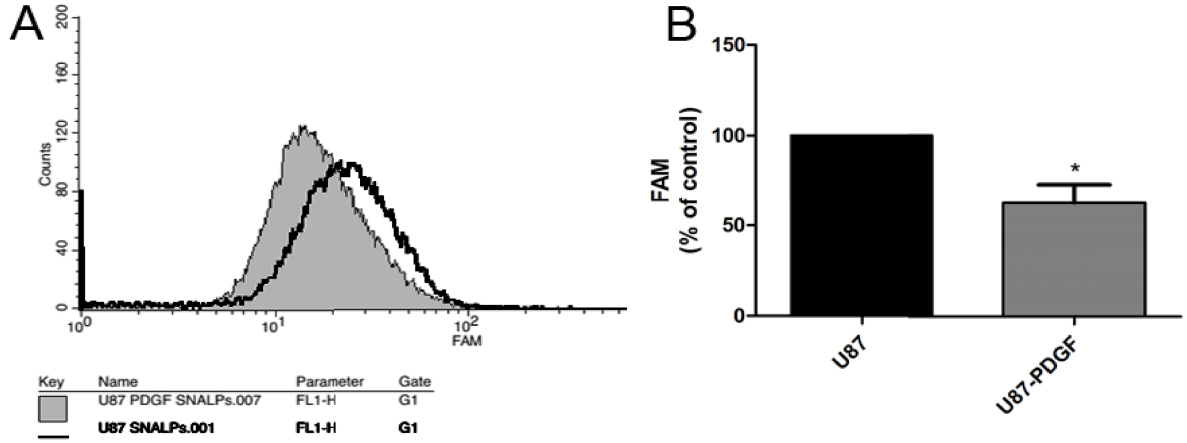

Figure 23. SNALP internalization in parental U87 and U87-PDGF cells. Parental U87 and U87-PDGF cells were plated in 12-well plates. After 24 hours, the cells were transfected Cltx-targetted SNALP particles containing FAM-labelled oligonucleotides The intracellular FAM content was quantified by flow cytometry **(A)**. Result are expressed as the percentage of the fluorescence geometric mean of U87-PDGF cells with respect to parental U87 cells and are representative of two indipendent experiments. * $p<0.05$.

protocol to the one developed for MMP-2 silencing and were able to obtain a significant increase in SNALP internalization in all tested cell lines. U87 parental cells presented an increase of 36% in intracellular FAM fluorescence following TIMP-2 silencing, while U87-PDGF and GL261 cells presented increases of 16,5% and 38%, respectively (Figure 8C). In our opinion, these results suggest that other members of the MMP-2 regulatory complex, such as TIMP-2, can also contribute to Cltx-mediated SNALP internalization, and open new avenues of research concerning the properties and mechanism of action of this targeting ligand.

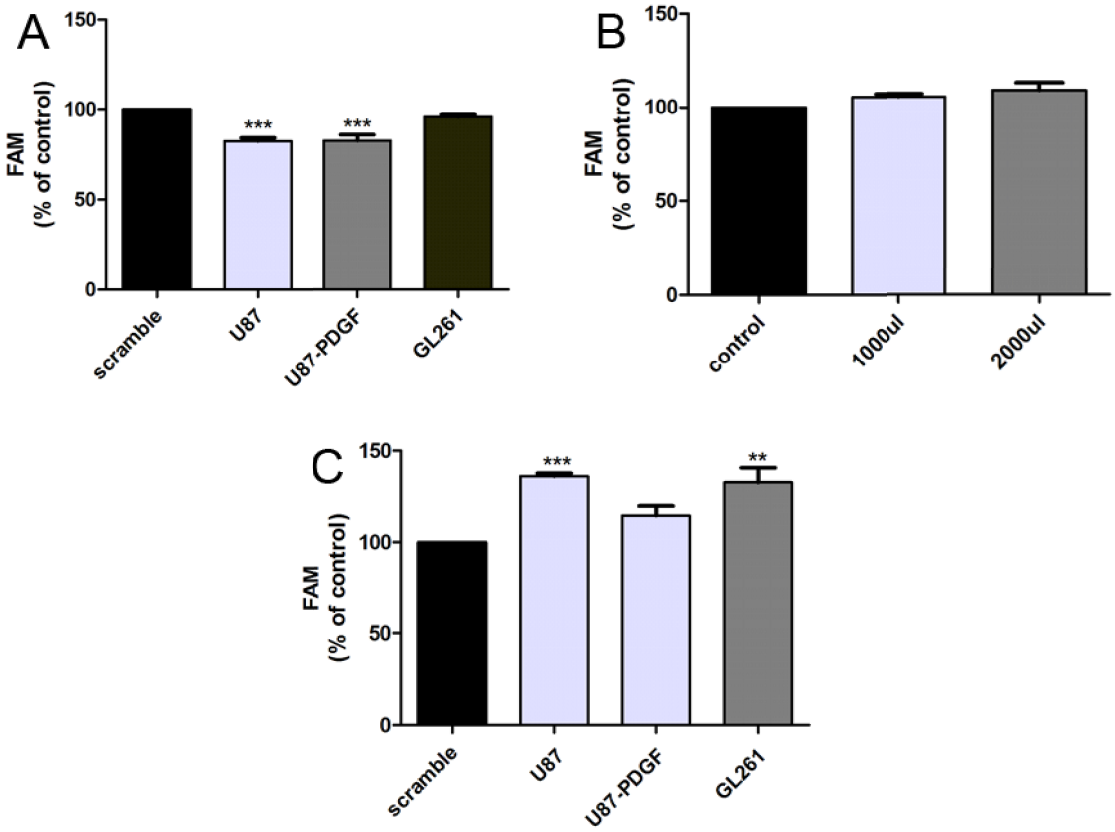

Figure 24. SNALP internalization following modulation of MMP-2 protein levels. Parental U87, U87-PDGF or GL261 cells were plated in 12-well plates and transfected after 24 hours with Tf-associated liposomes containing 50nM of anti-MMP-2, anti-TIMP-2 or scramble siRNAs **(A** and **C**). In parallel experiments, U87 cells were treated with 1000 or 2000µl of U87-PDGF conditioned medium **(B)**. The cells were mantained in culture for 72 hours **(A** and **C)** or 24h **(B)** before cell transfection with Cltx-targetted SNALP particles containing FAM-labelled oligonucleotides The intracellular FAM content was quantified by flow cytometry. Result are expressed as the percentage of the fluorescence geometric mean of MMP-2 or TIMP-2 silenced cells with respect to scramble transfected cells **(A** and **C)** or as the percentage of the fluorescence geometric mean of conditioned medium treated cells with respect to parental U87 cells **(B)** and are representative of two independent experiments**.** ** $p<0.01$ and *** $p<0.001$.

Conclusions and future perspectives

5. Conclusions and future perspectives.

The results presented in this work led to the following main conclusions:

The first part of this work concerned the influence of PDGF stimulation on MMP-2 and the characterization of the pathways involved the regulatory mechanisms of this metalloproteinase. We observed that in U87 glioma cells, MMP-2 protein levels can be regulated by PDGF trough both the AKT and the c-Jun pathways. The observed upregulation of AKT levels upon PDGF stimulation was supposed to have a positive influence on MMP-2 gene expression, but was also shown to activate a negative feedback loop through PDCD4, which repressed AP-2 positive regulation of the MMP-2 gene. Moreover, it was shown that PDGF can be related to a direct, albeit modest, increase in c-Jun protein levels. Since c-Jun has the ability to upregulate the SP-1 protein, which is an enhancer of MMP-2 gene activity, this transcription factor was also shown to contribute to MMP-2 expression and to constitute a viable second pathway by which PDGF can regulate MMP-2 levels.

In this work, we also demonstrated the presence of a latency period between PDGF stimulation and the activation of the AKT or c-Jun pathways. This observation led us to suppose the existence of an initial negative regulatory mechanism that could explain the low levels of MMP-2 mRNA observed after 24 hours of stimulation and the notable increase observed in MMP-2 gene expression after 48 hours.

In what concerns PTEN, another molecular intervenient in the MMP-2 regulatory pathways, despite reports stating that this protein is mutated in glioblastoma, we observed level fluctuations compatible with AKT-mediated protein downregulation, which led us to suppose that PTEN mutation can present a heterozygous character or it can only partially compromise the activity of the protein, not affecting directly all of its regulatory functions.

Overall, we observed that MMP-2 levels are positively regulated by PDGF in parental U87 cells. However, this regulation was shown to be deficient in U87 cells which have been retrorvirally modified to overexpress PDGF. We believe that the presence of continuous autocrine and paracrince stimulation led to the sustained activation of a negative feedback loop which downregulates MMP-2 protein levels in the modified cell line. Moreover, we considered that the discrepancy in MMP-2 mRNA levels between U87

cells stimulated with PDGF two times (immediately after plating and after 24 hours in culture) and U87 cells stimulated only once (immediately after plating) constitutes another evidence of a limiting feedback mechanism activated by massive PDGF stimulation.

Finally, and still concerning the regulation of MMP-2 cellular levels in glioma cells, we were able to detect the presence of extracellular vesicles containing MMP-2 in the culture medium of both U87 and GL261 glioma cell lines. The accumulation of MMP-2 in these structures reveals the presence of a second pool of intracellular MMP-2 protein, separated from the cytoplasmic MMP-2, which can help to explain the delayed MMP-2 protein level variations observed in response to the PDGF stimulus.

The second part of this work concerned the characterization of the influence of the MMP-2 protein on the internalization of Cltx-associated SNALPs. In this context, our research showed that Tf-lipoplexes presented the same efficiency and toxicity profile in U87 cells than the commercial reagent Lipofectamine and, therefore, could be used as a delivery system for siRNAs in these cells. We performed the optimization of a transfection protocol employing these lipoplexes in order to achieve efficient downregulation of MMP-2 levels before performing adhesion studies with Cltx-associated SNALPs.

We found SNALP internalization to be only slightly reduced following siRNA-mediated silencing of MMP-2. Moreover, the increase in particle internalization was also inferior to what was expected following MMP-2 upregulation induced by cell stimulation with U87-PDGF conditioned medium. In parallel, we also observed that siRNA-mediated downregulation of TIMP-2, an inhibitor of MMP-2 activation, was able to induce a remarkable increase in SNALP internalization. However, although silencing of the MMP-2 inhibitor was shown to achieve more efficient results in terms of transfection potentiation, we cannot exclude that the presence of MMP-2-containing vesicles in U87 cells may mask the effects of MMP-2 siRNA silencing, which would help to explain the discrepancies observed in the adhesion studies.

Overall, we can conclude that MMP-2 is involved in the ability of Cltx to bind glioma cells but that this protein is not the only intervenient in the internalization process, since the modification of both MMP-2 and TIMP-2 levels is able to partially modify Cltx-mediated SNALP cellular uptake.

The logic next steps in this line of research would be to better investigate the role of PDGF in vesicle externalization, in order to completely clarify PDGF contribution to the MMP-2 regulatory process, from gene transduction to protein secretion. In addition, and taking in consideration the good results obtained with TIMP-2 manipulation, it would be interesting to investigate the contribution of this inhibitor to MMP-2 extracellular pro-form levels and the possible role of TIMP-2 in a regulatory feedback mechanism of the MMP-2 pathway.

We expect that this work will help to clarify the relation between MMP-2 and Chlorotoxin-mediated SNALP internalization, while also contributing to advance our understanding on the role of PDGF in the regulatory mechanism of this metalloproteinase. Gaining extra knowledge on these mechanisms can, on one hand, open new perspectives on how to reduce glioma cell invasiveness and, on the other hand, contribute to improve the efficiency of SNALP-based therapies against Glioblastoma and other tumors types that present MMP-2 overexpression.

References

6. References

1. Dolecek, T.A., et al., *CBTRUS statistical report: primary brain and central nervous system tumors diagnosed in the United States in 2005–2009.* Neuro-Oncology, 2012. **14**(suppl 5): p. v1-v49.
2. Stupp, R., et al., *Radiotherapy plus concomitant and adjuvant temozolomide for glioblastoma.* N Engl J Med, 2005. **352**(10): p. 987-96.
3. Ohgaki, H., *Epidemiology of brain tumors.* Methods Mol Biol, 2009. **472**: p. 323-42.
4. Fisher, J.L., et al., *Epidemiology of brain tumors.* Neurol Clin, 2007. **25**(4): p. 867-90, vii.
5. Bondy, M.L., et al., *Brain tumor epidemiology: consensus from the Brain Tumor Epidemiology Consortium.* Cancer, 2008. **113**(7 Suppl): p. 1953-68.
6. Wrensch, M., et al., *Epidemiology of primary brain tumors: current concepts and review of the literature.* Neuro Oncol, 2002. **4**(4): p. 278-99.
7. Louis, D.N., et al., *The 2007 WHO classification of tumours of the central nervous system.* Acta Neuropathol, 2007. **114**(2): p. 97-109.
8. Ohgaki, H. and P. Kleihues, *Genetic pathways to primary and secondary glioblastoma.* Am J Pathol, 2007. **170**(5): p. 1445-53.
9. Ohgaki, H. and P. Kleihues, *Population-based studies on incidence, survival rates, and genetic alterations in astrocytic and oligodendroglial gliomas.* J Neuropathol Exp Neurol, 2005. **64**(6): p. 479-89.
10. Furnari, F.B., et al., *Malignant astrocytic glioma: genetics, biology, and paths to treatment.* Genes Dev, 2007. **21**(21): p. 2683-710.
11. Sherr, C.J. and F. McCormick, *The RB and p53 pathways in cancer.* Cancer Cell, 2002. **2**(2): p. 103-12.
12. Albanese, C., et al., *Transforming P21(Ras) Mutants and C-Ets-2 Activate the Cyclin D1 Promoter through Distinguishable Regions.* Journal of Biological Chemistry, 1995. **270**(40): p. 23589-23597.
13. Weinberg, R.A., *The retinoblastoma protein and cell cycle control.* Cell, 1995. **81**(3): p. 323-30.
14. James, C.D., et al., *Clonal genomic alterations in glioma malignancy stages.* Cancer Res, 1988. **48**(19): p. 5546-51.
15. Reifenberger, G., et al., *Amplification of Multiple Genes from Chromosomal Region 12q13-14 in Human-Malignant Gliomas - Preliminary Mapping of the Amplicons Shows Preferential Involvement of Cdk4, Sas, and Mdm2.* Cancer Research, 1994. **54**(16): p. 4299-4303.
16. Serrano, M., G.J. Hannon, and D. Beach, *A new regulatory motif in cell-cycle control causing specific inhibition of cyclin D/CDK4.* Nature, 1993. **366**(6456): p. 704-7.
17. Jen, J., et al., *Deletion of p16 and p15 genes in brain tumors.* Cancer Res, 1994. **54**(24): p. 6353-8.
18. Molofsky, A.V., et al., *Increasing p16INK4a expression decreases forebrain progenitors and neurogenesis during ageing.* Nature, 2006. **443**(7110): p. 448-52.
19. Schmidt, E.E., et al., *CDKN2 (p16/MTS1) gene deletion or CDK4 amplification occurs in the majority of glioblastomas.* Cancer Res, 1994. **54**(24): p. 6321-4.
20. Holland, E.C., et al., *Combined activation of Ras and Akt in neural progenitors induces glioblastoma formation in mice.* Nat Genet, 2000. **25**(1): p. 55-7.
21. Vousden, K.H. and X. Lu, *Live or let die: the cell's response to p53.* Nat Rev Cancer, 2002. **2**(8): p. 594-604.

22. Hoh, J., et al., *The p53MH algorithm and its application in detecting p53-responsive genes.* Proc Natl Acad Sci U S A, 2002. **99**(13): p. 8467-72.
23. el-Deiry, W.S., et al., *WAF1, a potential mediator of p53 tumor suppression.* Cell, 1993. **75**(4): p. 817-25.
24. Louis, D.N. and W.K. Cavenee, *Molecular biology of central nervous system tumors*, 2003.
25. Kamijo, T., et al., *Tumor spectrum in ARF-deficient mice.* Cancer Res, 1999. **59**(9): p. 2217-22.
26. Shvarts, A., et al., *MDMX: A novel p53-binding protein with some functional properties of MDM2.* Embo Journal, 1996. **15**(19): p. 5349-5357.
27. Fujita, T., et al., *CHD5, a tumor suppressor gene deleted from 1p36.31 in neuroblastomas.* J Natl Cancer Inst, 2008. **100**(13): p. 940-9.
28. Schlaepfer, D.D. and T. Hunter, *Focal adhesion kinase overexpression enhances Ras-dependent integrin signaling to ERK2/mitogen-activated protein kinase through interactions with and activation of c-Src.* Journal of Biological Chemistry, 1997. **272**(20): p. 13189-13195.
29. Guha, A., et al., *Proliferation of human malignant astrocytomas is dependent on Ras activation.* Oncogene, 1997. **15**(23): p. 2755-2765.
30. Hawkins, P.T., et al., *Signalling through class I PI3Ks in mammalian cells.* Biochemical Society Transactions, 2006. **34**: p. 647-662.
31. Chang, S.M., et al., *Phase II study of CCI-779 in patients with recurrent glioblastoma multiforme.* Invest New Drugs, 2005. **23**(4): p. 357-61.
32. Samuels, Y., et al., *High frequency of mutations of the PIK3CA gene in human cancers.* Science, 2004. **304**(5670): p. 554.
33. Li, C., et al., *Identification of pancreatic cancer stem cells.* Cancer Res, 2007. **67**(3): p. 1030-7.
34. Ohgaki, H., et al., *Genetic pathways to glioblastoma: a population-based study.* Cancer Res, 2004. **64**(19): p. 6892-9.
35. Fraser, M.M., et al., *Pten loss causes hypertrophy and increased proliferation of astrocytes in vivo.* Cancer Res, 2004. **64**(21): p. 7773-9.
36. Xiao, A., et al., *Somatic induction of Pten loss in a preclinical astrocytoma model reveals major roles in disease progression and avenues for target discovery and validation.* Cancer Res, 2005. **65**(12): p. 5172-80.
37. Stiles, B., et al., *Essential role of AKT-1/protein kinase Bα in PTEN-controlled tumorigenesis.* Molecular and cellular biology, 2002. **22**(11): p. 3842-3851.
38. Mora, A., et al. *PDK1, the master regulator of AGC kinase signal transduction*. in *Seminars in cell & developmental biology*. 2004. Elsevier.
39. Sarbassov, D.D., S.M. Ali, and D.M. Sabatini, *Growing roles for the mTOR pathway.* Curr Opin Cell Biol, 2005. **17**(6): p. 596-603.
40. Stambolic, V., et al., *Regulation of PTEN transcription by p53.* Mol Cell, 2001. **8**(2): p. 317-25.
41. Seoane, J., et al., *Integration of Smad and forkhead pathways in the control of neuroepithelial and glioblastoma cell proliferation.* Cell, 2004. **117**(2): p. 211-23.
42. Shin, I., et al., *PKB/Akt mediates cell-cycle progression by phosphorylation of p27Kip1 at threonine 157 and modulation of its cellular localization.* Nature medicine, 2002. **8**(10): p. 1145-1152.
43. You, H., et al., *P53-dependent inhibition of FKHRL1 in response to DNA damage through-protein kinase SGK1.* Proceedings of the National Academy of Sciences of the United States of America, 2004. **101**(39): p. 14057-14062.
44. Courtois-Cox, S., et al., *A negative feedback signaling network underlies oncogene-induced senescence.* Cancer Cell, 2006. **10**(6): p. 459-72.
45. Sporn, M.B. and A.B. Roberts, *Peptide growth factors and their receptors/contributors, K.-I. Arai...[et al.]*1990: Springer-Verlag, Berlin; New York.
46. Heldin, C.H., U. Eriksson, and A. Ostman, *New members of the platelet-derived growth factor family of mitogens.* Arch Biochem Biophys, 2002. **398**(2): p. 284-90.

47. Ostman, A., et al., *Identification of a cell retention signal in the B-chain of platelet-derived growth factor and in the long splice version of the A-chain.* Cell Regul, 1991. **2**(7): p. 503-12.
48. Ostman, A., et al., *Assignment of intrachain disulfide bonds in platelet-derived growth factor B-chain.* J Biol Chem, 1993. **268**(18): p. 13372-7.
49. Ostman, A. and C.H. Heldin, *Involvement of platelet-derived growth factor in disease: development of specific antagonists.* Adv Cancer Res, 2001. **80**: p. 1-38.
50. Ostman, A., et al., *PDGF-AA and PDGF-BB biosynthesis: proprotein processing in the Golgi complex and lysosomal degradation of PDGF-BB retained intracellularly.* J Cell Biol, 1992. **118**(3): p. 509-19.
51. Muller, Y.A., et al., *Vascular endothelial growth factor: crystal structure and functional mapping of the kinase domain receptor binding site.* Proc Natl Acad Sci U S A, 1997. **94**(14): p. 7192-7.
52. Murray-Rust, J., et al., *Topological similarities in TGF-β2, PDGF-BB and NGF define a superfamily of polypeptide growth factors.* Structure, 1993. **1**(2): p. 153-159.
53. Heldin, C.H., A. Ostman, and L. Ronnstrand, *Signal transduction via platelet-derived growth factor receptors.* Biochim Biophys Acta, 1998. **1378**(1): p. F79-113.
54. Blume-Jensen, P. and T. Hunter, *Oncogenic kinase signalling.* Nature, 2001. **411**(6835): p. 355-65.
55. Bergsten, E., et al., *PDGF-D is a specific, protease-activated ligand for the PDGF β-receptor.* Nature cell biology, 2001. **3**(5): p. 512-516.
56. Emaduddin, M., et al., *Functional co-operation between the subunits in heterodimeric platelet-derived growth factor receptor complexes.* Biochemical Journal, 1999. **341**(Pt 3): p. 523-528.
57. Kazlauskas, A. and J.A. Cooper, *Autophosphorylation of the PDGF receptor in the kinase insert region regulates interactions with cell proteins.* Cell, 1989. **58**(6): p. 1121-33.
58. Shimizu, A., et al., *Ligand stimulation reduces platelet-derived growth factor β-receptor susceptibility to tyrosine dephosphorylation.* Journal of Biological Chemistry, 2001. **276**(30): p. 27749-27752.
59. Beckmann, M.P., et al., *Comparison of biological properties and transforming potential of human PDGF-A and PDGF-B chains.* Science, 1988. **241**(4871): p. 1346-9.
60. Doolittle, R.F., et al., *Simian sarcoma virus onc gene, v-sis, is derived from the gene (or genes) encoding a platelet-derived growth factor.* Science (New York, NY), 1983. **221**(4607): p. 275.
61. Fleming, T.P., et al., *Amplification and/or overexpression of platelet-derived growth factor receptors and epidermal growth factor receptor in human glial tumors.* Cancer Res, 1992. **52**(16): p. 4550-3.
62. Lokker, N.A., et al., *Platelet-derived growth factor (PDGF) autocrine signaling regulates survival and mitogenic pathways in glioblastoma cells: Evidence that the novel PDGF-C and PDGF-D ligands may play a role in the development of brain tumors.* Cancer Research, 2002. **62**(13): p. 3729-3735.
63. Shamah, S.M., C.D. Stiles, and A. Guha, *Dominant-negative mutants of platelet-derived growth factor revert the transformed phenotype of human astrocytoma cells.* Mol Cell Biol, 1993. **13**(12): p. 7203-12.
64. Kilic, T., et al., *Intracranial inhibition of platelet-derived growth factor-mediated glioblastoma cell growth by an orally active kinase inhibitor of the 2-phenylaminopyrimidine class.* Cancer Res, 2000. **60**(18): p. 5143-50.
65. Newby, A.C., *Dual role of matrix metalloproteinases (matrixins) in intimal thickening and atherosclerotic plaque rupture.* Physiol Rev, 2005. **85**(1): p. 1-31.
66. Spinale, F.G., *Matrix metalloproteinases: regulation and dysregulation in the failing heart.* Circ Res, 2002. **90**(5): p. 520-30.

67. Shah, P.K., *Inflammation, metalloproteinases, and increased proteolysis: an emerging pathophysiological paradigm in aortic aneurysm.* Circulation, 1997. **96**(7): p. 2115-7.
68. Nagase, H. and J.F. Woessner, Jr., *Matrix metalloproteinases.* J Biol Chem, 1999. **274**(31): p. 21491-4.
69. Hiller, O., et al., *Matrix metalloproteinases collagenase-2, macrophage elastase, collagenase-3, and membrane type 1-matrix metalloproteinase impair clotting by degradation of fibrinogen and factor XII.* J Biol Chem, 2000. **275**(42): p. 33008-13.
70. Lochter, A., et al., *Matrix metalloproteinase stromelysin-1 triggers a cascade of molecular alterations that leads to stable epithelial-to-mesenchymal conversion and a premalignant phenotype in mammary epithelial cells.* Journal of Cell Biology, 1997. **139**(7): p. 1861-1872.
71. Noe, V., et al., *Release of an invasion promoter E-cadherin fragment by matrilysin and stromelysin-1.* J Cell Sci, 2001. **114**(Pt 1): p. 111-118.
72. Lijnen, H.R., et al., *Inactivation of plasminogen activator inhibitor-1 by specific proteolysis with stromelysin-1 (MMP-3).* J Biol Chem, 2000. **275**(48): p. 37645-50.
73. Aimes, R.T. and J.P. Quigley, *Matrix Metalloproteinase-2 Is an Interstitial Collagenase INHIBITOR-FREE ENZYME CATALYZES THE CLEAVAGE OF COLLAGEN FIBRILS AND SOLUBLE NATIVE TYPE I COLLAGEN GENERATING THE SPECIFIC ¾-AND ¼-LENGTH FRAGMENTS.* Journal of Biological Chemistry, 1995. **270**(11): p. 5872-5876.
74. Patterson, M.L., et al., *Specific collagenolysis by gelatinase A, MMP-2, is determined by the hemopexin domain and not the fibronectin-like domain.* FEBS letters, 2001. **503**(2): p. 158-162.
75. Itoh, T., et al., *Unaltered secretion of β-amyloid precursor protein in gelatinase A (matrix metalloproteinase 2)-deficient mice.* Journal of Biological Chemistry, 1997. **272**(36): p. 22389-22392.
76. Martignetti, J.A., et al., *Mutation of the matrix metalloproteinase 2 gene (MMP2) causes a multicentric osteolysis and arthritis syndrome.* Nat Genet, 2001. **28**(3): p. 261-5.
77. Van Wart, H.E. and H. Birkedal-Hansen, *The cysteine switch: a principle of regulation of metalloproteinase activity with potential applicability to the entire matrix metalloproteinase gene family.* Proc Natl Acad Sci U S A, 1990. **87**(14): p. 5578-82.
78. Fessler, L.I., et al., *Characterization of the procollagen IV cleavage products produced by a specific tumor collagenase.* J Biol Chem, 1984. **259**(15): p. 9783-9.
79. Nagase, H., R. Visse, and G. Murphy, *Structure and function of matrix metalloproteinases and TIMPs.* Cardiovasc Res, 2006. **69**(3): p. 562-73.
80. Stocker, W. and W. Bode, *Structural features of a superfamily of zinc-endopeptidases: the metzincins.* Curr Opin Struct Biol, 1995. **5**(3): p. 383-90.
81. Morgunova, E., et al., *Structure of human pro-matrix metalloproteinase-2: activation mechanism revealed.* Science, 1999. **284**(5420): p. 1667-70.
82. Pickford, A.R., et al., *Solution structure of a type 2 module from fibronectin: implications for the structure and function of the gelatin-binding domain.* Structure, 1997. **5**(3): p. 359-70.
83. Murphy, G. and V. Knauper, *Relating matrix metalloproteinase structure to function: why the "hemopexin" domain?* Matrix Biol, 1997. **15**(8-9): p. 511-8.
84. Fernandez-Catalan, C., et al., *Crystal structure of the complex formed by the membrane type 1-matrix metalloproteinase with the tissue inhibitor of metalloproteinases-2, the soluble progelatinase A receptor.* EMBO J, 1998. **17**(17): p. 5238-48.
85. Cao, J., et al., *The C-Terminal Region of Membrane Type Matrix Metalloproteinase Is a Functional Transmembrane Domain Required for Pro-Gelatinase-C Activation.* Journal of Biological Chemistry, 1995. **270**(2): p. 801-805.
86. Butler, G.S., et al., *The TIMP2 membrane type 1 metalloproteinase "receptor" regulates the concentration and efficient activation of progelatinase AA kinetic study.* Journal of Biological Chemistry, 1998. **273**(2): p. 871-880.

87. Morgunova, E., et al., *Structural insight into the complex formation of latent matrix metalloproteinase 2 with tissue inhibitor of metalloproteinase 2.* Proc Natl Acad Sci U S A, 2002. **99**(11): p. 7414-7419.
88. Soroceanu, L., T.J. Manning, and H. Sontheimer, *Modulation of glioma cell migration and invasion using Cl- and K+ ion channel blockers.* Journal of Neuroscience, 1999. **19**(14): p. 5942-5954.
89. Wang, X., et al., *Co-recycling of MT1-MMP and MT3-MMP through the trans-Golgi network - Identification of DKV582 as a recycling signal.* Journal of Biological Chemistry, 2004. **279**(10): p. 9331-9336.
90. Deshane, J., C.C. Garner, and H. Sontheimer, *Chlorotoxin inhibits glioma cell invasion via matrix metalloproteinase-2.* J Biol Chem, 2003. **278**(6): p. 4135-44.
91. Anilkumar, N., et al., *Palmitoylation at Cys574 is essential for MT1-MMP to promote cell migration.* The FASEB journal, 2005. **19**(10): p. 1326-1328.
92. Stupp, R., et al., *Chemoradiotherapy in malignant glioma: standard of care and future directions.* J Clin Oncol, 2007. **25**(26): p. 4127-36.
93. Wen, P.Y. and A.A. Brandes, *Treatment of recurrent high-grade gliomas.* Curr Opin Neurol, 2009. **22**(6): p. 657-64.
94. Cohen, M.H., et al., *FDA drug approval summary: bevacizumab (AVASTIN®) as treatment of recurrent glioblastoma multiforme.* The oncologist, 2009. **14**(11): p. 1131-1138.
95. Van Meir, E.G., et al., *Exciting new advances in neuro-oncology: the avenue to a cure for malignant glioma.* CA Cancer J Clin, 2010. **60**(3): p. 166-93.
96. Sathornsumetee, S. and J.N. Rich, *Designer therapies for glioblastoma multiforme.* Ann N Y Acad Sci, 2008. **1142**(1): p. 108-32.
97. Chan, L.S., J. Daruwalla, and C. Christophi, *Selective targeting of the tumour vasculature.* ANZ J Surg, 2008. **78**(11): p. 955-67.
98. Chi, A.S., et al., *Angiogenesis as a Therapeutic Target in Malignant Gliomas.* Oncologist, 2009. **14**(6): p. 621-636.
99. Siemann, D.W., *Vascular-targeted therapies in oncology*2006: Wiley Online Library.
100. Sapra, P. and T.M. Allen, *Ligand-targeted liposomal anticancer drugs.* Prog Lipid Res, 2003. **42**(5): p. 439-62.
101. Simone, E., B.S. Ding, and V. Muzykantov, *Targeted delivery of therapeutics to endothelium.* Cell Tissue Res, 2009. **335**(1): p. 283-300.
102. Jain, R.K., et al., *Angiogenesis in brain tumours.* Nat Rev Neurosci, 2007. **8**(8): p. 610-22.
103. Fukumura, D. and R.K. Jain, *Tumor microvasculature and microenvironment: targets for anti-angiogenesis and normalization.* Microvasc Res, 2007. **74**(2-3): p. 72-84.
104. Cavaliere, R., P.Y. Wen, and D. Schiff, *Novel therapies for malignant gliomas.* Neurol Clin, 2007. **25**(4): p. 1141-71, x.
105. Lammers, T., W.E. Hennink, and G. Storm, *Tumour-targeted nanomedicines: principles and practice.* Br J Cancer, 2008. **99**(3): p. 392-7.
106. Chirasani, S.R., et al., *Transferrin-receptor-mediated iron accumulation controls proliferation and glutamate release in glioma cells.* J Mol Med (Berl), 2009. **87**(2): p. 153-67.
107. Husain, S.R. and R.K. Puri, *Interleukin-13 receptor-directed cytotoxin for malignant glioma therapy: from bench to bedside.* J Neurooncol, 2003. **65**(1): p. 37-48.
108. Weaver, M. and D.W. Laske, *Transferrin receptor ligand-targeted toxin conjugate (Tf-CRM107) for therapy of malignant gliomas.* J Neurooncol, 2003. **65**(1): p. 3-13.
109. Weber, F.W., et al., *Local convection enhanced delivery of IL4-Pseudomonas exotoxin (NBI-3001) for treatment of patients with recurrent malignant glioma.* Acta Neurochir Suppl, 2003. **88**(88): p. 93-103.
110. Lasch, J., V. Weissig, and M. Brandl, *Preparation of liposomes.* Liposomes: a practical approach, 2003. **2**: p. 24-25.

111. Drummond, D.C., et al., *Optimizing liposomes for delivery of chemotherapeutic agents to solid tumors.* Pharmacol Rev, 1999. **51**(4): p. 691-743.
112. Senior, J., J.C. Crawley, and G. Gregoriadis, *Tissue distribution of liposomes exhibiting long half-lives in the circulation after intravenous injection.* Biochimica Et Biophysica Acta, 1985. **839**(1): p. 1-8.
113. Allen, T., et al., *Liposomes containing synthetic lipid derivatives of poly (ethylene glycol) show prolonged circulation half-lives in vivo.* Biochimica et Biophysica Acta (BBA)-Biomembranes, 1991. **1066**(1): p. 29-36.
114. Allen, T.M., *Liposomes. Opportunities in drug delivery.* Drugs, 1997. **54 Suppl 4**(4): p. 8-14.
115. Liu, D., A. Mori, and L. Huang, *Role of liposome size and RES blockade in controlling biodistribution and tumor uptake of GM< sub> 1</sub>-containing liposomes.* Biochimica et Biophysica Acta (BBA)-Biomembranes, 1992. **1104**(1): p. 95-101.
116. Litzinger, D.C., et al., *Effect of liposome size on the circulation time and intraorgan distribution of amphipathic poly(ethylene glycol)-containing liposomes.* Biochimica Et Biophysica Acta, 1994. **1190**(1): p. 99-107.
117. Kamps, J. and G. Scherphof, *Liposomes in biological systems.* Liposomes: a practical approach, 2nd edn. Oxford University Press, Oxford, 2003: p. 267-286.
118. Park, Y.S., *Tumor-directed targeting of liposomes.* Biosci Rep, 2002. **22**(2): p. 267-81.
119. Park, J.W., et al., *Tumor targeting using anti-her2 immunoliposomes.* Journal of Controlled Release, 2001. **74**(1-3): p. 95-113.
120. Harding, J.A., et al., *Immunogenicity and pharmacokinetic attributes of poly(ethylene glycol)-grafted immunoliposomes.* Biochimica Et Biophysica Acta, 1997. **1327**(2): p. 181-92.
121. Maruyama, K., et al., *Targetability of Novel Immunoliposomes Modified with Amphipathic Poly(Ethylene Glycol)S Conjugated at Their Distal Terminals to Monoclonal-Antibodies.* Biochimica Et Biophysica Acta-Biomembranes, 1995. **1234**(1): p. 74-80.
122. Allen, T.M., et al., *A new strategy for attachment of antibodies to sterically stabilized liposomes resulting in efficient targeting to cancer cells.* Biochimica Et Biophysica Acta, 1995. **1237**(2): p. 99-108.
123. Zalipsky, S., et al., *Peptide attachment to extremities of liposomal surface grafted PEG chains: preparation of the long-circulating form of laminin pentapeptide, YIGSR.* Bioconjug Chem, 1995. **6**(6): p. 705-8.
124. Zalipsky, S., et al., *Long circulating, cationic liposomes containing amino-PEG-phosphatidylethanolamine.* FEBS Lett, 1994. **353**(1): p. 71-4.
125. Zalipsky, S., *Synthesis of an end-group functionalized polyethylene glycol-lipid conjugate for preparation of polymer-grafted liposomes.* Bioconjug Chem, 1993. **4**(4): p. 296-9.
126. Park, J.W., et al., *Immunoliposomes for cancer treatment.* Adv Pharmacol, 1997. **40**: p. 399-435.
127. Hamilton, A.J. and D.C. Baulcombe, *A species of small antisense RNA in posttranscriptional gene silencing in plants.* Science, 1999. **286**(5441): p. 950-2.
128. Haupenthal, J., et al., *Inhibition of RNAse A family enzymes prevents degradation and loss of silencing activity of siRNAs in serum.* Biochem Pharmacol, 2006. **71**(5): p. 702-10.
129. Haupenthal, J., et al., *RNAse A-like enzymes in serum inhibit the anti-neoplastic activity of siRNA targeting polo-like kinase 1.* Int J Cancer, 2007. **121**(1): p. 206-10.
130. Turner, J.J., et al., *MALDI-TOF mass spectral analysis of siRNA degradation in serum confirms an RNAse A-like activity.* Mol Biosyst, 2007. **3**(1): p. 43-50.
131. Behlke, M.A., *Chemical Modification of siRNAs for In Vivo Use.* Oligonucleotides, 2008. **18**(4): p. 305-319.
132. Kennedy, S., D. Wang, and G. Ruvkun, *A conserved siRNA-degrading RNase negatively regulates RNA interference in C. elegans.* Nature, 2004. **427**(6975): p. 645-9.

133. Zou, Y., et al., *Metabolite identification of small interfering RNA duplex by high-resolution accurate mass spectrometry.* Rapid Commun Mass Spectrom, 2008. **22**(12): p. 1871-81.
134. Morrissey, D.V., et al., *Potent and persistent in vivo anti-HBV activity of chemically modified siRNAs.* Nat Biotechnol, 2005. **23**(8): p. 1002-7.
135. Zimmermann, T.S., et al., *RNAi-mediated gene silencing in non-human primates.* Nature, 2006. **441**(7089): p. 111-4.
136. De Boer, A., I. Van der Sandt, and P. Gaillard, *The role of drug transporters at the blood-brain barrier.* Annual review of pharmacology and toxicology, 2003. **43**(1): p. 629-656.
137. Pardridge, W.M., *The blood-brain barrier: bottleneck in brain drug development.* NeuroRx, 2005. **2**(1): p. 3-14.
138. Rao, K.S., et al., *TAT-conjugated nanoparticles for the CNS delivery of anti-HIV drugs.* Biomaterials, 2008. **29**(33): p. 4429-38.
139. Zensi, A., et al., *Albumin nanoparticles targeted with Apo E enter the CNS by transcytosis and are delivered to neurones.* J Control Release, 2009. **137**(1): p. 78-86.
140. Cerletti, A., et al., *Endocytosis and transcytosis of an immunoliposome-based brain drug delivery system.* J Drug Target, 2000. **8**(6): p. 435-46.
141. Tosi, G., et al., *Sialic acid and glycopeptides conjugated PLGA nanoparticles for central nervous system targeting:< i> In vivo</i> pharmacological evidence and biodistribution.* Journal of Controlled Release, 2010. **145**(1): p. 49-57.
142. Ponka, P. and C.N. Lok, *The transferrin receptor: role in health and disease.* Int J Biochem Cell Biol, 1999. **31**(10): p. 1111-37.
143. Moos, T., et al., *Iron trafficking inside the brain.* J Neurochem, 2007. **103**(5): p. 1730-40.
144. Visser, C.C., et al., *Targeting liposomes with protein drugs to the blood-brain barrier in vitro.* Eur J Pharm Sci, 2005. **25**(2-3): p. 299-305.
145. Chang, J., et al., *Characterization of endocytosis of transferrin-coated PLGA nanoparticles by the blood-brain barrier.* Int J Pharm, 2009. **379**(2): p. 285-92.
146. Mishra, V., et al., *Targeted brain delivery of AZT via transferrin anchored pegylated albumin nanoparticles.* J Drug Target, 2006. **14**(1): p. 45-53.
147. Ulbrich, K., et al., *Transferrin- and transferrin-receptor-antibody-modified nanoparticles enable drug delivery across the blood-brain barrier (BBB).* Eur J Pharm Biopharm, 2009. **71**(2): p. 251-6.
148. Costa P., Cardoso A.L. et al., *Tumor-target chlorotoxin nanoparticles for nucleic acid delivery*
149. Campbell, M., *Lipofection reagents prepared by a simple ethanol injection technique.* Biotechniques, 1995. **18**(6): p. 1027.
150. Mendonça, L.S., et al., *Transferrin receptor-targeted liposomes encapsulating anti-BCR-ABL siRNA or asODN for chronic myeloid leukemia treatment.* Bioconjugate chemistry, 2009. **21**(1): p. 157-168.
151. Moreira, J.N., et al., *Use of the post-insertion technique to insert peptide ligands into pre-formed stealth liposomes with retention of binding activity and cytotoxicity.* Pharmaceutical research, 2002. **19**(3): p. 265-269.
152. Huang, T., et al., *A stable reagent for the Liebermann-Burchard reaction. Application to rapid serum cholesterol determination.* Analytical chemistry, 1961. **33**(10): p. 1405-1407.
153. Leamon, C.P. and P.S. Low, *Delivery of Macromolecules into Living Cells - a Method That Exploits Folate Receptor Endocytosis.* Proc Natl Acad Sci U S A, 1991. **88**(13): p. 5572-5576.
154. Taraboletti, G., et al., *Shedding of the matrix metalloproteinases MMP-2, MMP-9, and MT1-MMP as membrane vesicle-associated components by endothelial cells.* American Journal of Pathology, 2002. **160**(2): p. 673-680.